

# Two phase fluid mechanics

Instructor:

[Valid Taghikhani](#)

Fall 1388

[Department of Chemical and Petroleum Engineering, Sharif University of Technology](#)

## Course syllabus

- Introduction to multiphase flow
- Hydrocarbon reservoirs
- Liquid mixture properties
- Gas/liquid mixture properties
- Basic concepts of two phase flow
- Mechanistic/empirical models
- Steady state correlations for horizontal, vertical and inclined pipes.
- Pigging and slug catchers
- Unsteady state multiphase flow
- Software application (OLGA, pvt-sim, PIPEPHASE)

# What is Flow Assurance?

Flow assurance is an engineering analysis process to assure hydrocarbon fluids are transmitted economically from the reservoir to the end user over the life of a project in any environment, in which the knowledge of fluid properties and thermal-hydraulic analysis of the system is utilized to develop strategies for controlling the solids such as hydrates, wax, asphaltenes, and scale from the system.

The term “Flow Assurance” was first used by Petrobras in the early 1990s, it originally only covered the thermal hydraulics and production chemistry issues encountered during oil and gas production. While the term is relatively new, the problems related with flow assurance have been a critical issue in the oil/gas industry from very early days. Hydrates were observed causing blockages in gas pipelines as early as the 1930s and were solved by chemical inhibition using methanol by the pioneering work of Hammerschmidt.

# Flow Assurance Challenges

Flow assurance analysis is a recognized critical part in the design and operation of subsea oil/gas systems. Flow assurance challenges mainly focus on the prevention and control of solid deposits which could potentially block the flow path. The solids of concern generally are hydrates, wax and asphaltenes. Sometimes scale and sand are also included. For a given hydrocarbons fluid these solids appear at certain combinations of pressure and temperature and deposit on the walls of the production equipment and flowline. Figure 17.1 shows the hydrate and wax depositions formed in hydrocarbons flowlines, which ultimately may cause plugging and flow stoppage.

The solids control strategies of hydrates, wax and asphaltenes include:

- thermodynamic control -- keeping the pressure and temperature of whole system out of the regions where the solids may form;
- kinetic control -- controlling the conditions of solids formation so that deposits do not form;
- mechanical control -- allowing solids to deposit, but periodically removing them by pigging.



## References

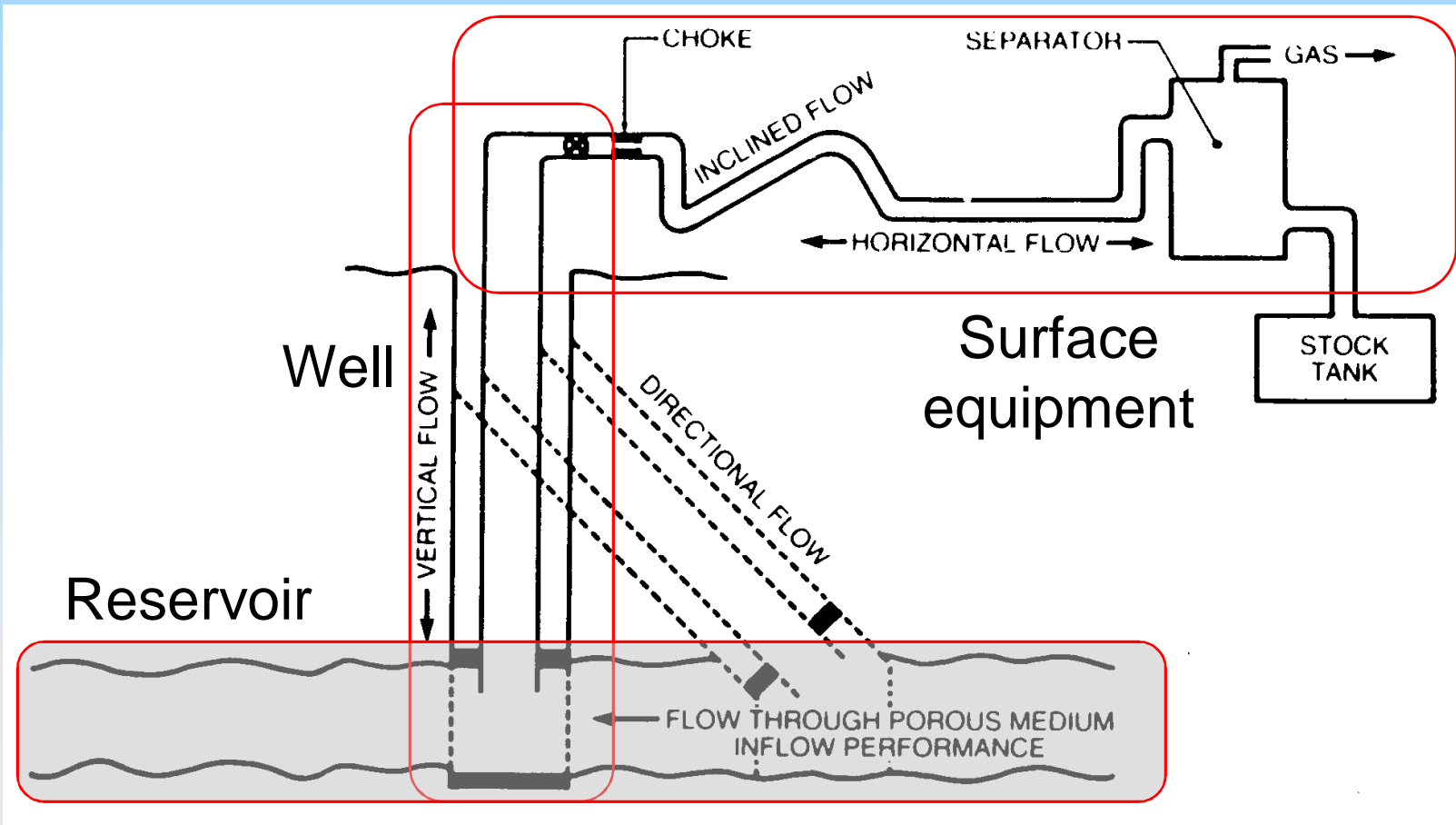
- Two phase flow in pipes, 6<sup>th</sup> ed., J P Brill, H P Beggs.
- Multiphase flow in wells, J P Brill, SPE communication.
- Some technical papers.

# Course grading scheme

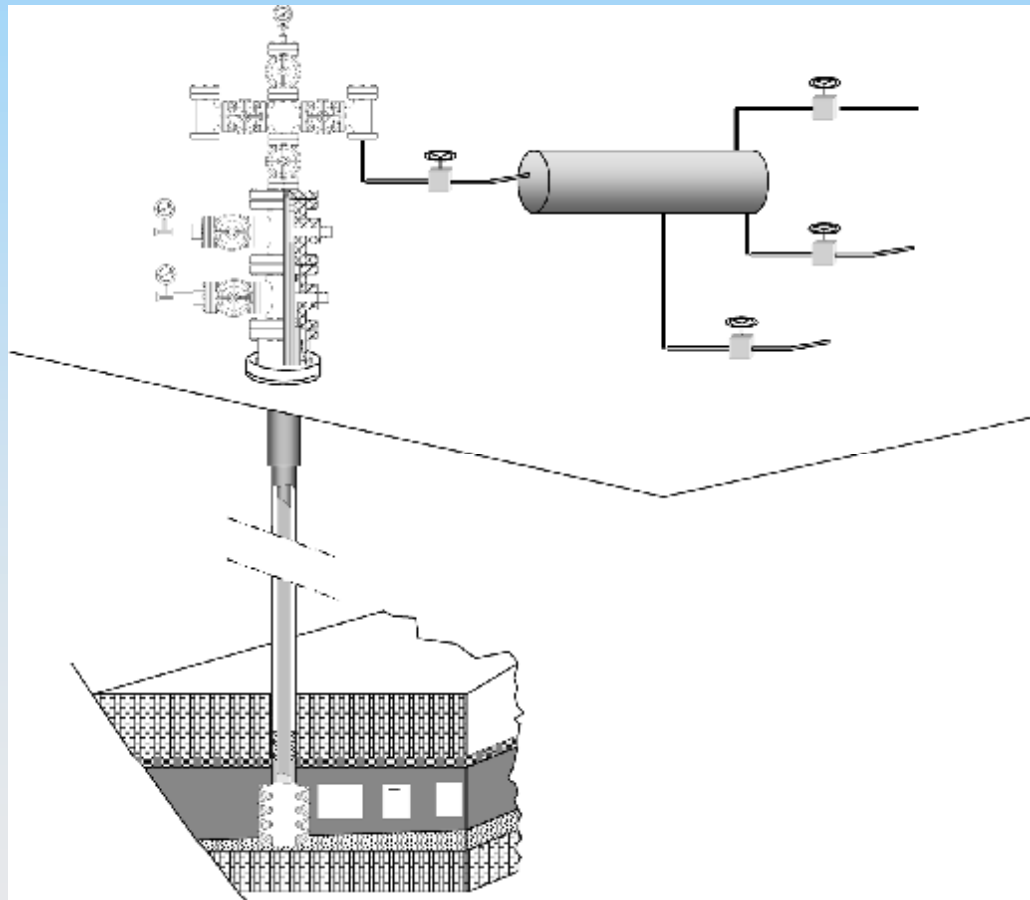
- Written exams (up to 80%)
- Assignments (up to 5%)
- Class projects (up to 15%)

A mailing list and a taker to moderate the mailing list required. Who is the taker!?

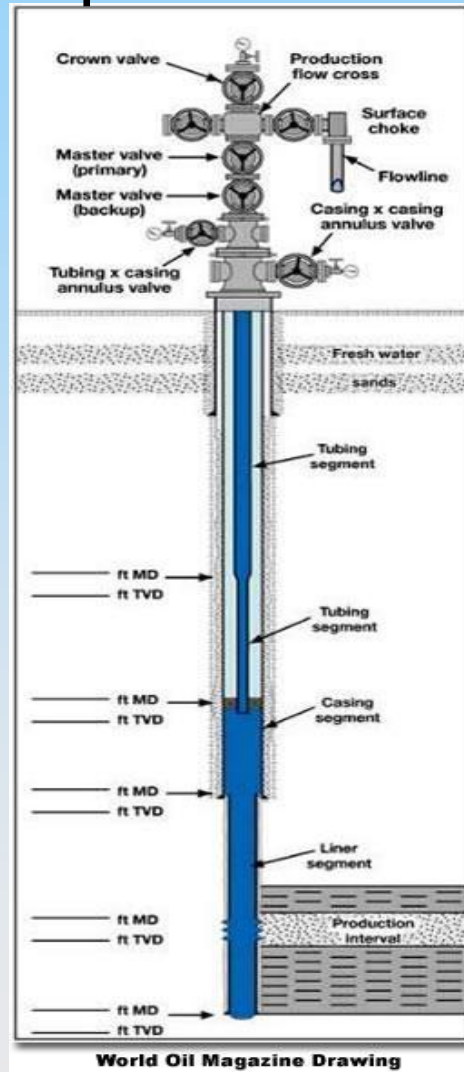
# Multiphase Production system

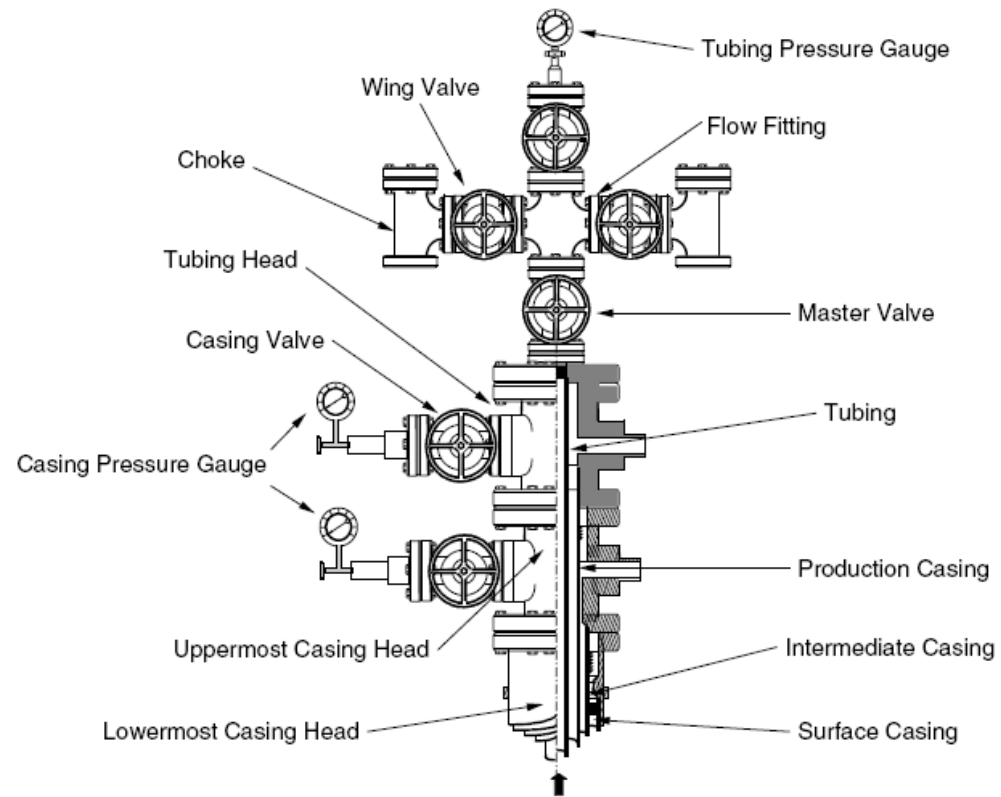


# Production system

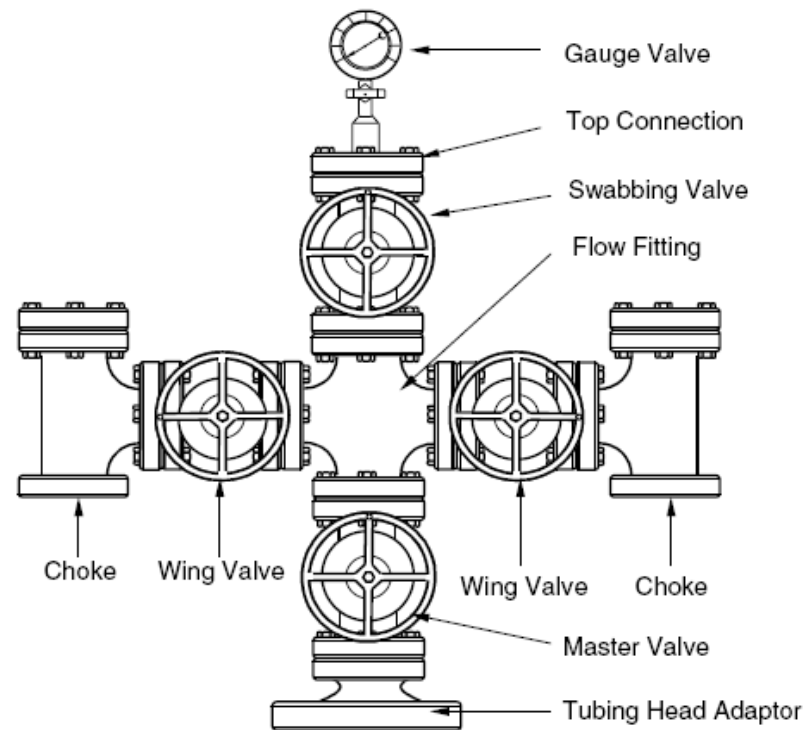


# Well completion components

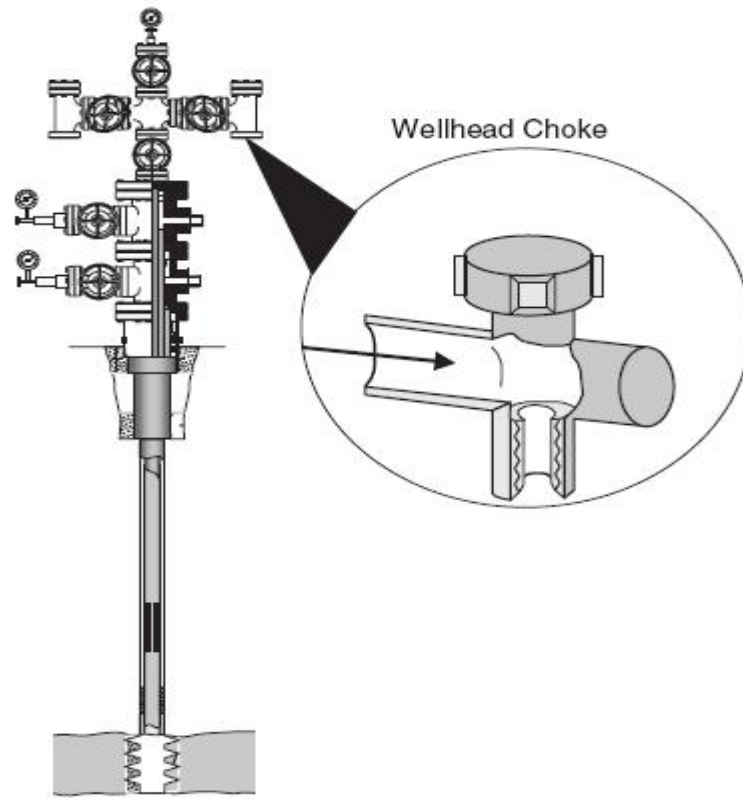




*Figure 1.7 A sketch of a wellhead.*

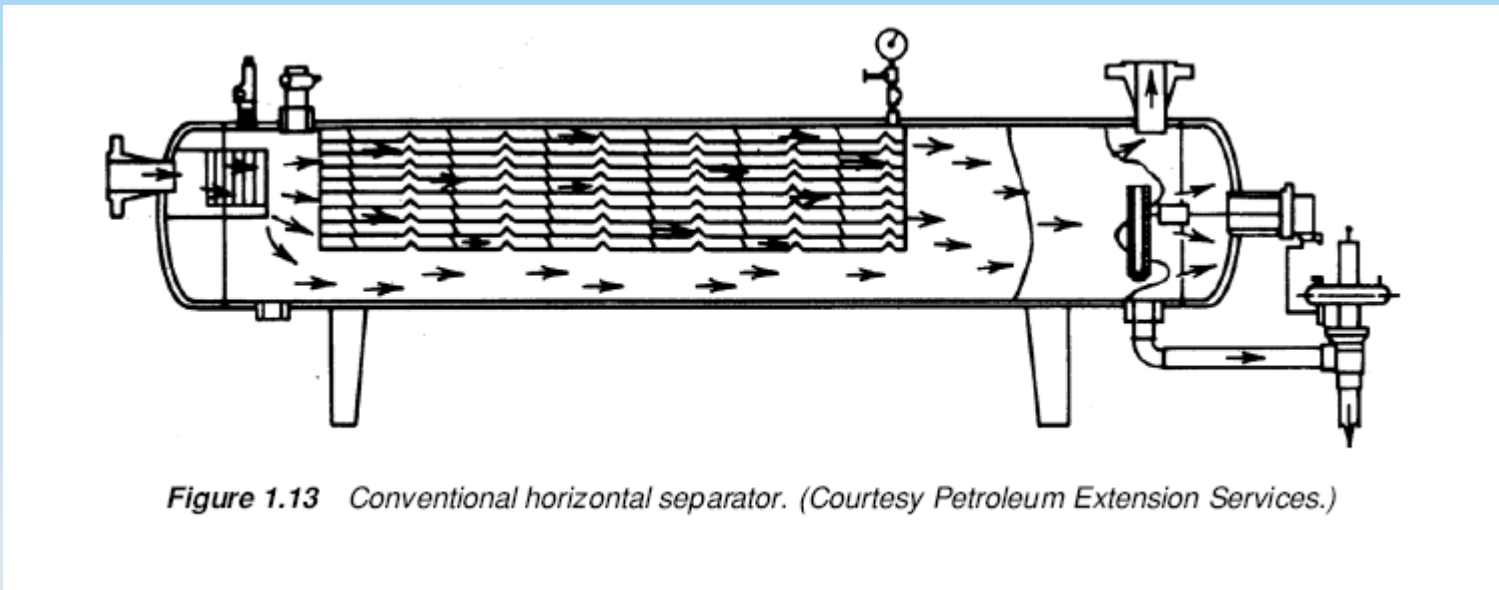


*Figure 1.10 A sketch of a "Christmas tree."*

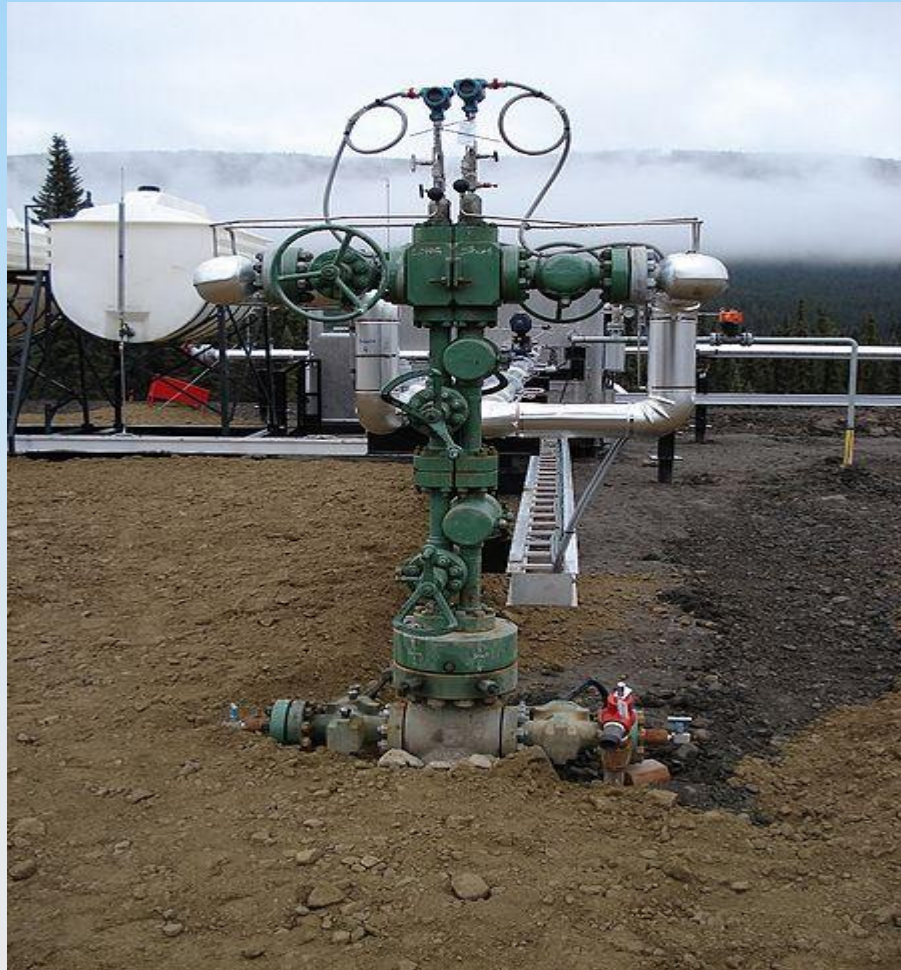


**Figure 1.12** A sketch of a wellhead choke.





*Figure 1.13 Conventional horizontal separator. (Courtesy Petroleum Extension Services.)*



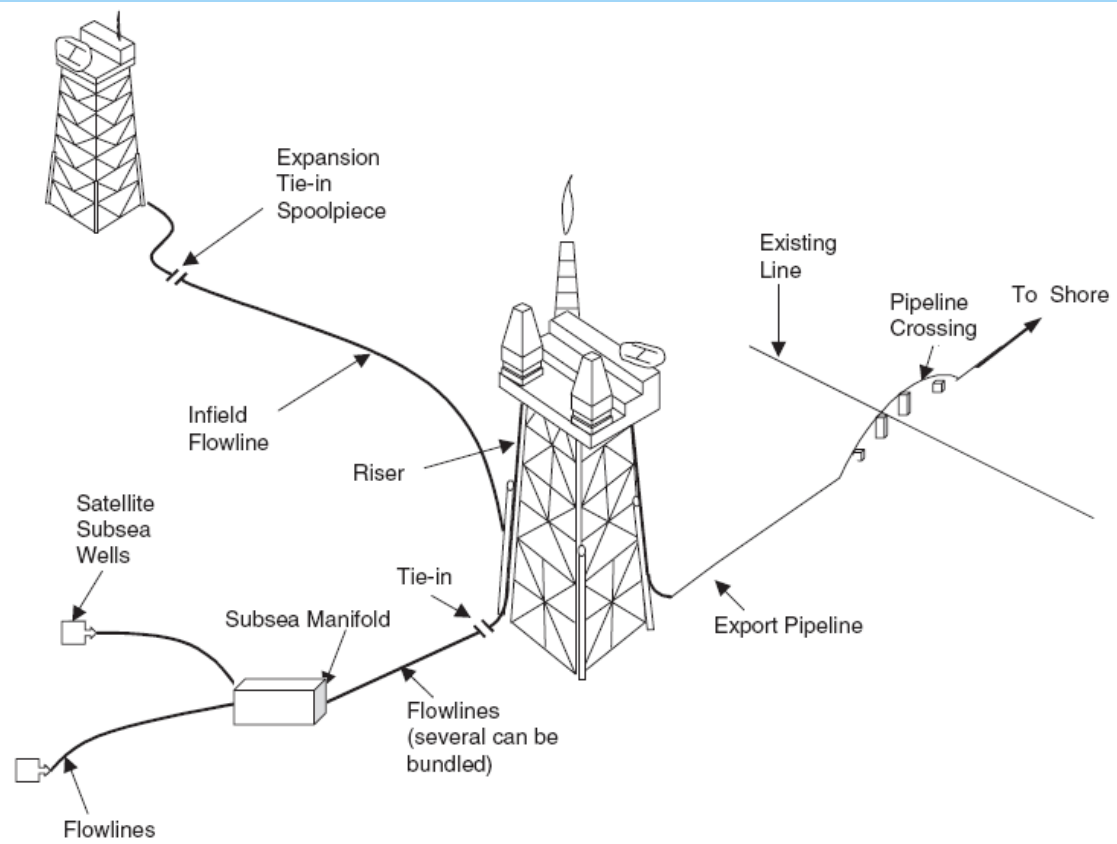


**Figure 1.16** Uses of offshore pipelines. (Guo et al., 2005.)

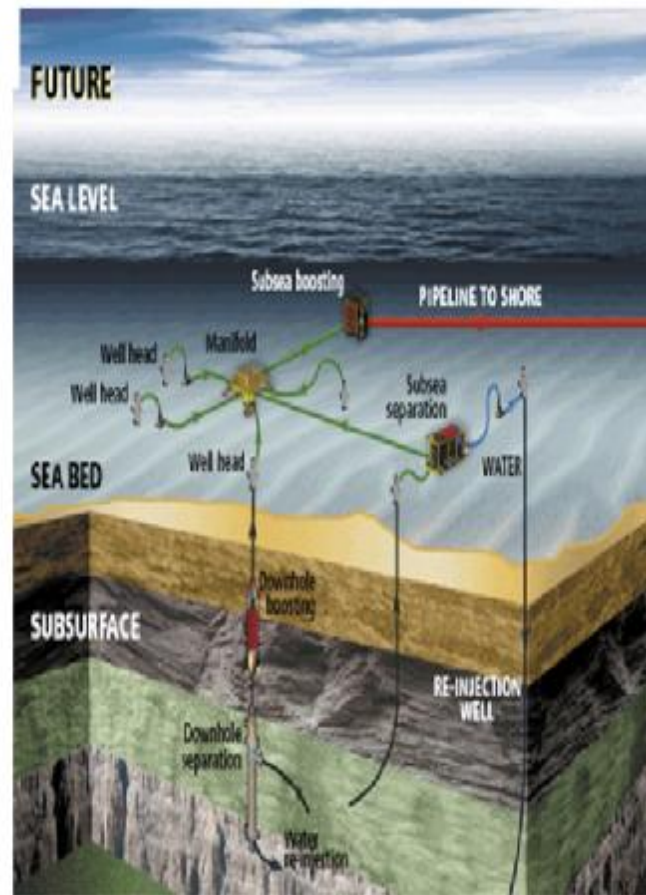
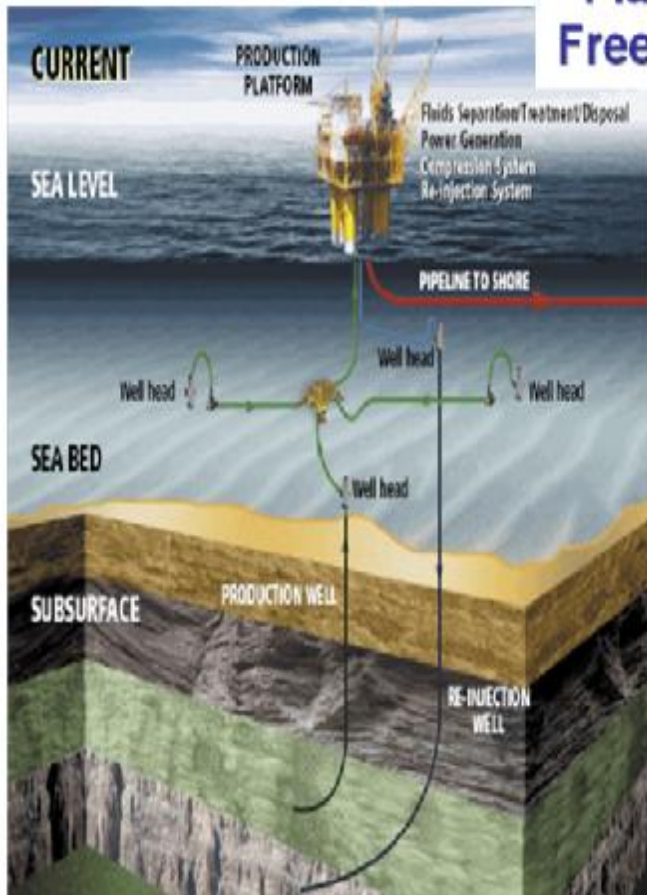
- **Sizing, routing and layout**
- **Operability analysis**
  - Slugging
  - Rate changes
  - Shut-down/Cool-down/Start-up
  - Blowdown
  - Liquid management/Pigging

- **Thermal management**

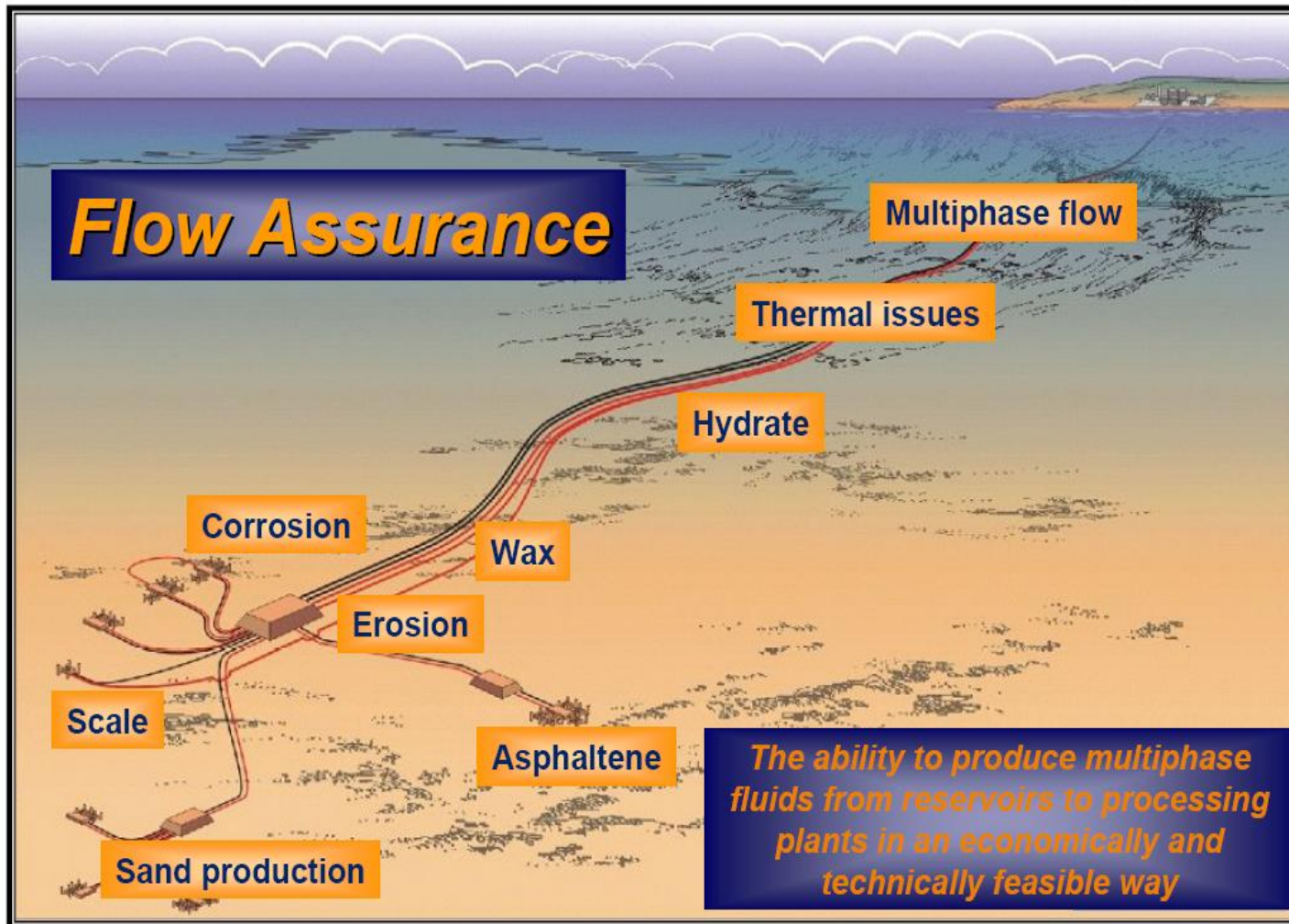
- Insulation/Burial
- Bundles/Complex risers
- Hydrates/Wax
- Inhibition



## Platform Free Fields

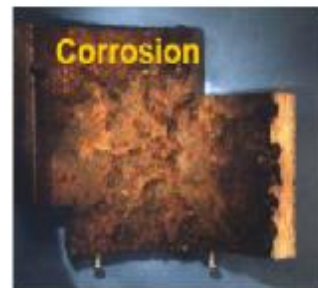


# The Flow Assurance Challenge



## Multiphase Oil Systems

### Fluid challenges



**Temperature!**



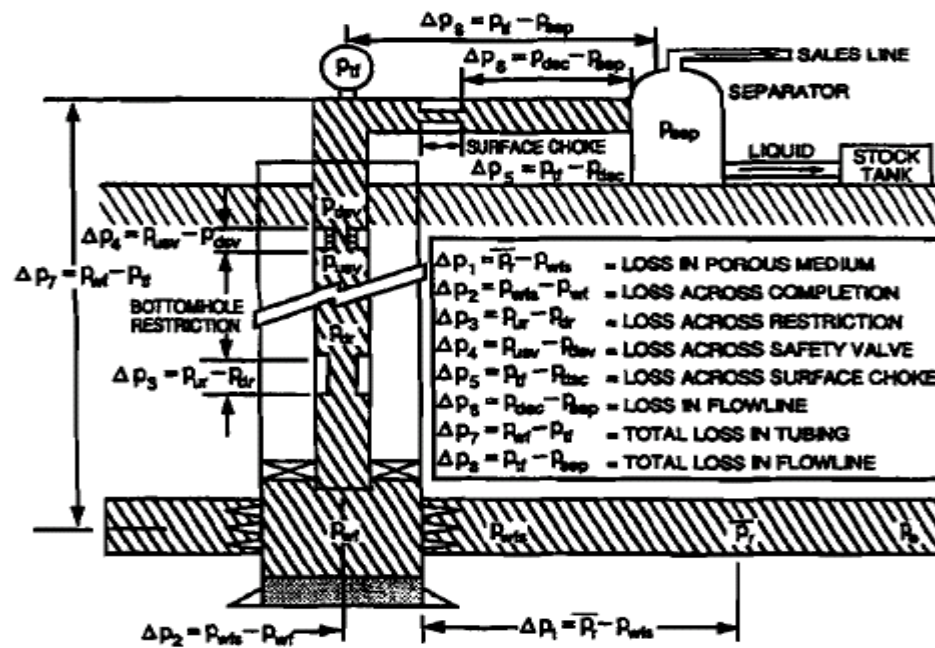
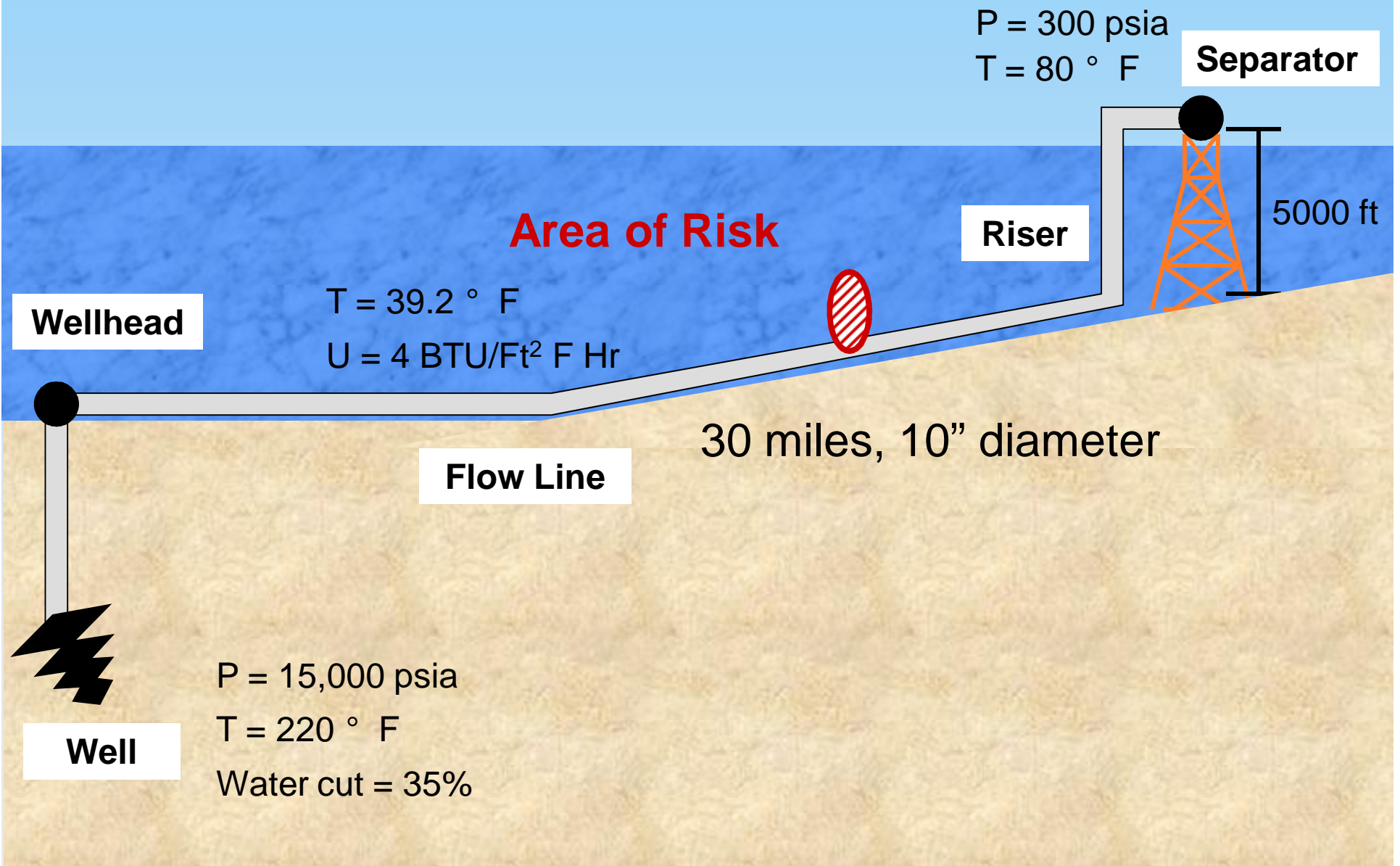


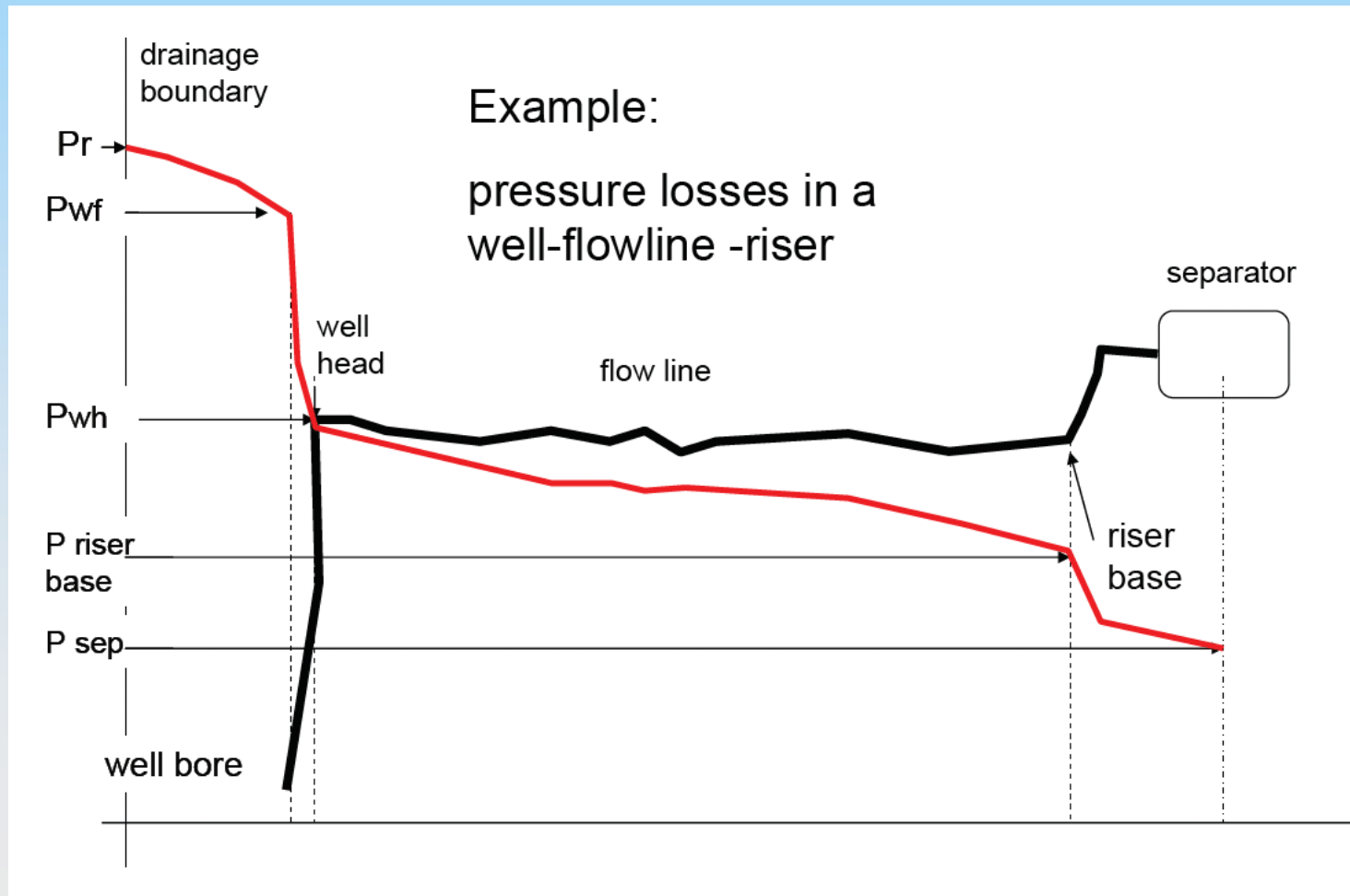
Fig. 6.1—Possible pressure losses in the producing system of a flowing well.<sup>6</sup>

$$p_{wf} = p_{sep} + \Delta p_h + (\Delta p_{fl} + \Delta p_t + \Delta p_{ch})_f + \Delta p_{acc},$$



# The Jomon Field Flow Line Schematic





**Session 2:**  
**Hydrocarbon phase behavior, flash calculations  
and pvt-sim**

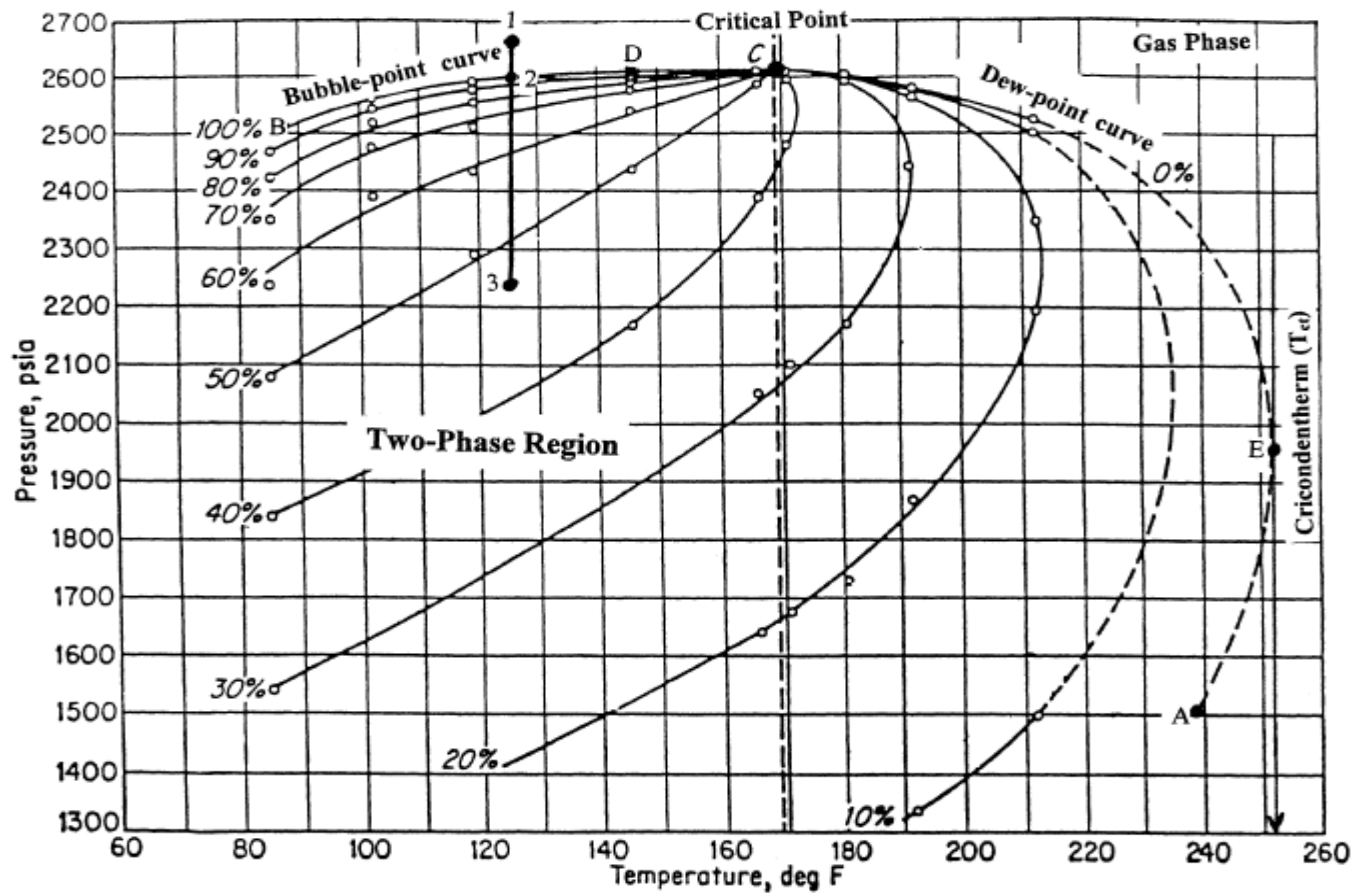


FIGURE 1-16 Typical  $p/T$  diagram for a multicomponent system.

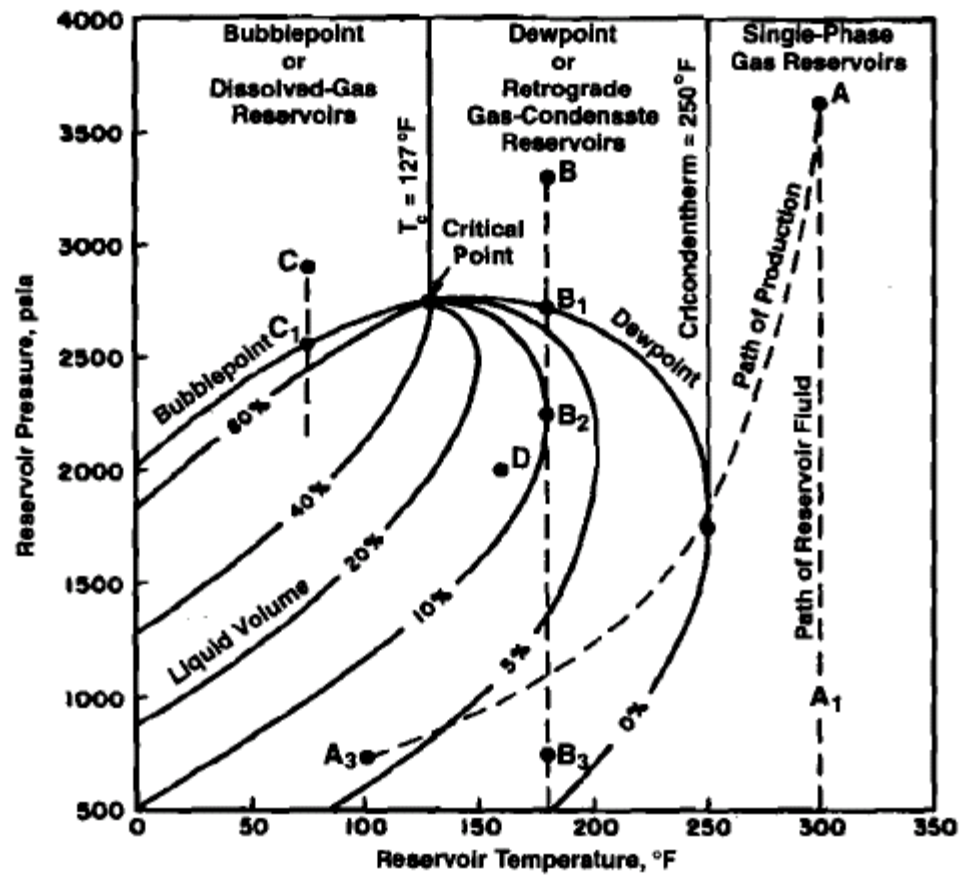


Fig. 3.1—Typical phase diagram.<sup>1</sup>

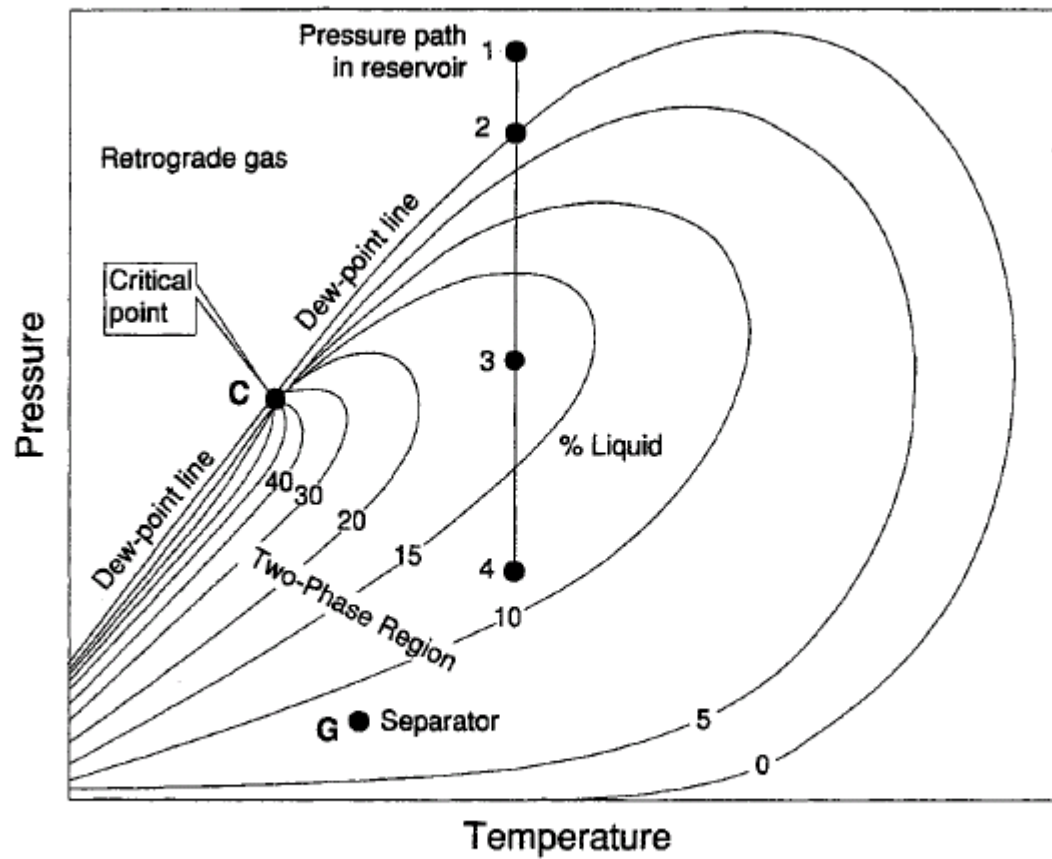


FIGURE 1-26 *Typical phase diagram of a retrograde system.*

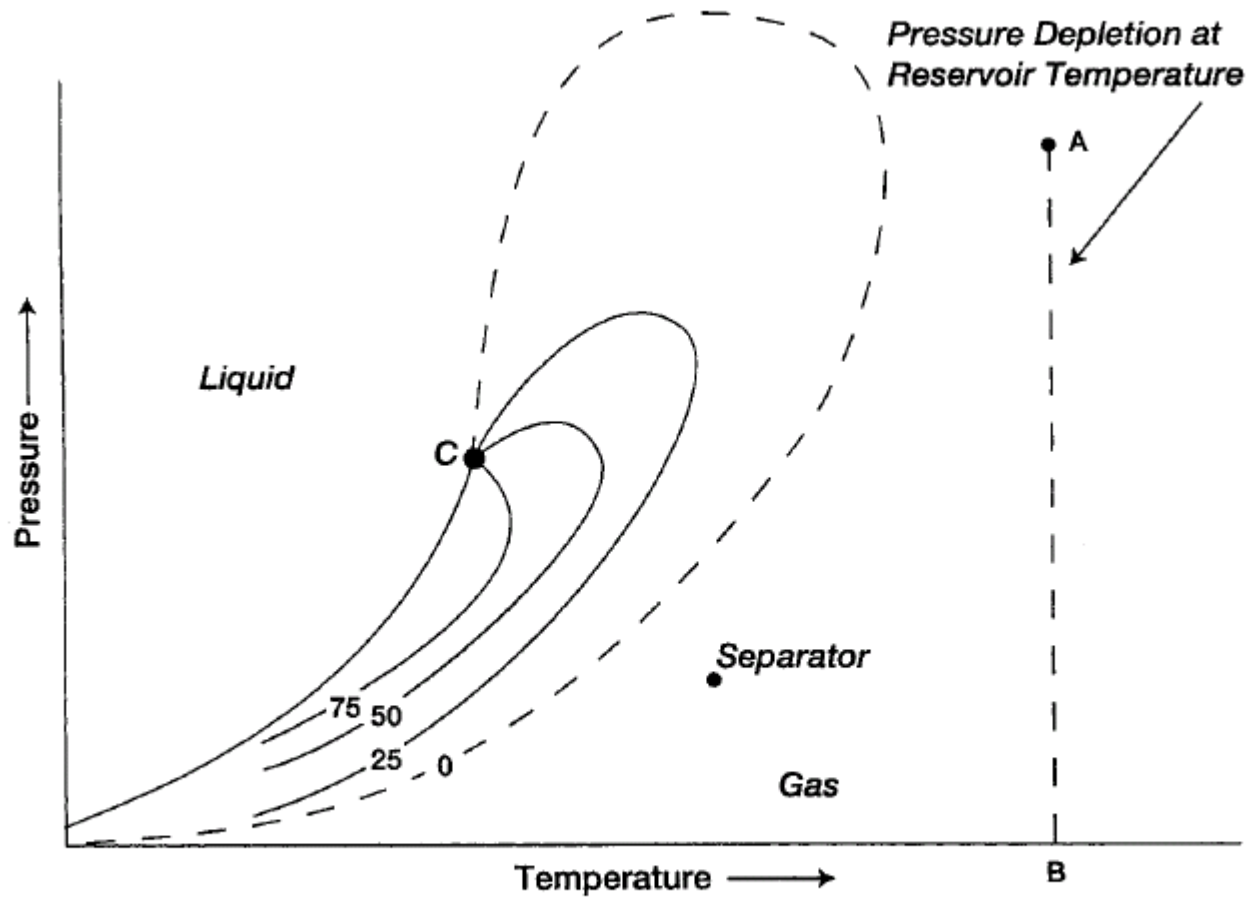


FIGURE 1-31 Phase diagram for a dry gas.

Source: After N. J. Clark, *Elements of Petroleum Reservoirs*, 2nd ed. Tulsa, OK: Society of Petroleum Engineers, 1969.

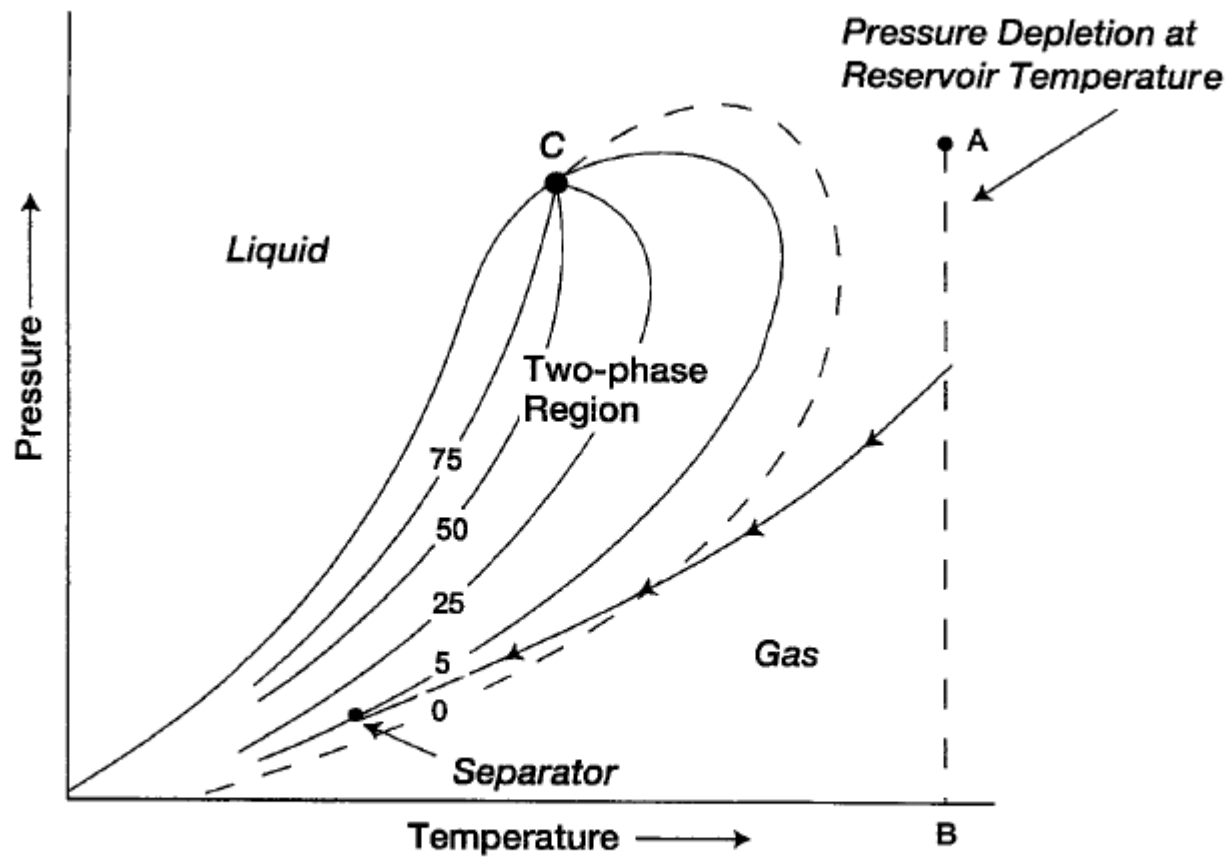
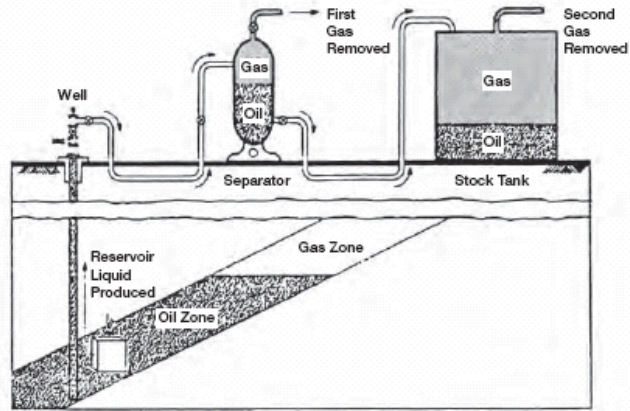


FIGURE 1-30 *Phase diagram for a wet gas.*

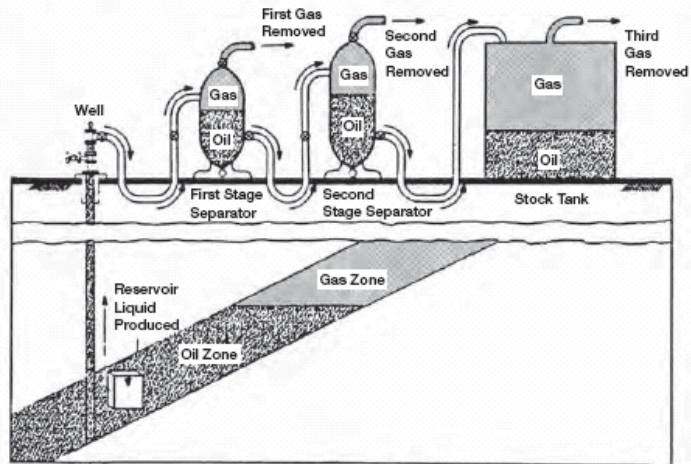
Source: After N. J. Clark, *Elements of Petroleum Reservoirs*, 2nd ed. Tulsa, OK: Society of Petroleum Engineers, 1969.



# Flash separation



One-stage separation



Two-stage separation

FIGURE 5-6 Schematic illustration of one- and two-stage separation processes.  
 Source: After N. Clark, *Elements of Petroleum Reservoirs*. Dallas: Society of Petroleum Engineers, 1960.

## Main objective of flash calculations

- Optimum separation conditions: P and T
- Composition of separated oil and gas phases
- Producing gas/oil ratio
- API gravity of the stock tank oil
- Oil formation volume factor

## Optimum conditions leads to:

- Minimum gas/oil ratio
- Minimum oil formation volume factor
- Maximum stock tank API gravity

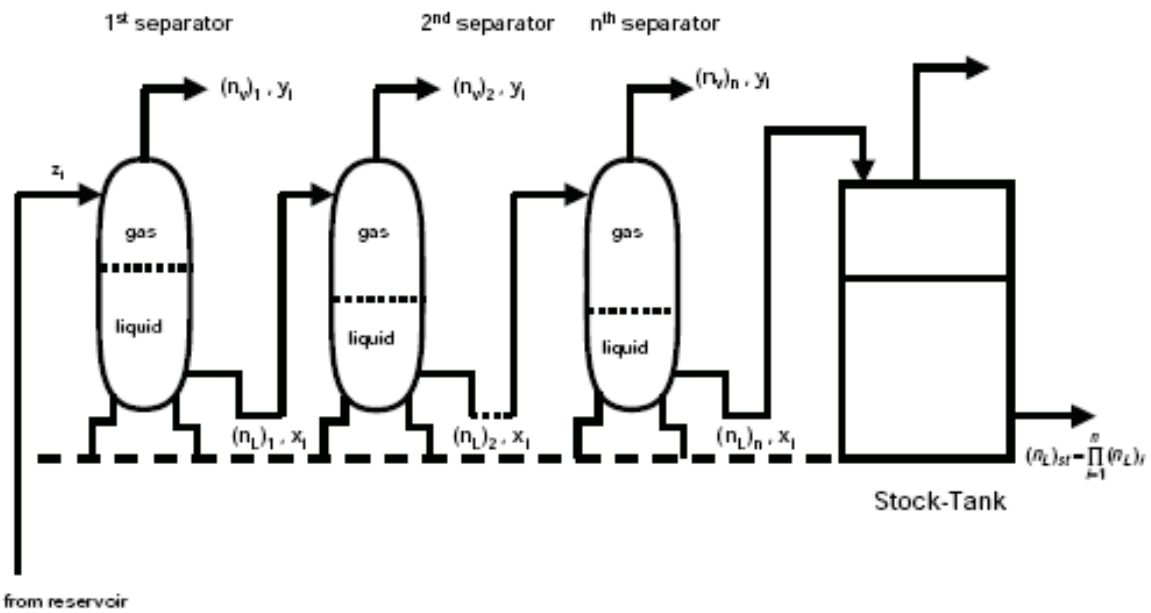


FIGURE 5-8 Schematic illustration of  $n$  separation stages.



PVTsim 16.0

File Edit View Fluid CharFluid Options Pure Component Utilities Window Help

Metric Units SRK Peneloux Standard Lumping Normal C7+ Char CSP Vec/Thermal cond

**Simulations Explorer**

- Database
  - Open Database
  - Create New Database
  - Import Fluids
  - Export Fluids
  - Duplicate Fluids
  - Delete Fluids
- Fluid
  - Select Fluid
  - New Plus Fluid
  - New No-Plus Fluid
  - New Char Fluid
  - New Hygro Fluid
  - New PRO/II Fluid
  - QC of Fluid
  - Plus Fluid Regression
  - Char Fluid Regression
  - Clean for Mud
  - Recombine
  - Mix
  - Weave
  - Same Pseudos
  - Delump
- CharFluid
  - Edit Current
  - Add to Database
  - Import
  - Create Current

**Fluid Management**


- Simulations
- Interfaces

**Output Explorer**

- Phase Envelope
- Property Generator
- ES-SAGD
- PVT Simulation
- Regression
- Wax
- Asphaltene
- Scale
- Hydrate
- DepoWax
- MMP
- Depth Gradient
- Cleaning for Mud
- QC
- Customized

**Plots**

- Spreadsheets



The splash screen features the PVTsim logo on the left, which includes a stylized drop icon. To the right of the logo, the text reads "VERSION 16 Copyright © 1988 - 2006 Calsep A/S". Below the logo is a photograph of an offshore oil rig at sea. At the bottom of the splash screen, the "calsep" logo is displayed.

VERSION 16 Copyright © 1988 - 2006 Calsep A/S

Revision 16.0.0  
FLEXim Version

Windows Genuine Advantage

**Your system may be at risk.**

This copy of Windows did not pass genuine Windows validation. Validation is required to receive many of the upgrades available from Microsoft. Click [here](#) to get help with this problem.

[Get Genuine Windows](#) | [More Details](#)

START

Presentation files pre... Microsoft PowerPoint... wordlin - Google Sear... untitled - Paint PVTsim 16.0

EN 4:23 PM

## **Fluid Management**

Simulations

Interfaces



**PVTsim 16.0**

File Edit View Fluid CharFluid Options Pure Component Utilities Window Help

Metric Units SRK ab Lumping Normal C7+ Char CSP Visc/Thermal cond

Current fluid: No fluid selected

### Simulations Explorer

- Database
  - Open Database
  - Create New Database
  - Import Fluids
  - Export Fluids
  - Duplicate Fluids
  - Delete Fluids
- Fluid
  - Select Fluid
  - New Plus Fluid
  - New No-Plus Fluid
  - New Char Fluid
  - New Hysys Fluid
  - New PRO/II Fluid
  - QC of Fluid
  - Plus Fluid Regression
  - Char Fluid Regression
  - Clean for Mud
  - Recombine
  - Mix
  - Weave
  - Same Pseudos
  - Delump
- CharFluid
  - Edit Current
  - Add to Database
  - Import
  - Export Current

**Fluid Management**

- Simulations
- Interfaces

### Output Explorer

- Flash
- Phase Envelope
- Property Generator
- H2S
- Unit Operations
- ES-SAGD
- Allocation
- PVT Simulation
- Regression
- Viscosity Tuning
- Wax
- Asphaltene
- Scale
- Hydrate
- DepoWax
- MMP
- Depth Gradient
- Cleaning for Mud

**Spreadsheets**

- Plots

Database: C:\Program Files\PVTsim 16\Demodata.fdb

start Microsoft PowerPoint ... PVTsim 16.0 Search Desktop 8:35 AM

Current fluid: No fluid selected

Simulations Explorer

- Flash & Unit Operations
    - Flash
    - Phase Envelope
    - Property Generator
    - H2S
    - Unit Operations
    - ES-SAGD
    - Allocation
  - Open Structure
    - Flash Open Structure
    - Hydrate Open Structure
  - PVT Simulations
    - Critical Point
    - Saturation Point
    - Separator Test
    - Const Mass Exp
    - Const Vol Depl
    - Diff Depletion
    - Viscosity
    - Swelling Test
    - Multiple Contact
  - Flow Assurance
    - Viscosity Tuning
    - Wax
    - Asphaltene
    - Scale
    - Hydrate
    - DepoWax
- Simulations**
- Interfaces
  - Fluid Management

Output Explorer

- Flash
  - Phase Envelope
  - Property Generator
  - H2S
  - Unit Operations
  - ES-SAGD
  - Allocation
  - PVT Simulation
  - Regression
  - Viscosity Tuning
  - Wax
  - Asphaltene
  - Scale
  - Hydrate
  - DepoWax
  - MMP
  - Depth Gradient
  - Cleaning for Mud
- Spreadsheets**
- Plots

Database: C:\Program Files\PVTsim 16\Demodata.fdb

**Simulations Explorer**

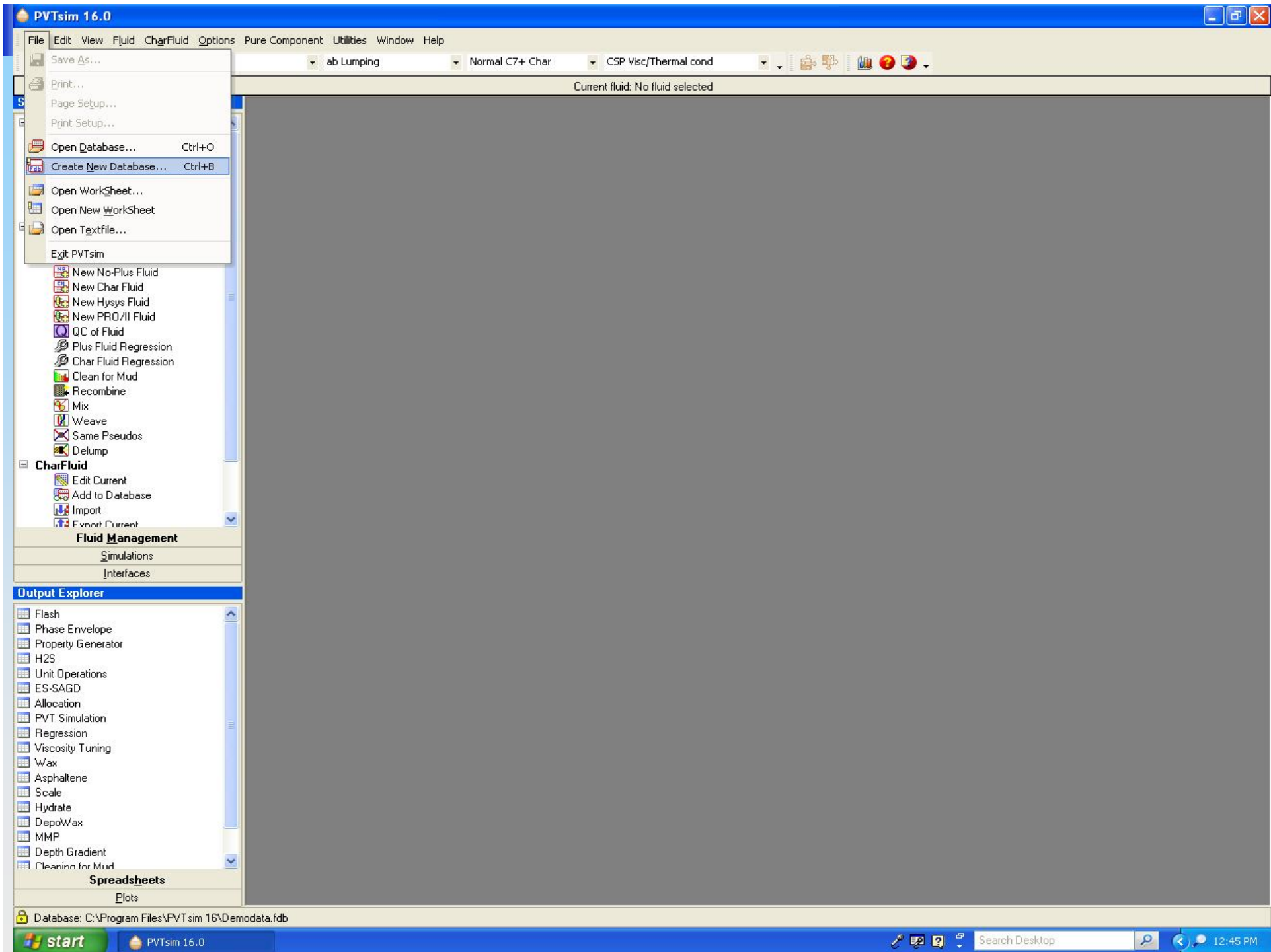
- Reservoir**
  - VIP Black Oil
  - VIP-COMP
  - MORE Black Oil
  - MORE EOS
  - Eclipse Black Oil
  - Eclipse Gi
  - Eclipse Comp
  - Eclipse Black Oil Corr
- Flow**
  - OLGA Compositional Tracking
  - OLGA
  - OLGA Wax
  - Pipesim
  - Multi Phase Meter
  - PipePhase
- Process**
  - PRO/II
  - Hysys
- Other**
  - Prosper-MBAL
  - Prosper-EDS
  - Saphir
  - WePs
  - Version 12 CHN-file format

- Interfaces**
- Fluid Management
  - Simulations

**Output Explorer**

- Flash
- Phase Envelope
- Property Generator
- H2S
- Unit Operations
- ES-SAGD
- Allocation
- PVT Simulation
- Regression
- Viscosity Tuning
- Wax
- Asphaltene
- Scale
- Hydrate
- DepoWax
- MMP
- Depth Gradient
- Cleaning for Mud

- Spreadsheets**
- Plots



PVTsim 16.0

File Edit View Fluid CharFluid Options Pure Component Utilities Window Help

Metric Units SRK ab Lumping Normal C7+ Char CSP Visc/Thermal cond

Current fluid: No fluid selected

### Create New Database

Save in: Desktop

- My Recent Documents
- Desktop
- My Documents
- My Computer
- My Network Places

- My Documents
- My Computer
- My Network Places
- Vahid
- 123.fdb
- fluid.fdb
- Shortcut to My Computer

File name:

Save as type: PVTsim fluid databases (\*.fdb)

Save Cancel

Add to Database  
Import  
Export Current

#### Fluid Management

- Simulations
- Interfaces

#### Output Explorer

- Flash
- Phase Envelope
- Property Generator
- H2S
- Unit Operations
- ES-SAGD
- Allocation
- PVT Simulation
- Regression
- Viscosity Tuning
- Wax
- Asphaltene
- Scale
- Hydrate
- DepoWax
- MMP
- Depth Gradient
- Cleaning for Mud

#### Spreadsheets

- Plots

Database: C:\Program Files\PVTsim 16\Demodata.fdb

start Mail :: Inbox (3) - Wi... PVTsim 16.0 Search Desktop 9:02 AM

**PVTsim 16.0**

File Edit View **Fluid** CharFluid Options Pure Component Utilities Window Help

Metric Units Database Ctrl+D ab Lumping Normal C7+ Char CSP Visc/Thermal cond

Enter New Fluid Ctrl+N

Current fluid: No fluid selected

**Simulations Expl**

- Database**
  - Open D
  - Create I
  - Import F
  - Export F
  - Duplica
  - Delete f
- Fluid**
  - Select F
  - New Pl
  - New Nc
  - New Cf
  - New Hy
  - New PF
  - QC of F
  - Plus Fluid Regression
  - Char Fluid Regression
  - Clean for Mud
  - Recombine
  - Mix
  - Weave
  - Same Pseudos
  - Delump
- CharFluid**
  - Edit Current
  - Add to Database
  - Import
  - Export Current

**Fluid Management**

- Simulations
- Interfaces

**Output Explorer**

- Flash
- Phase Envelope
- Property Generator
- H2S
- Unit Operations
- ES-SAGD
- Allocation
- PVT Simulation
- Regression
- Viscosity Tuning
- Wax
- Asphaltene
- Scale
- Hydrate
- DepoWax
- MMP
- Depth Gradient
- Cleaning for Mud

**Spreadsheets**

- Plots

Database: C:\Program Files\PVTsim 16\Demodata.fdb

start PVTsim 16.0 untitled - Paint Microsoft PowerPoint ... Search Desktop 12:46 PM



Current fluid: TEST 3B HEAVY COND + SALTWATER

**Simulations Explorer**

- Reservoir**
  - VIP Black Oil
  - VIP-COMP
  - MORE Black Oil
  - MORE EOS
  - Eclipse Black Oil
  - Eclipse Gi
  - Eclipse Comp
  - Eclipse Black Oil Corr
- Flow**
  - OLGA Compositional Tracking
  - OLGA
  - OLGA Wax
  - Pipesim
  - Multi Phase Meter
  - PipePhase
- Process**
  - PRO/II
  - Hysys
- Other**
  - Prosper-MBAL
  - Prosper-EDS
  - Saphir
  - WePs
  - Version 12 CHN-file format

**Interfaces**

- Fluid Management
- Simulations

**Output Explorer**

- Flash
- Phase Envelope
- Property Generator
- H2S
- Unit Operations
- ES-SAGD
- Allocation
- PVT Simulation
- Regression
- Viscosity Tuning
- Wax
- Asphaltene
- Scale
- Hydrate
- DepoWax
- MMP
- Depth Gradient
- Cleaning for Mud

**Spreadsheets**

- Plots

**Enter New Fluid**

Fluid

Well:  Test:  Fluid:

Sample:  Text:

History:

Composition

Component	Mol %	Mol wt	Liquid Density g/cm <sup>3</sup>
N2		28.014	
CO2		44.010	
H2S		34.080	
C1		16.043	
C2		30.070	
C3		44.097	
iC4		58.124	
nC4		58.124	
iC5		72.151	
nC5		72.151	
C6		86.178	0.6640
C7		96.000	0.7380
C8		107.000	0.7650
C9		121.000	0.7810
Total %	0.000		

Input composition in:

- Mol%
- Weight%

Input wsg fraction

Options:

- Save Char Fluid
- Adjust to Sat point

Fluid type:

- Plus fraction
- No-Plus fraction
- Characterized

Buttons: OK, Cancel, Print, Char Options, Interact Param, PVT Data, Visc Data

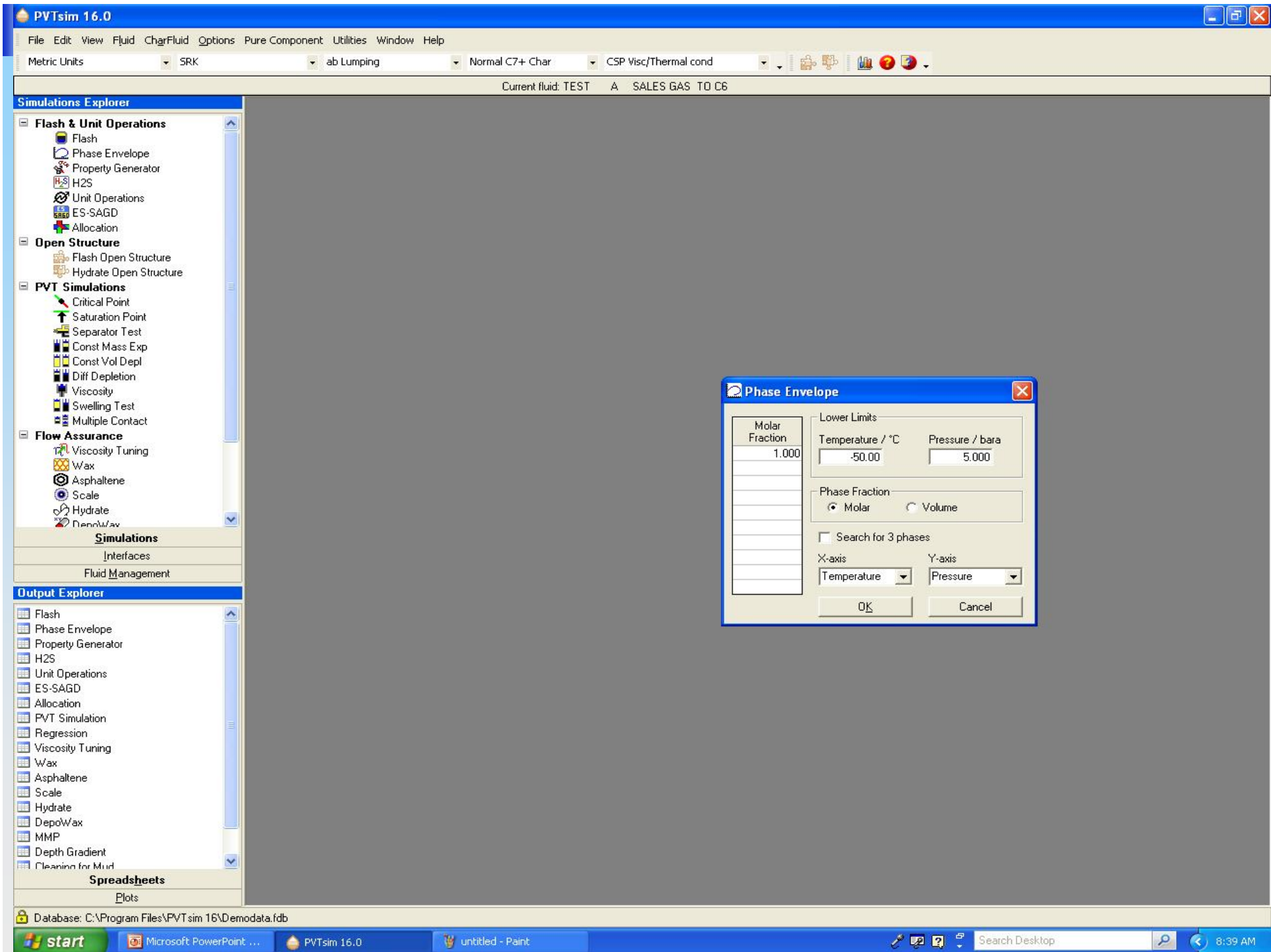
Buttons: Normalize, Clear, Add Comps, Mol to Weight, Complete

**Simulations**

Interfaces

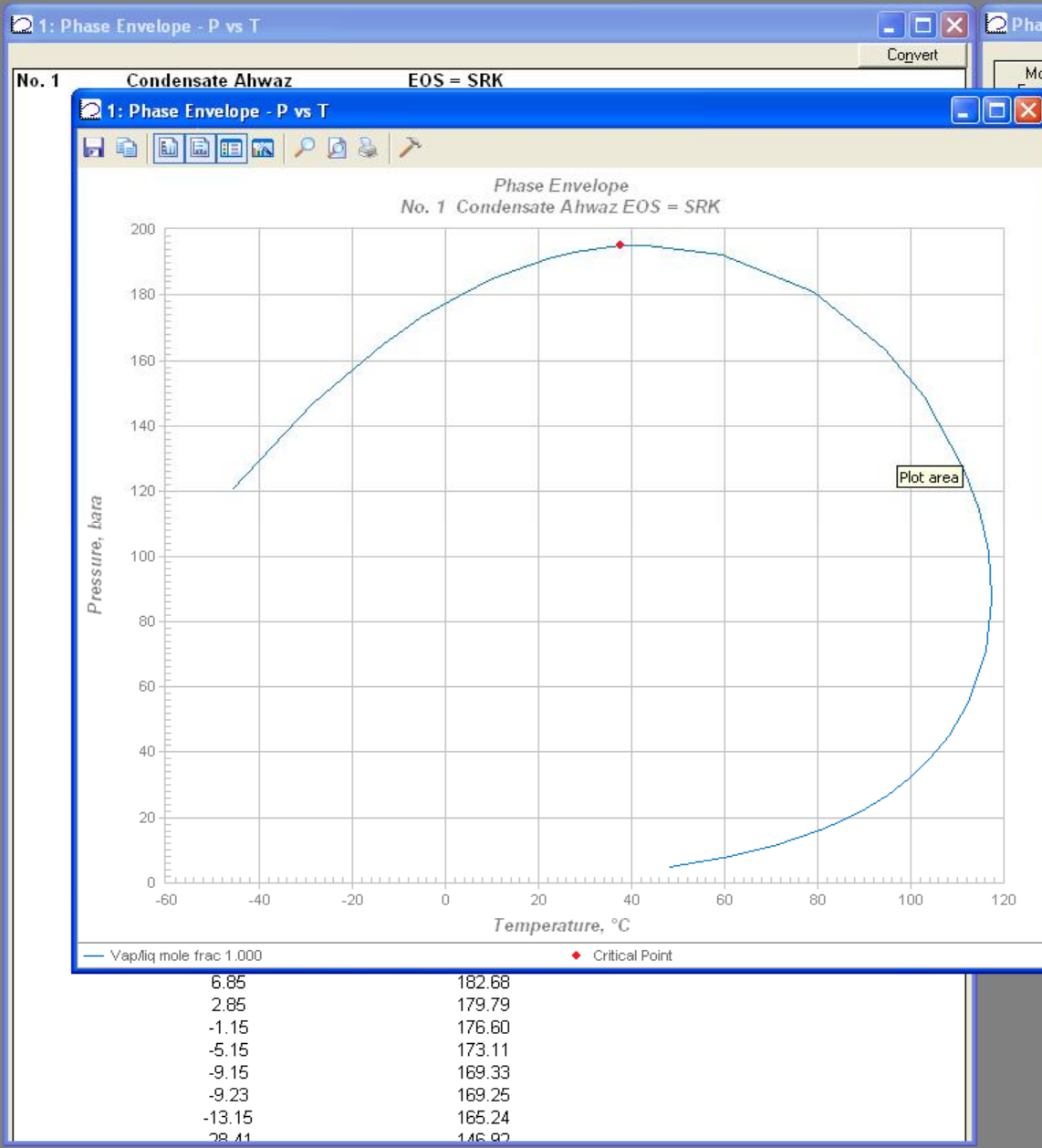
Fluid Management





- Simulations Explorer**
- Flash & Unit Operations
    - Flash
    - Phase Envelope
    - Property Generator
    - H2S
    - Unit Operations
    - ES-SAGD
    - Allocation
  - Open Structure
    - Flash Open Structure
    - Hydrate Open Structure
  - PVT Simulations
    - Critical Point
    - Saturation Point
    - Separator Test
    - Const Mass Exp
    - Const Vol Depl
    - Diff Depletion
    - Viscosity
    - Swelling Test
    - Multiple Contact
  - Flow Assurance
    - Viscosity Tuning
    - Wax
    - Asphaltene
    - Scale
    - Hydrate
    - DepoWax
- Simulations**
- Interfaces
  - Fluid Management

- Output Explorer**
- Flash
  - Phase Envelope (1)
    - 1: Phase Envelope - P vs T
  - Property Generator
  - H2S
  - Unit Operations
  - ES-SAGD
  - Allocation
  - PVT Simulation
  - Regression
  - Viscosity Tuning
  - Wax
  - Asphaltene
  - Scale
  - Hydrate
  - DepoWax
  - MMP
  - Depth Gradient
- Spreadsheets**
- Plots



**Phase Envelope**

Convert

Molar Fraction: 1.000

Lower Limits

Temperature / °C: -50.00

Pressure / bara: 5.000

Phase Fraction

Molar  Volume

Search for 3 phases

X-axis: Temperature

Y-axis: Pressure

OK Cancel

**Simulations Explorer**

- Flash & Unit Operations
  - Flash
  - Phase Envelope
  - Property Generator
  - H2S
  - Unit Operations
  - ES-SAGD
  - Allocation
- Open Structure
  - Flash Open Structure
  - Hydrate Open Structure
- PVT Simulations
  - Critical Point
  - Saturation Point
  - Separator Test
  - Const Mass Exp
  - Const Vol Depl
  - Diff Depletion
  - Viscosity
  - Swelling Test
  - Multiple Contact
- Flow Assurance
  - Viscosity Tuning
  - Wax
  - Asphaltene
  - Scale
  - Hydrate
  - DepoWax
- Simulations
  - Interfaces
  - Fluid Management

**Output Explorer**

- Flash
- Phase Envelope (1)
  - 1: Phase Envelope - P vs T
- Property Generator
- H2S
- Unit Operations
- ES-SAGD
- Allocation
- PVT Simulation
- Regression
- Viscosity Tuning
- Wax
- Asphaltene
- Scale
- Hydrate
- DepoWax
- MMP
- Depth Gradient

**Spreadsheets**

- Plots

**1: Phase Envelope - P vs T**

No. 1 Condensate Ahwaz EOS = SRK

Convert

Phase Envelope (mole)  
Vap/liq frac = 1.000

Temperature/°C	Pressure/bara
48.17	5.00
53.07	6.04
56.53	6.86
61.18	8.14
65.92	9.66
70.73	11.46
75.60	13.60
80.50	16.14
85.40	19.15
90.27	22.73
95.06	26.97
99.70	32.01
104.13	37.98
108.21	45.07
112.47	55.35
116.15	70.83
117.37	86.27
117.38	87.73
116.69	101.01
114.60	114.59
111.57	126.77
102.90	148.99
94.41	163.50
79.08	180.82
59.27	192.48
43.21	195.23
42.97	195.23
37.65	194.95
27.55	192.90
26.85	192.69
22.85	191.28
18.85	189.58
14.85	187.58
10.85	185.28
9.84	184.65
6.85	182.68
2.85	179.79
-1.15	176.60
-5.15	173.11
-9.15	169.33
-9.23	169.25
-13.15	165.24
-28.41	146.00

**Phase Envelope**

Lower Limits

Temperature / °C: -50.00 Pressure / bara: 5.000

Molar Fraction: 1.000

Phase Fraction:  Molar  Volume

Search for 3 phases

X-axis: Temperature Y-axis: Pressure

OK Cancel

**Simulations Explorer**

- Flash & Unit Operations
  - Flash
  - Phase Envelope
  - Property Generator
  - H2S
  - Unit Operations
  - ES-SAGD
  - Allocation
- Open Structure
  - Flash Open Structure
  - Hydrate Open Structure
- PVT Simulations
  - Critical Point
  - Saturation Point
  - Separator Test
  - Const Mass Exp
  - Const Vol Depl
  - Diff Depletion
  - Viscosity
  - Swelling Test
  - Multiple Contact
- Flow Assurance
  - Viscosity Tuning
  - Wax
  - Asphaltene
  - Scale
  - Hydrate
  - DepoWax

**Simulations**

- Interfaces
- Fluid Management

**Output Explorer**

- Flash
- Phase Envelope
- Property Generator
- H2S
- Unit Operations
- ES-SAGD
- Allocation
- PVT Simulation
- Regression
- Viscosity Tuning
- Wax
- Asphaltene
- Scale
- Hydrate
- DepoWax
- MMP
- Depth Gradient
- Cleaning for Mud

**Spreadsheets**

- Plots

**Flash**

P (bara)	T (°C)

PT non-aqueous     PH  
 PT aqueous     PS  
 PT multi phase     VT  
 K-factor     UV  
 Split-factor     HS  
 P-Beta  
 T-Beta

OK Clear Cancel





Simulations Explorer

- Flash & Unit Operations
  - Flash
  - Phase Envelope
  - Property Generator
  - H2S
  - Unit Operations
  - ES-SAGD
  - Allocation
- Open Structure
  - Flash Open Structure
  - Hydrate Open Structure
- PVT Simulations
  - Critical Point
  - Saturation Point
  - Separator Test
  - Const Mass Exp
  - Const Vol Depl
  - Diff Depletion
  - Viscosity
  - Swelling Test
  - Multiple Contact
- Flow Assurance
  - Viscosity Tuning
  - Wax
  - Asphaltene
  - Scale
  - Hydrate
  - DepoWax

- SRK
- SRK Peneloux
- SRK Peneloux (T)
- PR
- PR Peneloux
- PR Peneloux (T)
- PR78
- PR78 Peneloux

Simulations

- Interfaces
- Fluid Management

Output Explorer

- Flash
- Phase Envelope
- Property Generator
- H2S
- Unit Operations
- ES-SAGD
- Allocation
- PVT Simulation
- Regression
- Viscosity Tuning
- Wax
- Asphaltene
- Scale
- Hydrate
- DepoWax
- MMP
- Depth Gradient
- Cleaning for Mud

Spreadsheets

- Plots

## **Interfaces**

Fluid Management

Simulations

Metric Units SRK ab Lumping Normal C7+ Char CSP Visc/Thermal cond  
 Current fluid: No. 1 Condensate Ahwaz

**Simulations Explorer**

- Reservoir
  - VIP Black Oil
  - VIP-COMP
  - MORE Black Oil
  - MORE EOS
  - Eclipse Black Oil
  - Eclipse Gi
  - Eclipse Comp
  - Eclipse Black Oil Corr
- Flow
  - OLGA Compositional Tracking
  - OLGA
  - OLGA Wax
  - Pipesim
  - Multi Phase Meter
  - PipePhase
- Process
  - PRO/II
  - Hysys
- Other
  - Prosper-MBAL
  - Prosper-EOS
  - Saphir
  - WePs
  - Version 12 CHN-file format

**Interfaces**

- Fluid Management
- Simulations

**Output Explorer**

- Flash
- Phase Envelope
- Property Generator
- H2S
- Unit Operations
- ES-SAGD
- Allocation
- PVT Simulation
- Regression
- Viscosity Tuning
- Wax
- Asphaltene
- Scale
- Hydrate
- DepoWax
- MMP
- Depth Gradient
- Cleaning for Mud

**Spreadsheets**

- Plots

**PVT tables to OLGA**

Fluid selection  
 Current Fluid  Fluid 2  Fluid 3  Fluid 4  Fluid 5  Fluid 6  Fluid 7  Fluid 8  Fluid 9  Fluid 10

Current Fluid

Water specification

Amount  %water cut

Composition

H2O		mole%
NaCl		
KCl		
NaBr		
CaCl2		
HCOONa		
Total	0.000	

Clear Normalize

Pressure and temperature

	Pressure/bara	Temperature/°C
Min	1.00	-20.00
Max	120.00	100.00
No of Points	50	50

Alternative P&T

Emulsion  IntelliGrid Grid Factor

Inhibitor specification

Amount  mol inhib/mol spec water

Composition

MeOH		mole%
EtOH		
PG		
PGME		
MEG		
DEG		
Total	0.000	

Clear Normalize

Experimental emulsion viscosity

Pal & Rhodes  Wat vol frac.  Rel visc.  Inv. point

Output table

Two phase  Three Phase

Extrapolation method

Derivatives  Compositional

Water properties

EOS  Water Package

Composition No. 1 Condensate Ahwaz

Save Fluid Fluid Label  Clear

Output File  Table format  Key  Fixed  Bold artificial properties

OK Cancel

Database: C:\Documents and Settings\Collin\Desktop\fluid.fdb

start how to remove a mail... PVTsim 16.0 Flexible License Mana... Microsoft PowerPoint ... Search Desktop 5:13 PM



PVTsim 16.0

File Edit View Fluid CharFluid Options Pure Component Utilities Window Help

Metric Units SRK ab Lumping Normal C7+ Char CSP Visc/Thermal cond

Current fluid: No. 1 Condensate Ahwaz

**Simulations Explorer**

- Reservoir
  - VIP Black Oil
  - VIP-COMP
  - MORE Black Oil
  - MORE EOS
  - Eclipse Black Oil
  - Eclipse Gi
  - Eclipse Comp
  - Eclipse Black Oil Corr
- Flow
  - OLGA Compositional Tracking
  - OLGA
  - OLGA Wax
  - Pipesim
  - Multi Phase Meter
  - PipePhase
- Process
  - PRO/II
  - Hysys
- Other
  - Prosper-MBAL
  - Prosper-EDS
  - Saphir
  - WePs
  - Version 12 CHN-file format

**Interfaces**

- Fluid Management
- Simulations

**Output Explorer**

- Flash
- Phase Envelope
- Property Generator
- H2S
- Unit Operations
- ES-SAGD
- Allocation
- PVT Simulation
- Regression
- Viscosity Tuning
- Wax
- Asphaltene
- Scale
- Hydrate
- DepoWax
- MMP
- Depth Gradient
- Cleaning for Mud

**Spreadsheets**

- Plots

Database: C:\Documents and Settings\Collin\Desktop\fluid.fdb

**PVT tables to OLGA**

Fluid selection: Current Fluid

Current Fluid: No. 1 Condensate Ahwaz OLGA

Water specific Amount Composition

Inhibitor spec Amount Composition

Total: 0.000

Normalize

Compositional

Water Package

Composition: No. 1 Condensate Ahwaz

Save Fluid:  Fluid Label: GasCond

Output File: C:\Documents and Settings\Collin\Desktop\GasCon.tab

Table format:  Key  Fixed

Bold artificial properties

OK Cancel

```

PVTTABLE LABEL = "GasCond", PHASE = TWO, \
!'ENTROPY ' No. 1 Condensate Ahwaz OLGA
interface
EOS = "SRK", \
COMPONENTS =
("N2", "CO2", "H2S", "C1", "C2", "C3", "nC4", "iC5", "nC5", "C6")
, \
MOLES = (.500000E+01, .600000E+01, .100000E+01, .700000E+
02, .200000E+01, .300000E+01, .500000E+00, .100000E+
01, .150000E+01, .100000E+02), \
MOLWEIGHT = (.280135E+02, .440098E+02, .340800E+
02, .160429E+02, .300698E+02, .440968E+02, .581237E+
02, .721506E+02, .721506E+02, .861780E+02) g/mol, \
DENSITY = (.000000E+00, .000000E+00, .000000E+00, .000000E+
00, .000000E+00, .000000E+00, .000000E+00, .000000E+
00, .000000E+00, .664000E+00) g/cm3, \
STDPRESSURE = .100000E+01 ATM, \
STDTEMPERATURE = .288150E+03 K, \
GOR = -.999000E+03 Sm3/Sm3, \
GLR = -.999000E+03 Sm3/Sm3, \
STDGASEDENSITY = .120133E+01 kg/m3, \
STDOILDENSITY = .000000E+00 kg/m3, \
  
```

Temperature/°C: -20.00  
Pressure: 100.00  
Density: 50

Fluid Factor: 1  
Inv. point: 0.7000

Current fluid: No fluid selected

Simulations Explorer

**Database**

- Open Database
- Create New Database
- Import Fluids
- Export Fluids
- Duplicate Fluids
- Delete Fluids

**Fluid**

- Select Fluid
- New Plus Fluid
- New No-Plus Fluid
- New Char Fluid
- New Hysys Fluid
- New PRO/II Fluid
- QC of Fluid
- Plus Fluid Regression
- Char Fluid Regression
- Clean for Mud
- Recombine
- Mix
- Weave
- Same Pseudos
- Delump

**CharFluid**

- Edit Current
- Add to Database
- Import
- Export Current

**Fluid Management**

- Simulations
- Interfaces

**Database**

No	Well	Test	Fluid	Sample	Text	Type
1	TEST1	DST1	GAS COND	RECOMBINED TO C10+	TEST LAB	Plus
2	TEST1	DST1	GAS COND	RECOMBINED TO C20+	PVT LAB	Plus
3	SEP GAS	PT1	SEPGAS	BOTTLE A#16000	PVT LAB	No-Plus
4	SEP LIQ	PPT1	SEP LIQUID	BOTTLE #K6000	PVT LAB	Plus
5	TEST 4	BHS	OIL	C10+	OIL LAB	Plus
6	TEST 4	BHS	OIL+H2S	C20+	OIL LAB	Plus
7	TEST	A	OIL	DIFF LIB DATA	DIFF LAB	Plus
8	TEST	B	CONDENSATE	CVD DATA	CVD LAB	Plus
9	TEST	G	1	NATURAL GAS 90.4 MOL% C1	GAS LAB	No-Plus
10	TEST	A	SALES GAS	TO C6	GAS LAB	No-Plus
11	TEST	3B	HEAVY COND	HEAVILY LUMPED	TBP LAB	Plus
12	TEST	3C	HEAVY COND	GC COMP TO C20+	GC LAB	Plus
13	TEST	3B	HEAVY COND	+ SALTWATER	TBP LAB EDS= SRK	Char
14	TEST	3B	HEAVY COND	HEAVILY LUMPED	TBP LAB EDS= SRK	Char
15	TEST	F&U	CO2	100% PURE	RESEARCH LAB	No-Plus
16	# 1	DST1	COND	3162.5 m	SPE 14410	Plus
17	# 2	DST 3	HEAVY COND	3179.5 m	REFERENCE, SPE 14410	Plus
18	# 2	DST 2	VOL OIL	3204.5 m	SPE 14410	Plus
19	# 2	DST 2	OIL	3241 m	SPE 14410	Plus
20	OIL	V	CONTAM	13.7% OF STO	MUD LAB	Plus
21	OIL C36+	V	CONTAM	EST MUD	MUD LAB	Plus
22	CHEMICAL	1	ULTRAMUD	BASE OIL	MUD LAB	No-Plus

History Last Modified Select Import Delete Duplicate Export Close

Output Explorer

- Flash
- Phase Envelope
- Property Generator
- H2S
- Unit Operations
- ES-SAGD
- Allocation
- PVT Simulation
- Regression
- Viscosity Tuning
- Wax
- Asphaltene
- Scale
- Hydrate
- DepoWax
- MMP
- Depth Gradient
- Cleaning for Mud

**Spreadsheets**

- Plots

Database: C:\Program Files\PVT sim 16\Demodata.fdb

PVTsim 16.0

File Edit View Fluid CharFluid Options Pure Component Utilities Window Help

Metric Units SRK ab Lumping Normal C7+ Char CSP Visc/Thermal cond

Current fluid: No fluid selected

### Simulations Explorer

- Database
  - Open Database
  - Create New Database
  - Import Fluids
  - Export Fluids
  - Duplicate Fluids
  - Delete Fluids
- Fluid
  - Select Fluid
  - New Plus Fluid
  - New No-Plus Fluid
  - New Char Fluid
  - New Hysys Fluid
  - New PRD/II Fluid
  - QC of Fluid
  - Plus Fluid Regression
  - Char Fluid Regression
  - Clean for Mud
  - Recombine
  - Mix
  - Weave
  - Same Pseudos
  - Delump
- CharFluid
  - Edit Current
  - Add to Database
  - Import
  - Export Current

### Fluid Management

- Simulations
- Interfaces

### Output Explorer

- Flash
- Phase Envelope
- Property Generator
- H2S
- Unit Operations
- ES-SAGD
- Allocation
- PVT Simulation
- Regression
- Viscosity Tuning
- Wax
- Asphaltene
- Scale
- Hydrate
- DepoWax
- MMP
- Depth Gradient
- Cleaning for Mud

### Spreadsheets

- Plots

### Selected Fluid

Fluid

Well: TEST Test: 3B Fluid: HEAVY COND

Sample: HEAVILY LUMPED Text: TBP LAB

History: Component parameters updated to PVT sim 16.

Composition

Component	Mol %	Mol wt	Liquid Density g/cm <sup>3</sup>
H2O	1.000	18.015	0.9990
NaCl	1.000	58.443	2.1650
N2	0.340	28.014	
CO2	3.587	44.010	
C1	67.368	16.043	
C2	9.013	30.070	
C3	4.307	44.097	
iC4	0.929	58.124	
nC4	1.709	58.124	
iC5	0.739	72.151	
nC5	0.849	72.151	
C6	1.129	86.178	0.6640
C7	1.749	90.570	0.7380
C8	1.689	104.480	0.7540
Total %	102.001		

Input composition in:  Mol%  Weight%

Input wax fraction

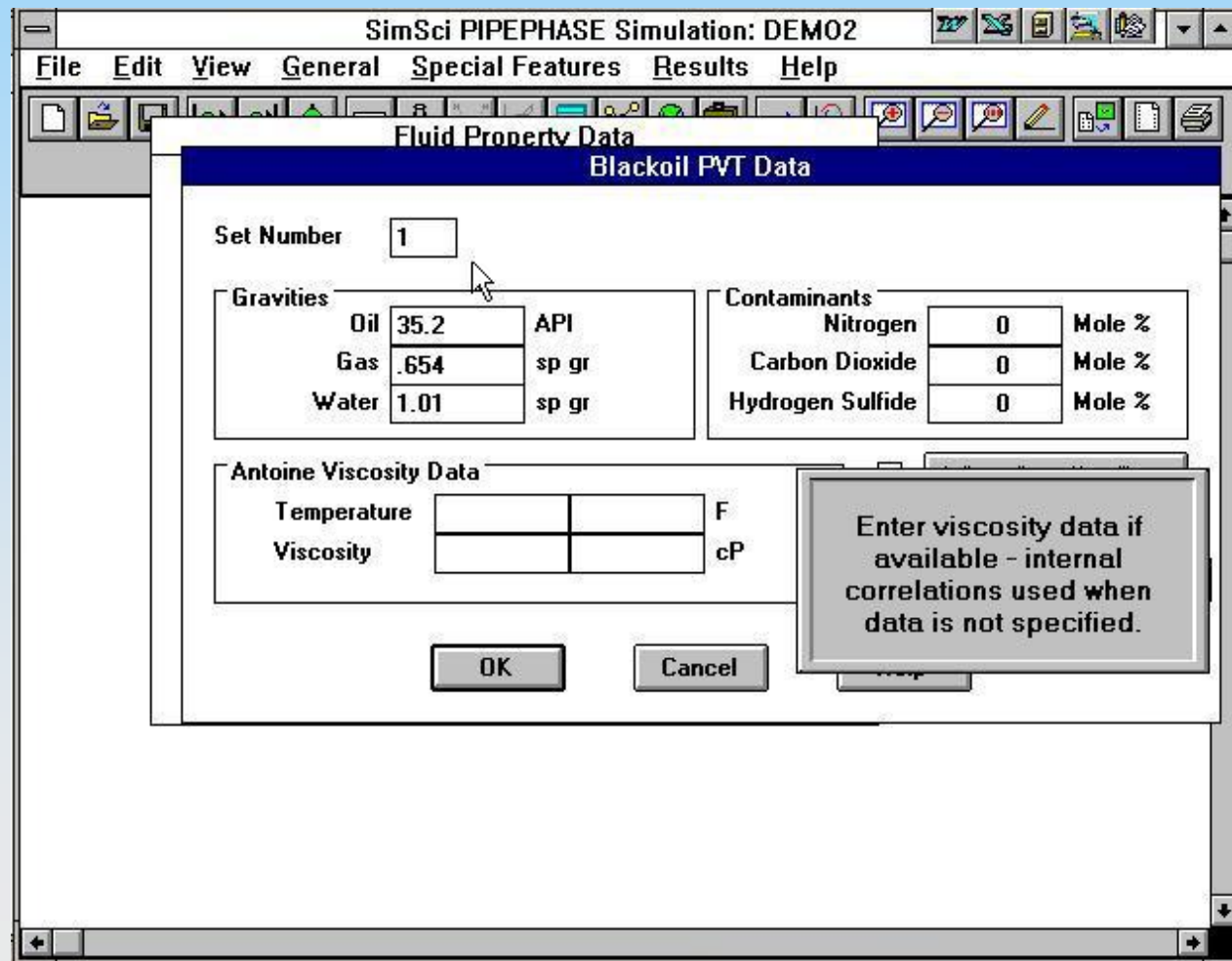
Options:  Save Char Fluid  Adjust to Sat point

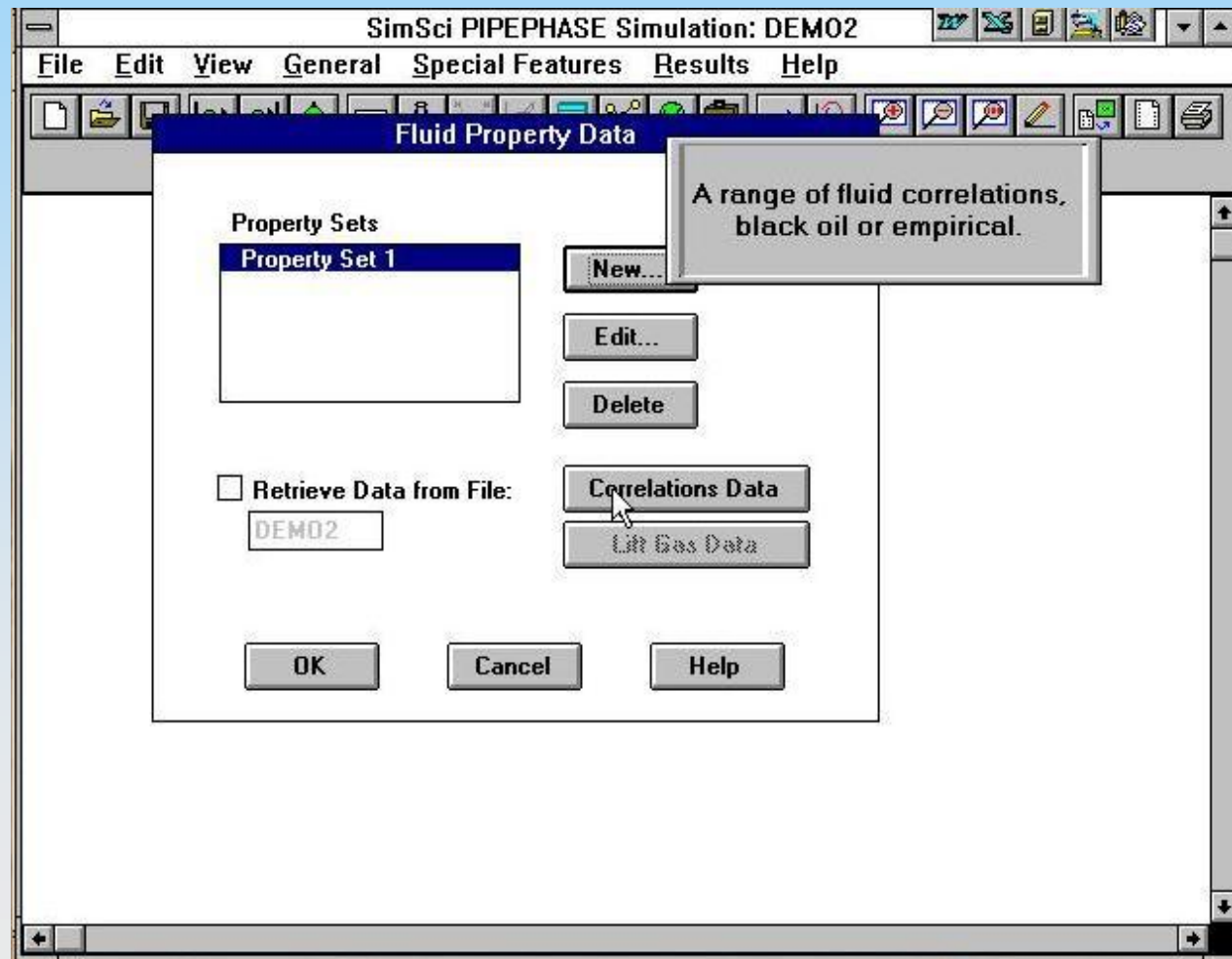
Fluid type:  Plus fraction  No-Plus fraction  Characterized

Buttons: OK, Cancel, Print, Char Options, Interact Param, PVT Data, Visc Data

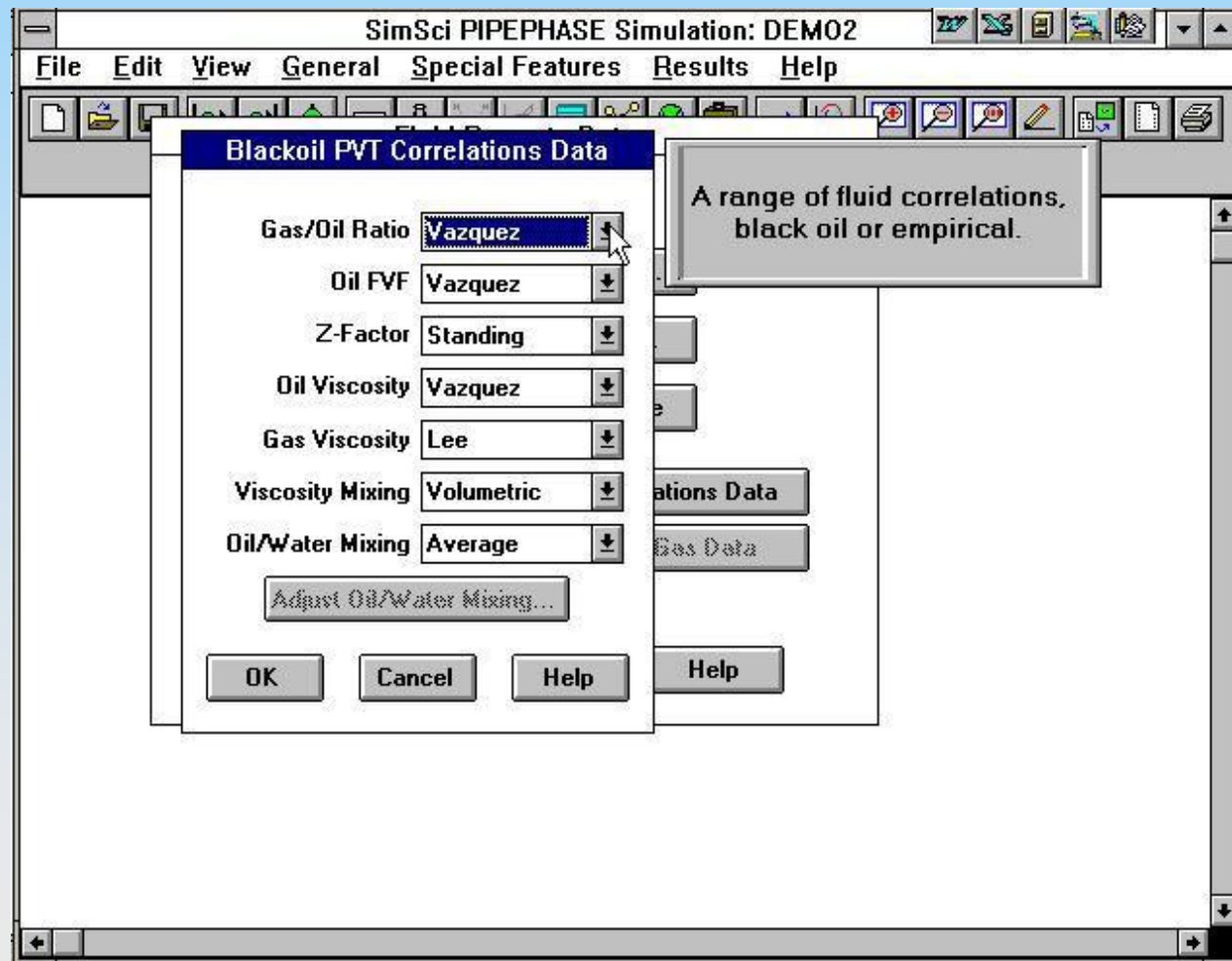
Buttons: Normalize, Clear, Add Comps, Mol to Weight, Complete

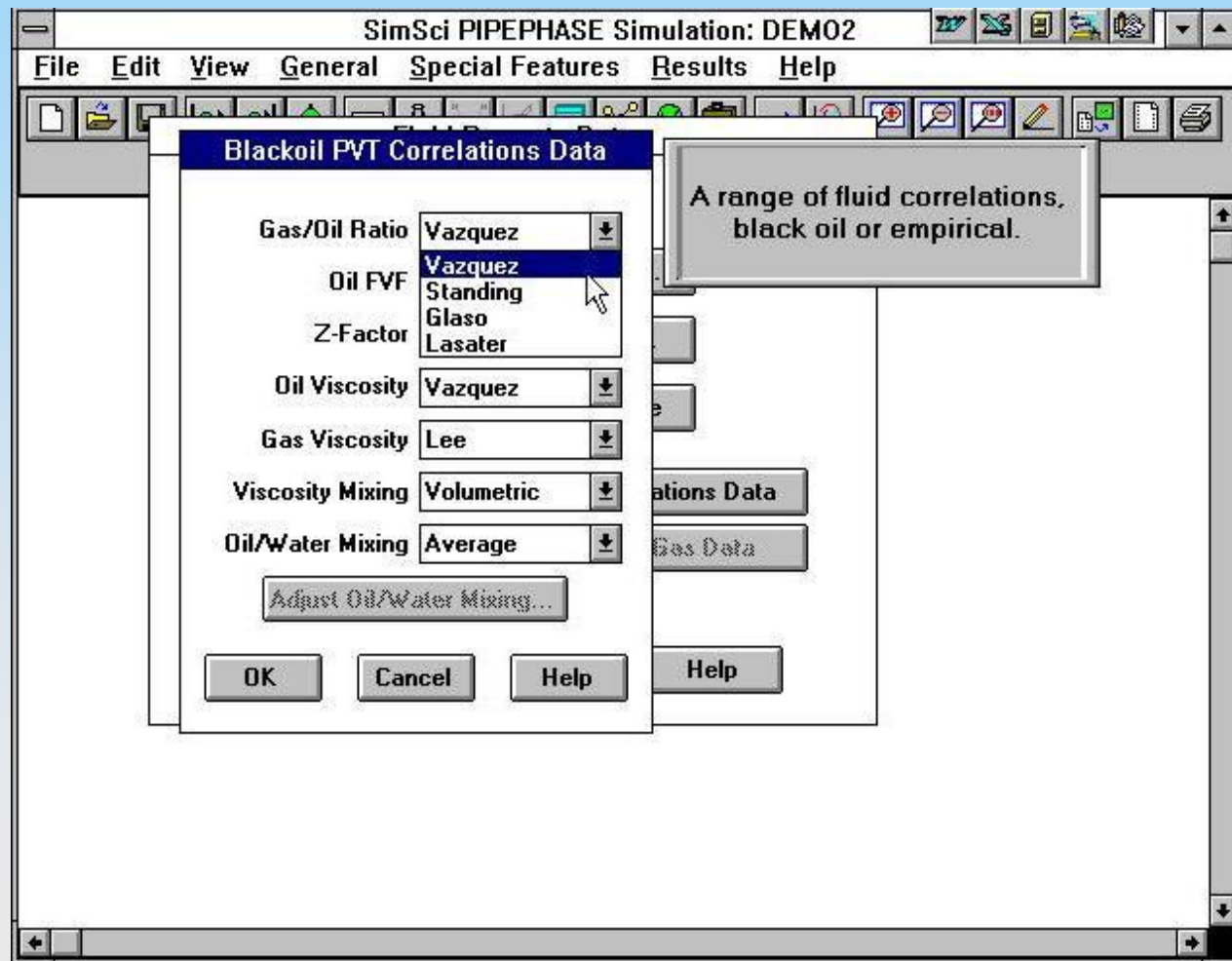
Sessions 3 and 4:  
(black oil and compositional models for  
Gas/liquid mixtures )













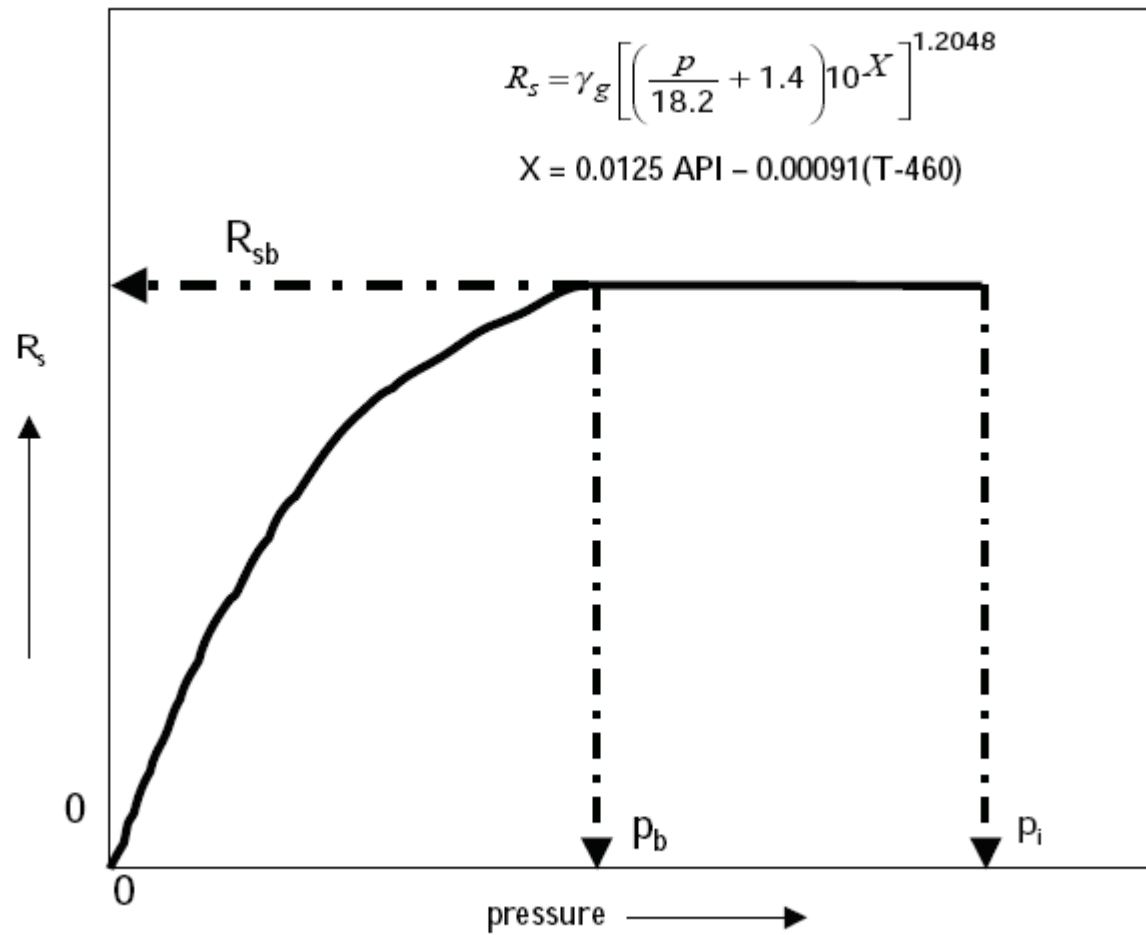


FIGURE 4-6 Typical gas solubility/pressure relationship.

## Standing's correlation

$$R_s = \gamma_g \left[ \left( \frac{p}{18.2} + 1.4 \right) 10^x \right]^{1.2048}$$

with

$$x = 0.0125\text{API} - 0.00091(T - 460)$$

where:

$R_s$  = gas solubility, scf/STB

$T$  = temperature, °R

$p$  = system pressure, psia

$\gamma_g$  = solution gas specific gravity

API = oil gravity, °API

# Vasquez-Begg's correlation

$$R_s = C_1 \gamma_{gs} p^{C_2} \exp \left[ C_3 \left( \frac{\text{API}}{T} \right) \right]$$

Values for the coefficients are as follows:

COEFFICIENTS	API ≤ 30	API > 30
C <sub>1</sub>	0.362	0.0178
C <sub>2</sub>	1.0937	1.1870
C <sub>3</sub>	25.7240	23.931

$$\gamma_{gs} = \gamma_g \left[ 1 + 5.912(10^{-5})(\text{API})(T_{\text{sep}} - 460) \log \left( \frac{p_{\text{sep}}}{114.7} \right) \right]$$

where

$\gamma_{gs}$  = gas gravity at the reference separator pressure

$\gamma_g$  = gas gravity at the actual separator conditions of  $p_{\text{sep}}$  and  $T_{\text{sep}}$

$p_{\text{sep}}$  = actual separator pressure, psia

$T_{\text{sep}}$  = actual separator temperature, °R

### *Glaser's Correlation*

Glaser (1980) proposed a correlation for estimating the gas solubility as a function of the API gravity, the pressure, the temperature, and the gas specific gravity. The correlation was developed from studying 45 North Sea crude oil samples. Glaser reported an average error of 1.28% with a standard deviation of 6.98%. The proposed relationship has the following form:

$$R_s = \gamma_g \left\{ \left[ \frac{\text{API}^{0.989}}{(T - 460)^{0.172}} \right] (A) \right\}^{1.2255} \quad (4-26)$$

The parameter  $A$  is a pressure-dependent coefficient defined by the following expression:

$$A = 10^X$$

with the exponent  $X$  as given by

$$X = 2.8869 - [14.1811 - 3.3093 \log(p)]^{0.5}$$

**EXAMPLE 4-10**

Rework Example 4-8 and solve for the gas solubility using Glaso's correlation.

**SOLUTION**

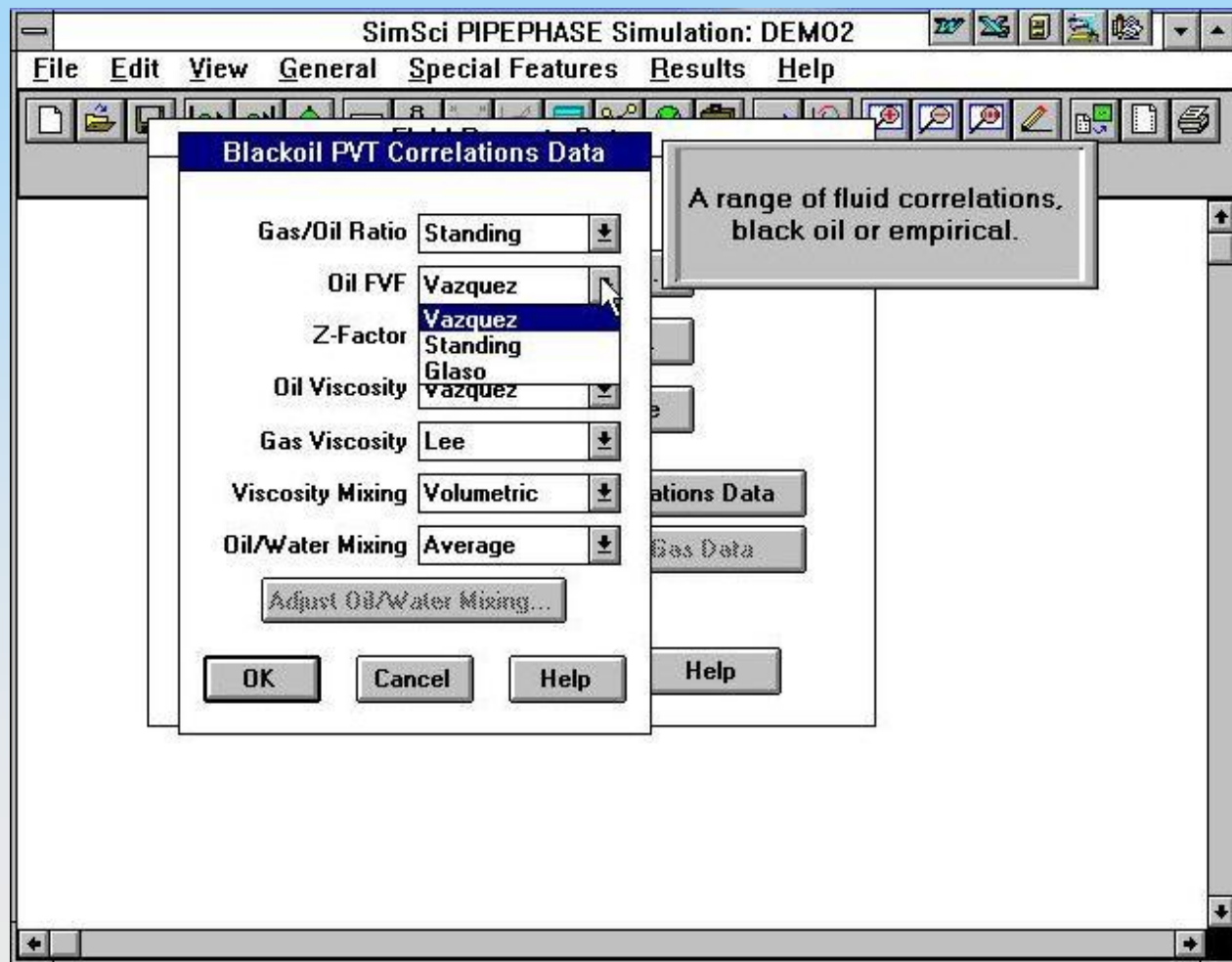
The results are shown in the table below.

Oil	$p$	$X$	$A$	Predicted $R_s$ , Equation (4-26)	Measured $R_s$	% Error
1	2377	1.155	14.286	737	751	-1.84
2	2620	1.196	15.687	714	768	-6.92
3	2051	1.095	12.450	686	693	-0.90
4	5884	1.237	17.243	843	968	-12.92
5	3045	1.260	18.210	868	943	-7.94
6	4239	1.413	25.883	842	807	4.34
					AAE	5.8%

$$X = 2.8869 - [14.1811 - 3.3093 \log(p)]^{0.5}$$

$$A = 10^X$$

$$R_s = \gamma_g \left[ \left( \frac{\text{API}^{0.989}}{(T-460)^{0.172}} \right) (A) \right]^{1.2255}$$



The oil formation volume factor,  $B_o$ , is defined as the ratio of the volume of oil (plus the gas in solution) at the prevailing reservoir temperature and pressure to the volume of oil at standard conditions. Evidently,  $B_o$  always is greater than or equal to unity. The oil formation volume factor can be expressed mathematically as

$$B_o = \frac{(V_o)_{p,T}}{(V_o)_{sc}} \quad (4-37)$$

where

$B_o$  = oil formation volume factor, bbl/STB

$(V_o)_{p,T}$  = volume of oil under reservoir pressure,  $p$ , and temperature,  $i$ , bbl

$(V_o)_{sc}$  = volume of oil is measured under standard conditions, STB

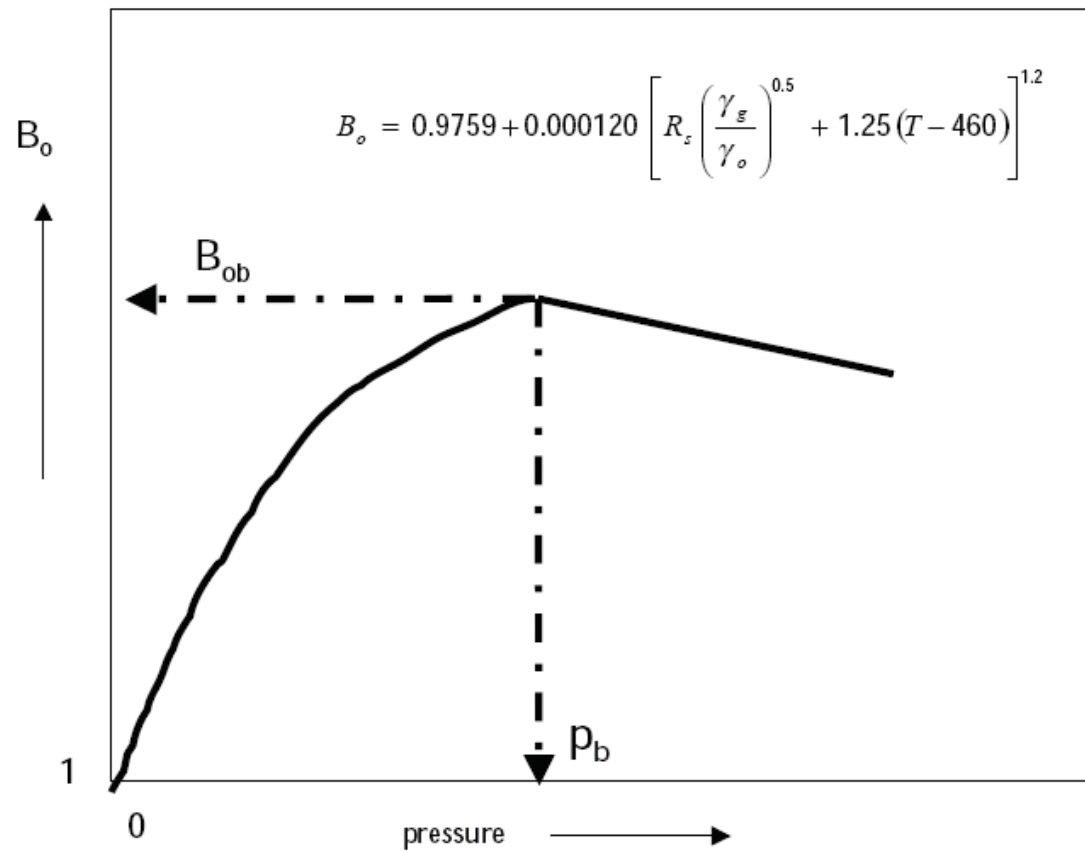


FIGURE 4-7 Typical oil formation volume factor/pressure relationship.

$$B_o = f(R_s, \gamma_g, \gamma_o, T)$$



### *Standing's Correlation*

Standing (1947) presented a graphical correlation for estimating the oil formation volume factor with the gas solubility, gas gravity, oil gravity, and reservoir temperature as the correlating parameters. This graphical correlation originated from examining 105 experimental data points on 22 California hydrocarbon systems. An average error of 1.2% was reported for the correlation.

Standing (1981) showed that the oil formation volume factor can be expressed more conveniently in a mathematical form by the following equation:

$$B_o = 0.9759 + 0.000120 \left[ R_s \left( \frac{\gamma_g}{\gamma_o} \right)^{0.5} + 1.25(T - 460) \right]^{1.2} \quad (4-38)$$

$T$  = temperature, °R

$\gamma_o$  = specific gravity of the stock-tank oil, 60°/60°

$\gamma_g$  = specific gravity of the solution gas

### *Vasquez and Beggs's Correlation*

Vasquez and Beggs (1980) developed a relationship for determining  $B_o$  as a function of  $R_s$ ,  $\gamma_o$ ,  $\gamma_g$ , and  $T$ . The proposed correlation was based on 6000 measurements of  $B_o$  at various pressures. Using the regression analysis technique, Vasquez and Beggs found the following equation to be the best form to reproduce the measured data:

$$B_o = 1.0 + C_1 R_s + (T - 520) \left( \frac{\text{API}}{\gamma_{gs}} \right) [C_2 + C_3 R_s] \quad (4-39)$$

where

$R$  = gas solubility, scf/STB

$T$  = temperature, °R

$\gamma_{gs}$  = gas specific gravity as defined by equation 4-25:

$$\gamma_{gs} = \gamma_g \left[ 1 + 5.912(10^{-5})(\text{API})(T_{\text{sep}} - 460) \log \left( \frac{P_{\text{sep}}}{114.7} \right) \right]$$

Values for the coefficients  $C_1$ ,  $C_2$ , and  $C_3$  of equation (4-39) follow:

COEFFICIENT	API ≤ 30	API > 30
$C_1$	$4.677 \times 10^{-4}$	$4.670 \times 10^{-4}$
$C_2$	$1.751 \times 10^{-5}$	$1.100 \times 10^{-5}$
$C_3$	$-1.811 \times 10^{-8}$	$1.337 \times 10^{-9}$

Vasquez and Beggs reported an average error of 4.7% for the proposed correlation.

### *Glaser's Correlation*

Glaser (1980) proposed the following expressions for calculating the oil formation volume factor:

$$B_o = 1.0 + 10^A \quad (4-40)$$

where

$$A = -6.58511 + 2.91329 \log B_{ob}^* - 0.27683(\log B_{ob}^*)^2 \quad (4-41)$$

$B_{ob}^*$  is a "correlating number," defined by the following equation:

$$B_{ob}^* = R_s \left( \frac{\gamma_g}{\gamma_o} \right)^{0.526} + 0.968(T - 460) \quad (4-42)$$

where  $T$  = temperature, °R, and  $\gamma_o$  = specific gravity of the stock-tank oil, 60°/60°. These correlations were originated from studying PVT data on 45 oil samples. The average error of the correlation was reported at -0.43% with a standard deviation of 2.18%.

# Real Gas Z-Factor Standing-Katz Chart/correlation

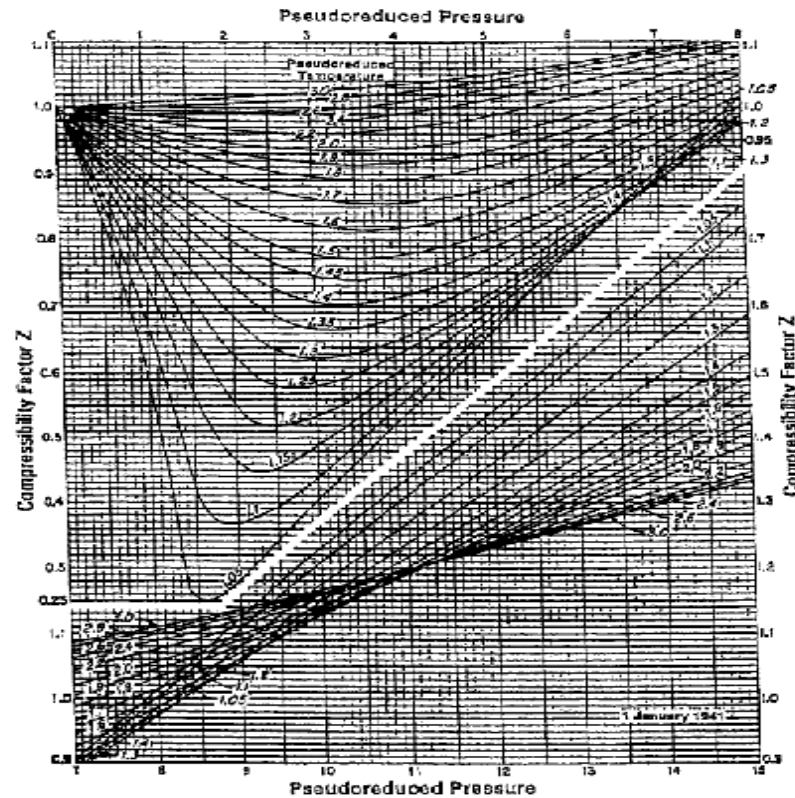
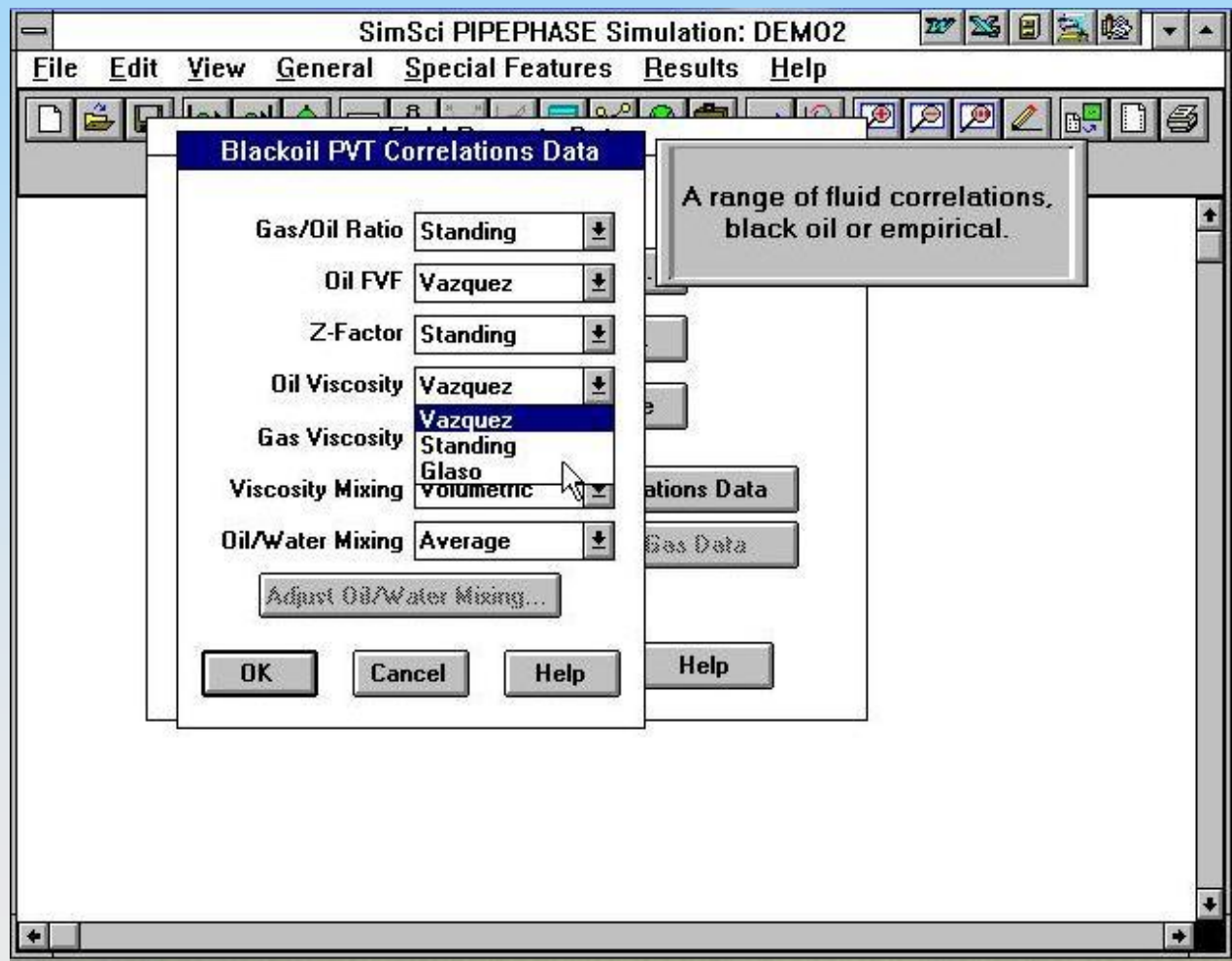


FIGURE 3-1 Standing and Katz pseudoreduced compressibility factors chart.  
 Source: *GPSSA Engineering Data Book*, 10th ed., Tulsa, OK: Gas Processors Suppliers Association, 1987. Courtesy of the Gas Processors Suppliers Association.

$$Z = 1 - \frac{3.53 p_{pr}}{10^{0.9813 T_{pr}}} + \frac{0.274 p_{pr}^2}{10^{0.8157 T_{pr}}}$$

For example, at  $p_{pr} = 3$  and  $T_{pr} = 2$ , the  $Z$ -factor from the preceding equation is

$$Z = 1 - \frac{3.53 p_{pr}}{10^{0.9813 T_{pr}}} + \frac{0.274 p_{pr}^2}{10^{0.8157 T_{pr}}} = 1 - \frac{3.53(3)}{10^{0.9813(2)}} + \frac{0.274(3)^2}{10^{0.8157(2)}} = 0.9422$$



- *Dead oil viscosity*,  $\mu_{od}$ . The dead oil viscosity (oil with no gas in the solution) is defined as the viscosity of crude oil at *atmospheric pressure* and system temperature,  $T$ .
- *Saturated oil viscosity*,  $\mu_{ob}$ . The saturated (bubble-point) oil viscosity is defined as the viscosity of the crude oil at any pressure less than or equal to the bubble-point pressure.
- *Undersaturated oil viscosity*,  $\mu_o$ . The undersaturated oil viscosity is defined as the viscosity of the crude oil at a pressure above the bubble-point and reservoir temperature.

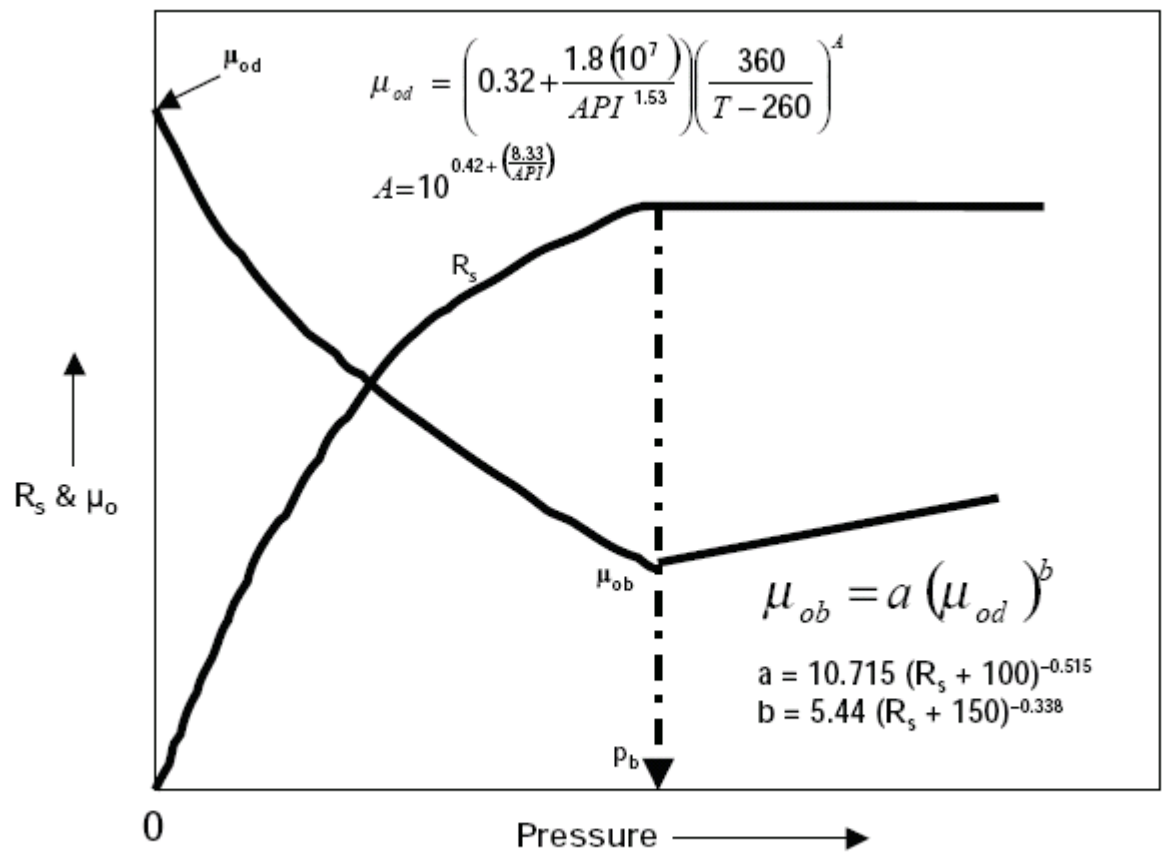


FIGURE 4-14 Crude oil viscosity as a function of  $R_s$  and  $p$ .



Based on these three categories, predicting the oil's viscosity follows a similar three-step procedure.

*Step 1* Calculate the dead oil viscosity,  $\mu_{od}$ , at the specified reservoir temperature and atmospheric pressure without dissolved gas:  $R_s = 0$ .

*Step 2* Adjust the dead oil viscosity to any specified reservoir pressure ( $p \leq p_b$ ) according to the gas solubility at  $p$ .

*Step 3* For pressures above the bubble-point pressure, a further adjustment is made to  $\mu_{ob}$  to account for the compression of the oil above  $p_b$ .

### *Glaser's Correlation*

Glaser (1980) proposed a generalized mathematical relationship for computing the dead oil viscosity. The relationship was developed from experimental measurements on 26 crude oil samples. The correlation has the following form:

$$\mu_{od} = [3.141(10^{10})](T - 460)^{-3.444} [\log(\text{API})]^A \quad (4-78)$$

The temperature  $T$  is expressed in °R and the coefficient  $A$  is given by

$$A = 10.313[\log(T - 460)] - 36.447$$

This expression can be used within the range of 50–300°F for the system temperature and 20–48° for the API gravity of the crude. Sutton and Farashad (1984) concluded that Glaser's correlation showed the best accuracy of the three previous correlations.

### *Beggs-Robinson Correlation*

From 2073 saturated oil viscosity measurements, Beggs and Robinson (1975) proposed an empirical correlation for estimating the saturated oil viscosity. The proposed mathematical expression has the following form:

$$\mu_{ob} = a(\mu_{od})^b \quad (4-80)$$

where:

$$a = 10.715(R_s + 100)^{-0.515}$$

$$b = 5.44(R_s + 150)^{-0.338}$$

The reported accuracy of the correlation is  $-1.83\%$  with a standard deviation of  $27.25\%$ . The ranges of the data used to develop Beggs and Robinson's equation are

*Pressure:* 132–5265 psia

*Temperature:* 70–295°F

*API gravity:* 16–58

*Gas solubility:* 20–2070 scf/STB

### *Vasquez-Beggs's Correlation*

Vasquez and Beggs proposed a simple mathematical expression for estimating the viscosity of the oil above the bubble-point pressure. From 3593 data points, Vasquez and Beggs (1980) proposed the following expression for estimating the viscosity of undersaturated crude oil:

$$\mu_o = \mu_{ob} \left( \frac{p}{p_b} \right)^m \quad (4-83)$$

where

$$m = 2.6p^{1.187}10^{-4}$$

$$A = -3.9(10^{-5})p - 5$$

The data used in developing the above correlation have the following ranges:

*Pressure:* 141–9151 psia

*Gas solubility:* 9.3–2199 scf/STB

*Viscosity:* 0.117–148 cp

*Gas gravity:* 0.511–1.351

*API gravity:* 15.3–59.5

The average error of the viscosity correlation is reported as –7.54%.

**3.2.3 Volumetric Flow Rates.** After mass transfer calculations are completed, it is possible to calculate the in-situ volumetric flow rates of each phase. For the black-oil model, volumetric flow rates are determined from

$$q_o = q_{o_{sc}} B_o, \dots\dots\dots (3.1)$$

$$q_w = q_{w_{sc}} B_w, \dots\dots\dots (3.2)$$

and

$$q_g = \left( q_{g_{sc}} - q_{o_{sc}} R_s - q_{w_{sc}} R_{sw} \right) B_g, \dots\dots\dots (3.3)$$

where  $B_g$  is derived from the engineering equation of state to be

$$B_g = p_{sc} ZT / pZ_{sc} T_{sc} . \dots\dots\dots (3.4)$$

**3.2.3 Volumetric Flow Rates.** After mass transfer calculations are completed, it is possible to calculate the in-situ volumetric flow rates of each phase. For the black-oil model, volumetric flow rates are determined from

$$q_o = q_{o_{sc}} B_o, \dots\dots\dots (3.1)$$

$$q_w = q_{w_{sc}} B_w, \dots\dots\dots (3.2)$$

and

$$q_g = (q_{g_{sc}} - q_{o_{sc}} R_s - q_{w_{sc}} R_{sw}) B_g, \dots\dots\dots (3.3)$$

where  $B_g$  is derived from the engineering equation of state to be

$$B_g = p_{sc} ZT / pZ_{sc} T_{sc} \dots\dots\dots (3.4)$$

Appendix B gives methods to predict gas compressibility,  $Z$ .

For the compositional model, volumetric flow rates are calculated from

$$q_L = \frac{w_l(1 - x_g)}{\rho_L} \dots\dots\dots (3.5)$$

and

$$q_g = w_l x_g / \rho_g, \dots\dots\dots (3.6)$$

where  $x_g$  is the no-slip quality or gas mass fraction and is obtained from the results of a VLE calculation as follows,

$$x_g = \frac{VM_g}{VM_g + LM_L} \dots\dots\dots (3.7)$$

**Example 3.2—Superficial Velocities: Black-Oil Model.** An oil well is flowing 10,000 STBO/D with a producing gas/oil ratio of 1,000 scf/STBO or a gas-production rate of 10 MMscf/D. At a location in the tubing where the pressure and temperature are 1,700 psia and 180°F, calculate the in-situ volumetric flow rates and superficial velocities of the liquid and gas phases. Also calculate the mixture velocity and the no-slip liquid holdup. The following is known from the pressure/volume/temperature (PVT) example problem given in Appendix B.

$$\begin{aligned} B_o &= 1.197 \text{ bbl/STBO} \\ B_g &= 0.0091 \text{ ft}^3/\text{scf} \\ R_s &= 281 \text{ scf/STBO} \\ d &= 6.0 \text{ in.} \end{aligned}$$

$$A_p = \frac{\pi}{4} d^2 = \frac{\pi}{4} \left( \frac{6}{12} \right)^2 = 0.196 \text{ ft}^2.$$

With Eq. 3.1,

$$\begin{aligned} q_o &= \frac{(10,000 \text{ STBO/D})(1.197 \text{ bbl/STBO})(5.614 \text{ ft}^3/\text{bbl})}{86,400 \text{ sec/D}} \\ &= 0.778 \text{ ft}^3/\text{sec.} \end{aligned}$$

With Eq. 3.10,

$$v_{SL} = \frac{q_L}{A_p} = \frac{0.778}{0.196} = 3.97 \text{ ft/sec.}$$

With Eq. 3.3,

$$q_g = \frac{[10 \times 10^6 - (10,000)(281)](0.0091)}{86,400} = 0.757 \text{ ft}^3/\text{sec.}$$

With Eq. 3.11,

$$v_{Sg} = q_g/A_p = 0.757/0.196 = 3.86 \text{ ft/sec.}$$

With Eq. 3.12,

$$v_m = v_{SL} + v_{Sg} = 3.97 + 3.86 = 7.83 \text{ ft/sec.}$$

With Eq. 3.8,

$$\lambda_L = \frac{q_L}{q_L + q_g} = \frac{0.778}{0.778 + 0.757} = 0.507.$$

**Example 3.1—Compositional-Model Flow Rates.** A gas-condensate well is flowing at a rate of 500,000 lbm/D. At a given location in the pipe, a VLE calculation is performed on the gas composition, yielding

$$L = 0.05 \left( \frac{\text{mole liquid}}{\text{mole feed}} \right) \quad V = 0.95 \left( \frac{\text{mole vapor}}{\text{mole feed}} \right),$$

$$M_L = 100 \left( \frac{\text{lbm}}{\text{mole liquid}} \right) \quad M_{gV} = 20 \left( \frac{\text{lbm}}{\text{mole vapor}} \right),$$

and

$$\rho_L = 50 \text{ lbm/ft}^3 \quad \rho_g = 5.0 \text{ lbm/ft}^3.$$

From Eq. 3.7,

$$\begin{aligned} x_g &= \frac{(0.95)(20.0)}{(0.95)(20.0) + (0.05)(100.0)} \\ &= 0.792 \text{ lbm vapor/lbm mixture.} \end{aligned}$$

With Eq. 3.5,

$$q_L = \frac{(500,000)(1 - 0.792)}{(86,400)(50)} = 0.024 \text{ ft}^3/\text{sec.}$$

With Eq. 3.6,

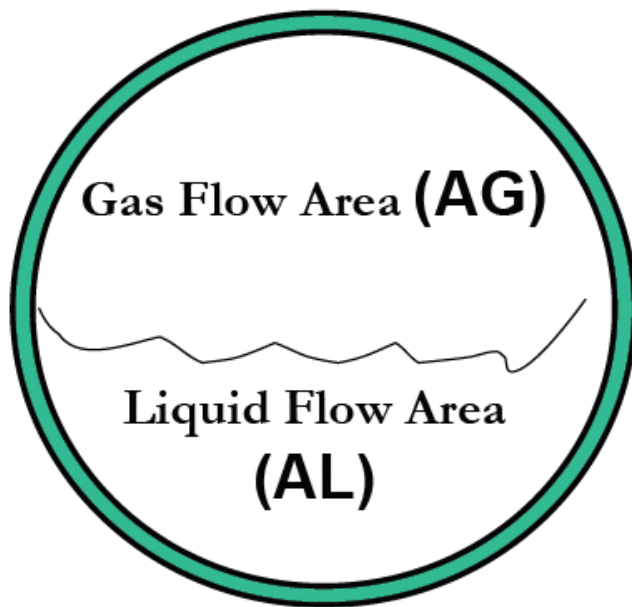
$$q_g = \frac{(500,000)(0.792)}{(86,400)(5.0)} = 0.917 \text{ ft}^3/\text{sec.}$$



Session 5 and 6:  
Basic concepts of two phase flow

- **Liquid Holdup is the local liquid volume fraction**
  - Gas fraction is the local gas volume fraction

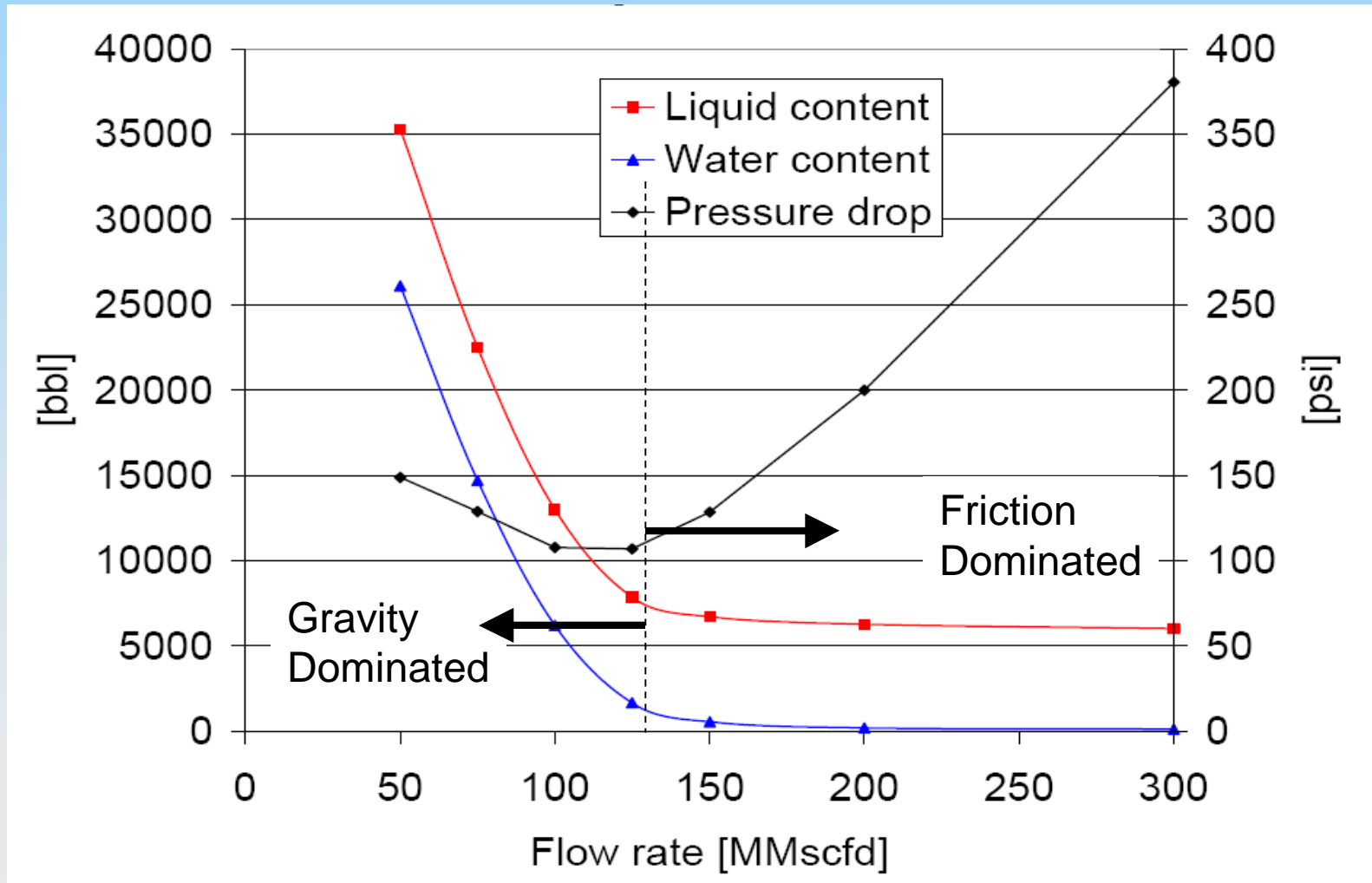
### **Pipe cross section with stratified flow**



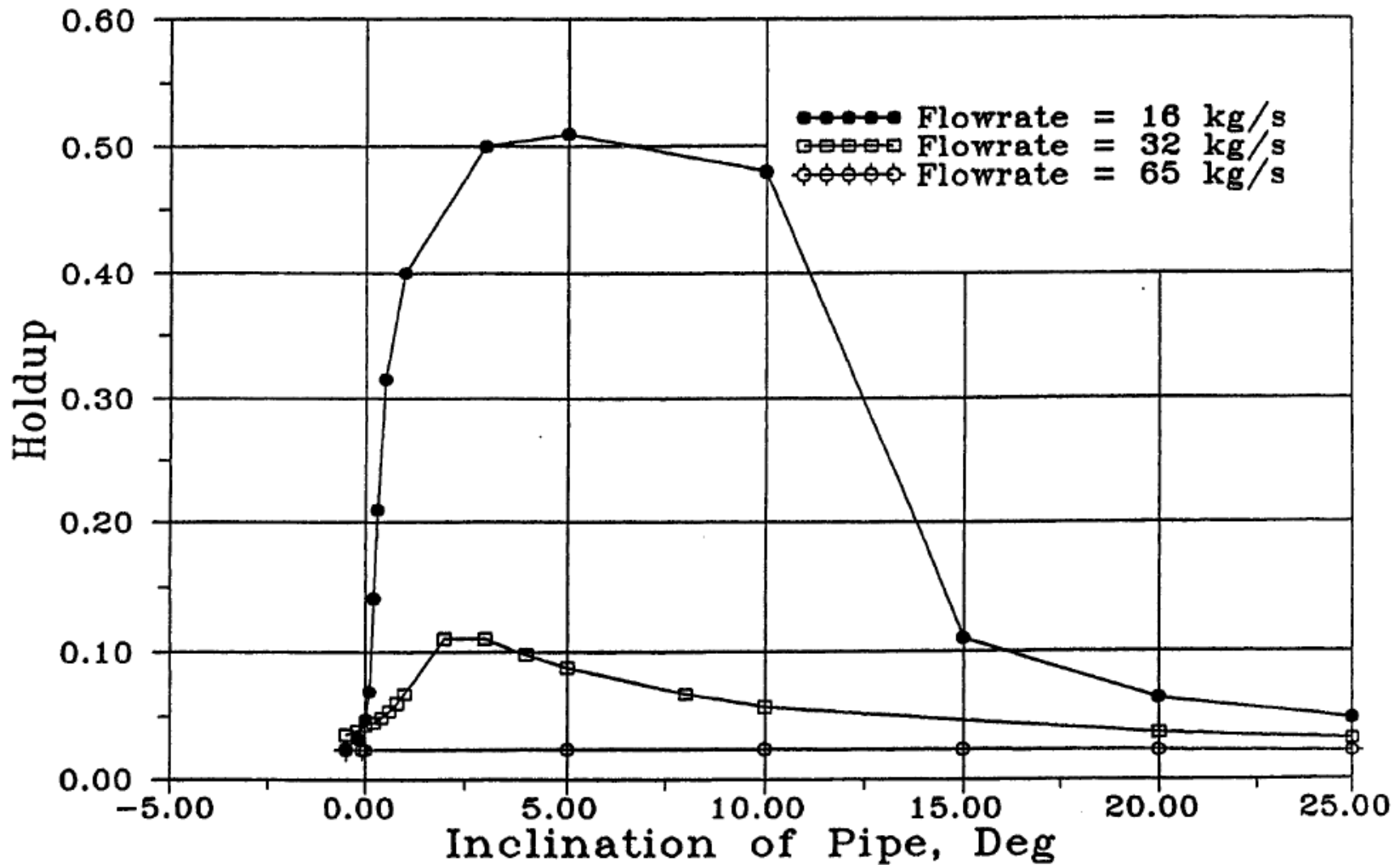
$$\text{Liquid holdup} = \frac{AL}{AG + AL}$$

$$\text{Liquid holdup} + \text{Gas fraction} = 1$$

# At Low Flow Rates Liquid Accumulates in the Flowline Increasing the Pressure Drop



## Liquid Holdup Depends on Flowline Geometry and Flowrate

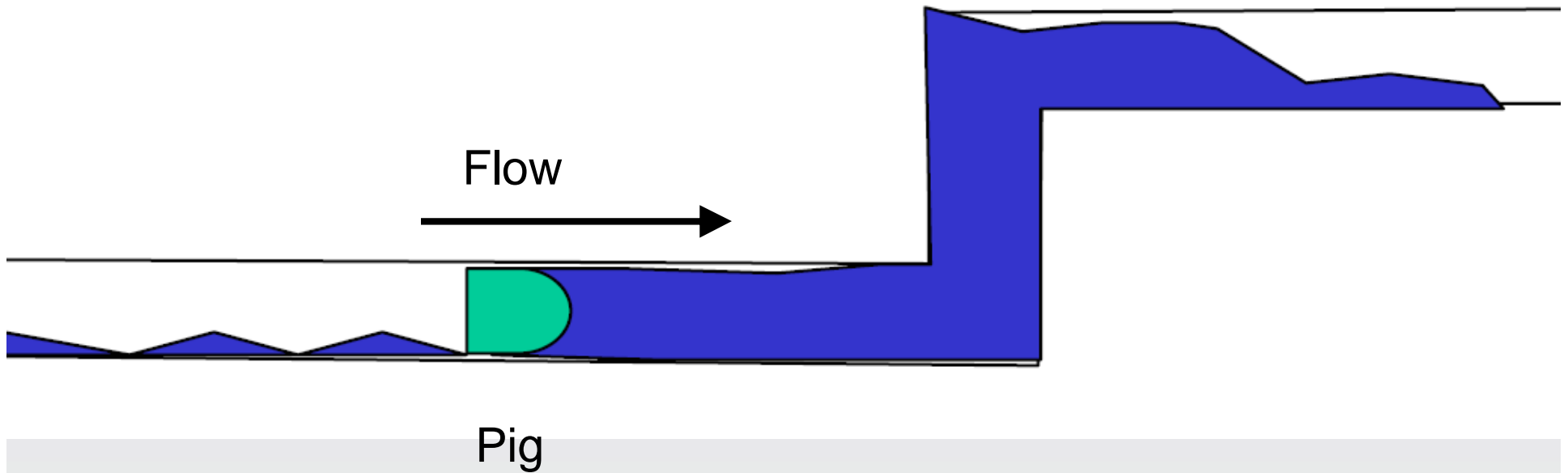


## Liquid Holdup Can Lead to Liquid Slugging

- There are two types of slugging:
  - Hydrodynamic: Induced by the holdup and superficial velocities
  - Terrain: Induced by geometry changes in which liquid can accumulate
- In Real Flowlines, Hydrodynamic and Terrain Slugs Can Interact:
  - Difficult to predict slug length and frequency
- Slugging can lead to surges of liquid that can overwhelm slugcatchers
- Liquid holdup leads to increased pressure drops and reduced flow
- Pigs can be used to periodically remove liquid from the flowline

## Pigging

- Gas lines in particular are periodically pigged to remove accumulated liquid
- The large liquid slug is caught in a large separator called a “Slug Catcher”



## Types of Pigs

- Spheres:
  - Easy to handle.
  - Can be re-inflated to compensate for wear.
  - Negotiate irregular bends.
  - Little energy for movement < 2psi.
- Foam Pigs:
  - Inexpensive and versatile.
  - Can be fitted with brushes to remove deposits.
- Steel Pigs:
  - Durable with replaceable sealing elements.
  - Can also be equipped with brushes and blades.
- Solid-Cast Pigs:
  - Light in weight, allow for longer and more efficient sealing.







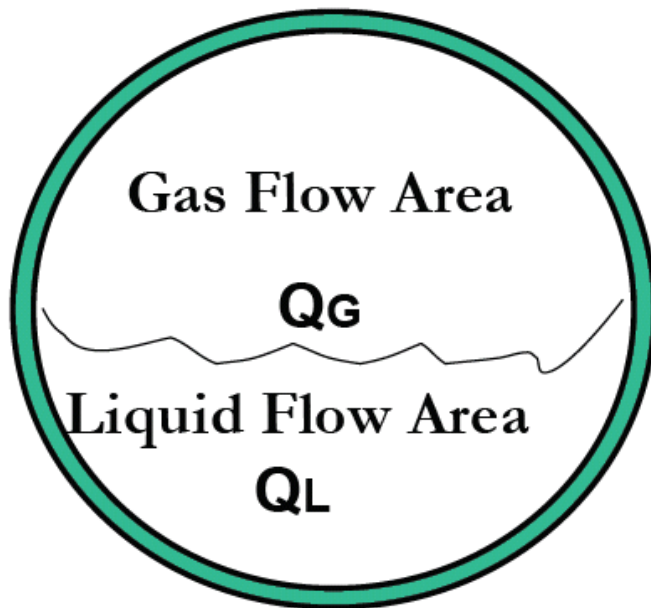


- **Phase velocities**

$Q$  = local volume flow rate

$$U_G = Q_G/A_G$$

$$U_L = Q_L/A_L$$



### **Superficial phase velocities (reduced phase velocities)**

$$A_T = A_G + A_L$$

$$U_{SG} = Q_G/A_T$$

$$U_{SL} = Q_L/A_T$$

### **Mixture velocity**

$$U_M = U_{SL} + U_{SG}$$

For the case of equal phase velocities, or no-slip conditions, the volume fraction of liquid in the pipe can be calculated analytically from a knowledge of the in-situ volumetric flow rates given in the previous section. Thus,

$$\lambda_L = \frac{q_L}{q_L + q_g} \dots \dots \dots (3.8)$$

where  $q_L$  is the sum of the oil and water flow rates for the black-oil model, or is given by Eq. 3.5 for the compositional model. If free water exists when the compositional model is used, the water flow rate must be added to the oil or condensate flow rate to account for all the liquid. Because the no-slip liquid holdup can be determined rigorously, it commonly is used as a correlating parameter to predict other multiphase-flow parameters, such as  $H_L$ .

When oil and water flow simultaneously in pipes, with or without gas, it is possible for slippage to occur between the oil and water phases. This type of slippage is normally small compared with the slippage that can occur between gas and liquid. However, slippage can be important when velocities are low, especially in horizontal wells where stratified flow can occur. Assuming no slippage, the oil fraction in a liquid phase is calculated from

$$f_o = \frac{q_o}{q_o + q_w} \dots \dots \dots (3.9)$$

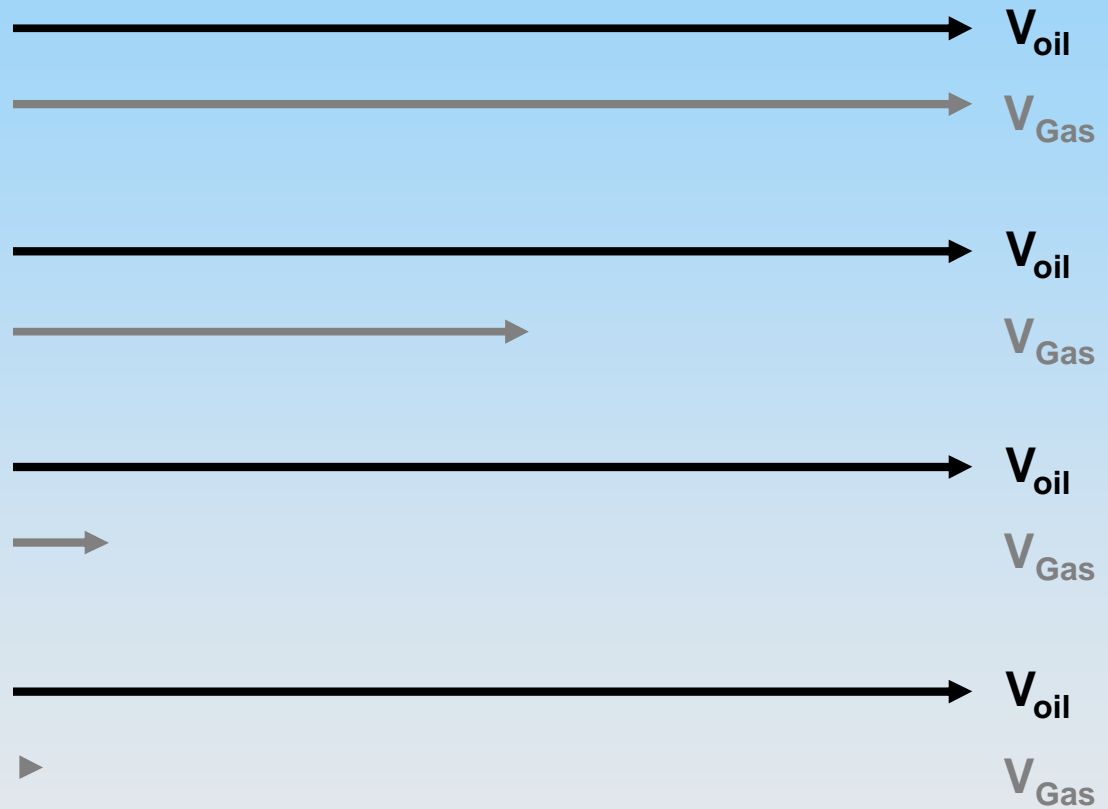
The water cut,  $f_w$ , based on in-situ rather than stock-tank flow rates, is simply  $1 - f_o$ .

- **Slip** is the ratio of the gas velocity to the liquid velocity

$$\text{Slip} = \frac{\text{average } U_{\text{Gas}}}{\text{average } U_{\text{Liq}}}$$

normally  $\geq 1$  for co-current horizontal or upwards flow  
for downward co-current flow the value may be  $< 1$

Slip velocity  
between oil  
and gas  
phases



If there were no slip between phases, both the gas and liquid would flow at the mixture velocity. Because of the slip between phases, the liquid typically flows at a velocity less than the mixture velocity, while the gas flows at a velocity greater than the mixture velocity. Time- and space-averaged velocities for each phase can be calculated from a knowledge of the time- and space-averaged liquid hold-up obtained from the empirical correlations. Thus,

$$v_L = v_{SL}/H_L \dots\dots\dots (3.13)$$

$$v_g = \frac{v_{Sg}}{1 - H_L} \dots\dots\dots (3.14)$$

A slip velocity can be defined as the difference between the actual phase velocities.

$$v_s = v_g - v_L \dots\dots\dots (3.15)$$

A variety of other velocities are encountered in multiphase flow that pertain to flow mechanisms in specific flow patterns. Examples are rise velocities of small bubbles and larger bullet-shaped bubbles that often occur in bubble- and slug-flow patterns. Chap. 4 describes these in detail.

$$\rho_L = \rho_o f_o + \rho_w f_w, \dots\dots\dots (3.16)$$

$$\sigma_L = \sigma_o f_o + \sigma_w f_w, \dots\dots\dots (3.17)$$

$$\mu_L = \mu_o f_o + \mu_w f_w. \dots\dots\dots (3.18)$$

$$f_o = \frac{q_o}{q_o + q_w}, \dots\dots\dots (3.9)$$

The water cut,  $f_w$ , based on in-situ rather than stock-tank flow rates, is simply  $1 - f_o$ .



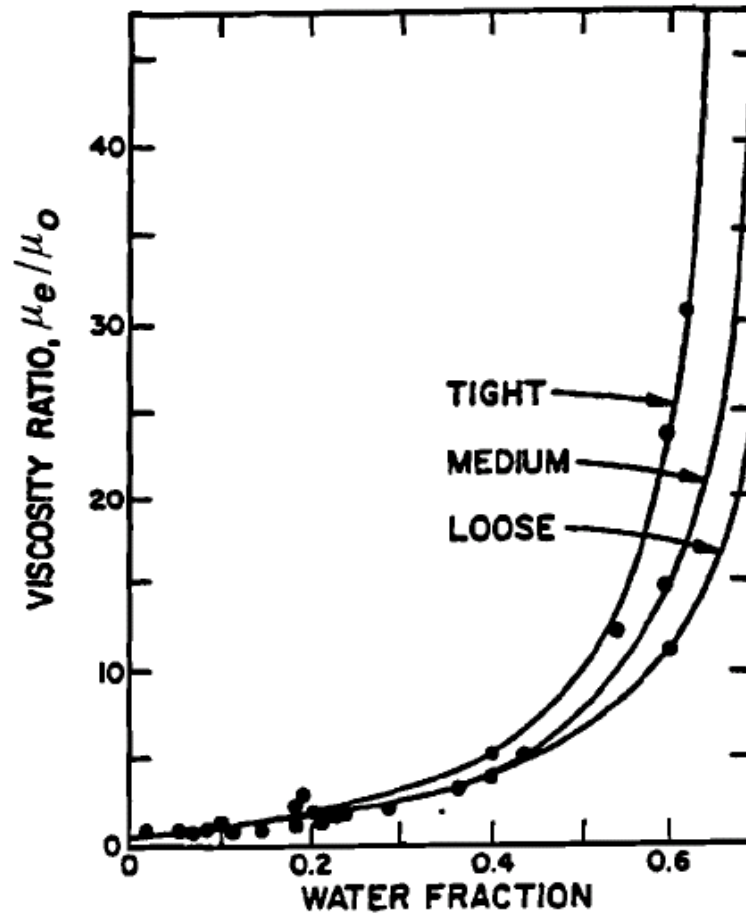


Fig 3.2—Effect of water on emulsion viscosity.<sup>2</sup>



**Gas/Liquid Mixture.** Numerous equations have been proposed to describe the physical properties of gas/liquid mixtures. In general, these equations are referred to as “slip” or “no-slip” properties, depending on whether  $H_L$  or  $\lambda_L$  is used as the volumetric weighting factor. Thus, for the case of two-phase viscosity,<sup>8</sup>

$$\mu_s = \mu_L H_L + \mu_g(1 - H_L) \dots\dots\dots (3.19)$$

or

$$\mu_s = (\mu_L^{H_L}) \times [\mu_g^{(1-H_L)}] \dots\dots\dots (3.20)$$

and

$$\mu_n = \mu_L \lambda_L + \mu_g(1 - \lambda_L). \dots\dots\dots (3.21)$$

The following expressions have been used to calculate multi-phase-flow mixture densities.<sup>8</sup>

$$\rho_s = \rho_L H_L + \rho_g(1 - H_L), \dots\dots\dots (3.22)$$

$$\rho_n = \rho_L \lambda_L + \rho_g(1 - \lambda_L), \dots\dots\dots (3.23)$$

and

$$\rho_k = \rho_L \frac{\lambda_L^2}{H_L} + \rho_g \frac{(1 - \lambda_L)^2}{(1 - H_L)}. \dots\dots\dots (3.24)$$

Eq. 3.24 contains the subscript *k* because it appears in the kinetic energy term for the specific case of a homogeneous-mixture, momentum-conservation equation.

When performing temperature-change calculations for multiphase flow in wells, it is necessary to predict the enthalpy of the multiphase mixture. Most VLE calculation methods include a provision to predict the enthalpies of the gas and liquid phases. If enthalpies are expressed per unit mass, the enthalpy of a multiphase mixture can be calculated from

$$h = h_L(1 - x_g) + h_g x_g \dots \dots \dots (3.25)$$

### 3.4 Pressure Gradient

The pressure-gradient equation derived in Sec. 2.3 for single-phase flow can be modified for multiphase flow by considering the fluids to be a homogeneous mixture. Thus,

$$\frac{dp}{dL} = \frac{f\rho_f v_f^2}{2d} + \rho_f g \sin \theta + \rho_f v_f \frac{dv_f}{dL}, \quad \dots \dots \dots (3.26)$$

where the definitions for  $\rho_f$  and  $v_f$  can vary with different investigators. For vertical flow,  $\theta = 90^\circ$ ,  $\sin \theta = 1$ ,  $dL = dZ$ , and the equation can be written as

$$\left(\frac{dp}{dZ}\right)_t = \left(\frac{dp}{dZ}\right)_f + \left(\frac{dp}{dZ}\right)_{el} + \left(\frac{dp}{dZ}\right)_{acc} \dots \dots \dots (3.27)$$

The pressure-drop component caused by friction losses requires evaluation of a two-phase friction factor. The pressure drop caused by elevation change depends on the density of the two-phase mixture which is usually calculated with Eq. 3.22. Except for conditions of high velocity, most of the pressure drop in vertical flow is caused by this component. The pressure-drop component caused by acceleration is normally negligible and is considered only for cases of high flow velocities.

## 2.2 Conservation of Mass

Conservation of mass simply means that for a given control volume, such as a segment of pipe, the mass in, minus the mass out, must equal the mass accumulation.<sup>1</sup> For a constant-area duct,

$$\frac{\partial p}{\partial t} + \frac{\partial(\rho v)}{\partial L} = 0. \quad \dots\dots\dots (2.1)$$

For steady-state flow, no mass accumulation can occur. Eq. 2.1 then becomes

$$\frac{\partial(\rho v)}{\partial L} = 0. \quad \dots\dots\dots (2.2)$$

It is evident from Eq. 2.2 that steady-state flow also is characterized by  $\rho v = \text{constant}$ .

## 2.3 Conservation of Momentum

Application of Newton's first law to fluid flow in pipes requires that the rate of momentum out, minus the rate of momentum in, plus the rate of momentum accumulation in a given pipe segment must equal the sum of all forces on the fluids.<sup>1</sup> Fig. 2.1 defines the control volume and pertinent variables. Conservation of linear momentum can be expressed as

$$\begin{aligned} & \frac{\partial}{\partial t}(\rho v) + \frac{\partial}{\partial L}(\rho v^2) \\ & = -\frac{\partial p}{\partial L} - \tau \frac{\pi d}{A} - \rho g \sin \theta. \quad \dots\dots\dots (2.3) \end{aligned}$$

### 2.4 Pressure-Gradient Equation

Combining Eqs. 2.2 and 2.3, and assuming steady-state flow to eliminate the rate of accumulation of linear momentum, gives

$$\rho v \frac{dv}{dL} = - \frac{dp}{dL} - \tau \frac{\pi d}{A} - \rho g \sin \theta. \quad \dots\dots\dots (2.4)$$

Solving for the pressure gradient obtains

$$\frac{dp}{dL} = - \tau \frac{\pi d}{A} - \rho g \sin \theta - \rho v \frac{dv}{dL}, \quad \dots\dots\dots (2.5)$$

which also frequently is called the mechanical energy balance equation. Thus, the steady-state, pressure-gradient equation is a result of applying the principles of conservation of mass and linear momentum.

Eq. 2.5 clearly shows that the steady-state pressure gradient is made up of three components. Thus

$$\left( \frac{dp}{dL} \right)_t = \left( \frac{dp}{dL} \right)_f + \left( \frac{dp}{dL} \right)_{el} + \left( \frac{dp}{dL} \right)_{acc} \quad \dots\dots\dots (2.6)$$

The first component in Eq. 2.5, described in greater detail in Eqs. 2.7 through 2.9, results from friction or shear stress at the pipe wall. Friction losses normally represent 5 to 20% of the total pressure drop in wells. The second term in Eq. 2.5 is the pressure gradient caused by elevation change (often called the hydrostatic head or elevation component). It is normally the predominant term in wells and contributes from 80 to 95% of the pressure gradient. The final component in Eq. 2.5 results from change in velocity (often called acceleration or the kinetic energy component). It is normally negligible and can become significant only if a compressible phase exists at relatively low pressures, such as in gas-lift wells near the surface.

For upward flow in a well, pressure always drops in the direction of flow. It is common to show the pressure drop as positive in the direction of flow. Eq. 2.5 must be multiplied by  $-1$  to yield a positive pressure gradient.

Evaluation of the wall shear stress or friction losses can be accomplished by defining a dimensionless friction factor that is the ratio of the wall shear stress to the kinetic energy of the fluid per unit volume.<sup>1</sup> Thus,

$$f' = \frac{\tau}{\rho v^2/2}, \dots\dots\dots (2.7)$$

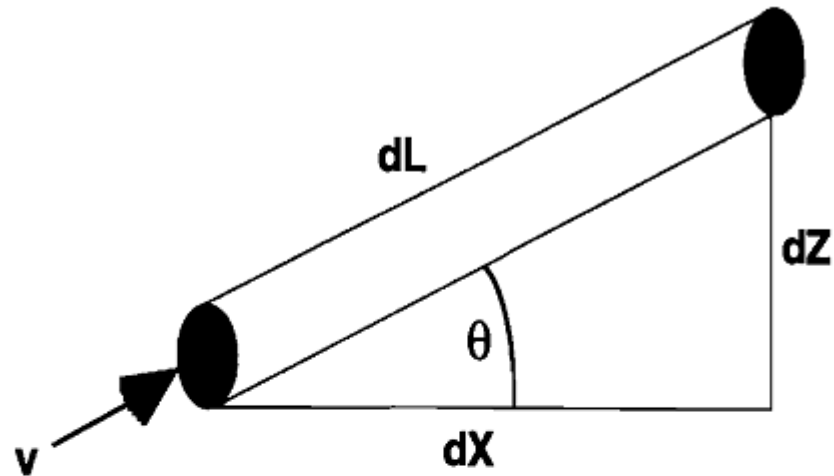


Fig. 2.1—Control volume.

Newtonian fluids and flow through annuli, Fanning friction factors are retained to preserve original equations. Eq. 2.7 can be solved for shear stress

$$\tau = f \frac{\rho v^2}{8} \dots \dots \dots (2.8)$$

Substituting Eq. 2.8 into Eq. 2.5, the frictional component of the pressure-gradient equation becomes

$$\left(\frac{dp}{dL}\right)_f = \left(\frac{f \rho v^2}{8}\right) \left(\frac{\pi d}{\pi d^2/4}\right) = \frac{f \rho v^2}{2d} \dots \dots \dots (2.9)$$



$$\frac{1}{\sqrt{f}} = 1.74 - 2 \log\left(\frac{2\varepsilon}{d}\right). \dots\dots\dots (2.16)$$

$$\frac{1}{\sqrt{f}} = 1.74 - 2 \log\left(\frac{2\varepsilon}{d} + \frac{18.7}{N_{\text{Re}} \sqrt{f}}\right). \dots\dots\dots (2.17)$$

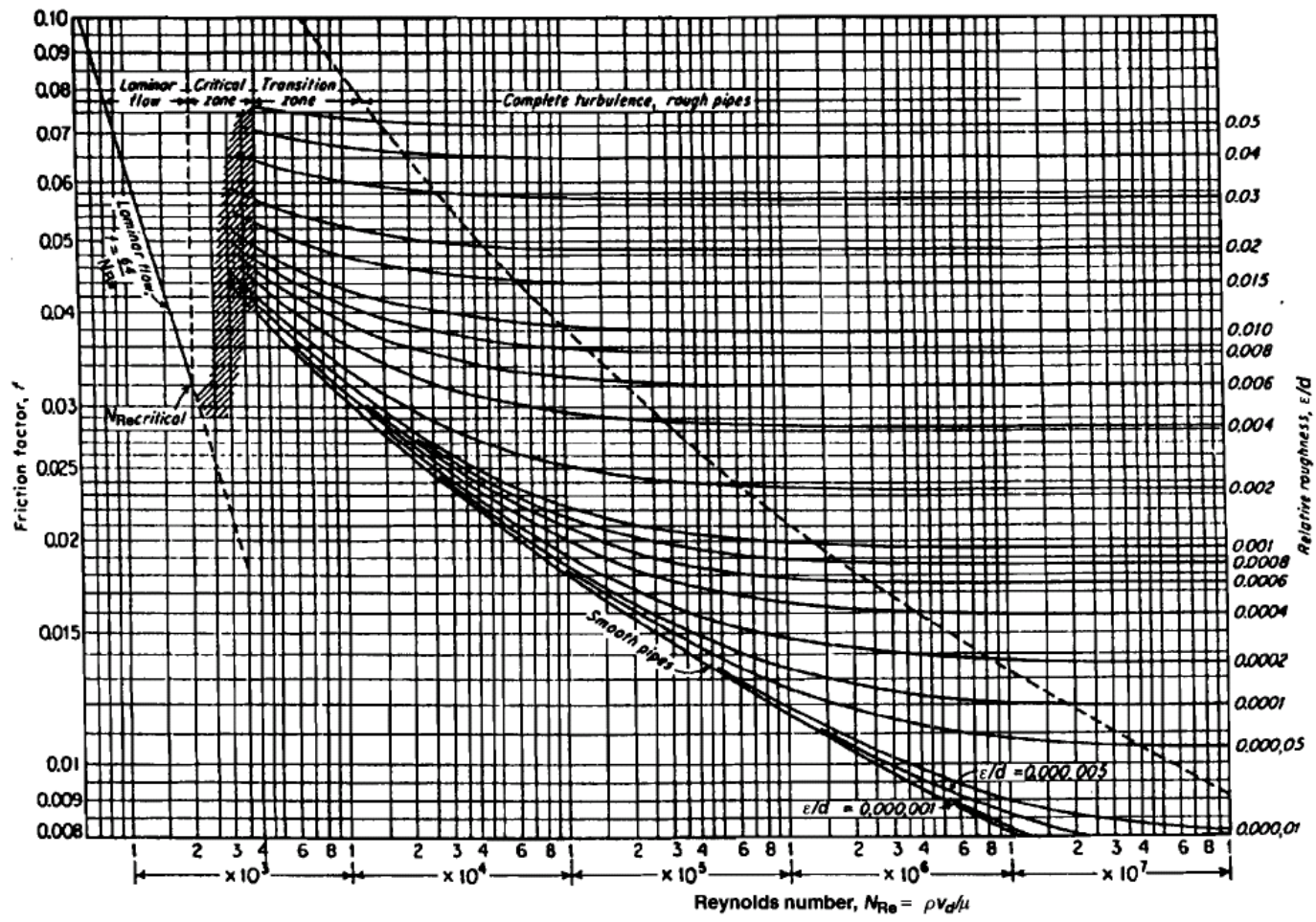


Fig. 2.2—Moody diagram.<sup>2</sup>

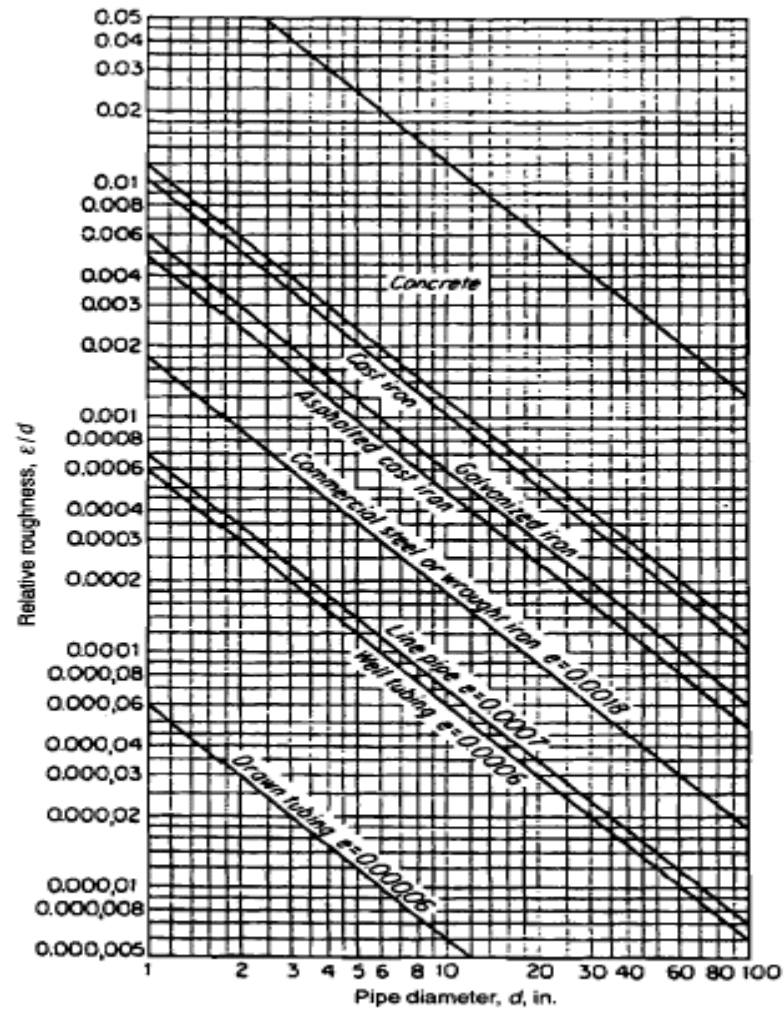
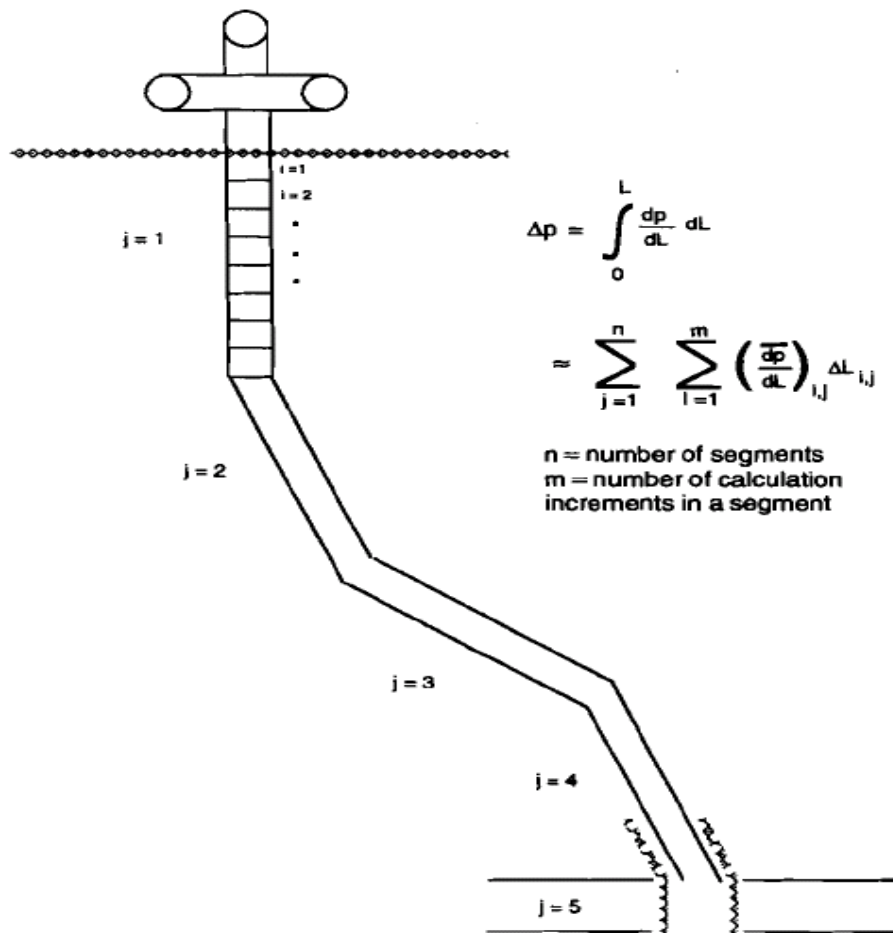


Fig. 2.3—Pipe roughness.<sup>2</sup>



**Fig. 3.9—Segmenting typical wellbore.**

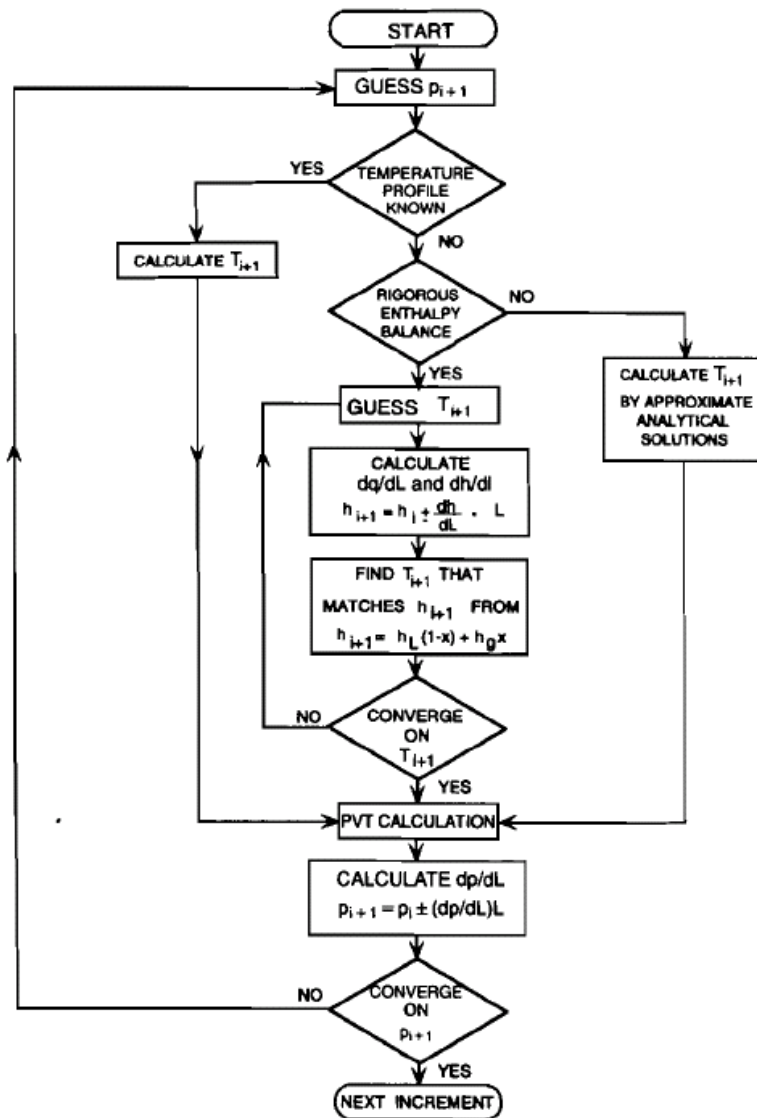


Fig. 3.10—Marching algorithm for a calculation increment.

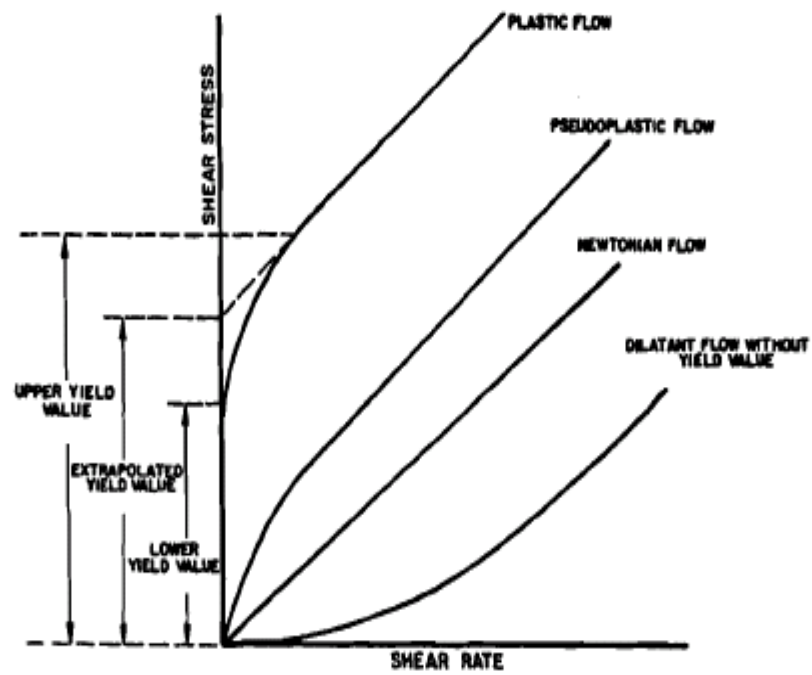


Fig 2.4—Rheological models.<sup>1</sup>

Sessions 7 and 8:  
two phase models for Vertical flow

**4.2.1 Empirical Correlations.** The empirical correlations to be discussed in this chapter can be placed in one of three categories:

Category “a.” No slip, no flow pattern consideration. The mixture density is calculated based on the input gas/liquid ratio. That is, the gas and liquid are assumed to travel at the same velocity. The only correlation required is for the two-phase friction factor. No distinction is made for different flow patterns.

Category “b.” Slip considered, no flow pattern considered. A correlation is required for both liquid holdup and friction factor. Because the liquid and gas can travel at different velocities, a method must be provided to predict the portion of the pipe occupied by liquid at any location. The same correlations used for liquid holdup and friction factor are used for all flow patterns.

Category “c.” Slip considered, flow pattern considered. Not only are correlations required to predict liquid holdup and friction factor, but methods to predict which flow pattern exists are necessary. Once the flow pattern is established, the appropriate holdup and friction-factor correlations are determined. The method used to calculate the acceleration pressure gradient also depends on flow pattern.



The following list gives the published empirical correlations for vertical upward flow and the categories in which they belong.

<u>Method</u>	<u>Category</u>
Poettmann and Carpenter <sup>1</sup>	a
Baxendell and Thomas <sup>2</sup>	a
Fancher and Brown <sup>3</sup>	a
Hagedorn and Brown <sup>4</sup>	b
Gray <sup>5</sup>	b
Asheim <sup>6</sup>	b
Duns and Ros <sup>7</sup>	c
Orkiszewski <sup>8</sup>	c
Aziz <i>et al.</i> <sup>9</sup>	c
Chierici <i>et al.</i> <sup>10</sup>	c
Beggs and Brill <sup>11</sup>	c
Mukherjee and Brill <sup>12</sup>	c

**Category “a.”** The three methods considered in this category differ only in the friction-factor correlation. In each method, field data based on Eq. 4.1 were used to calculate friction factors. For vertical flow of a homogeneous no-slip mixture, Eq. 3.26 can be expressed as

$$\frac{dp}{dZ} = \frac{f\rho_n v_m^2}{2d} + \rho_n g. \quad \dots\dots\dots (4.1)$$

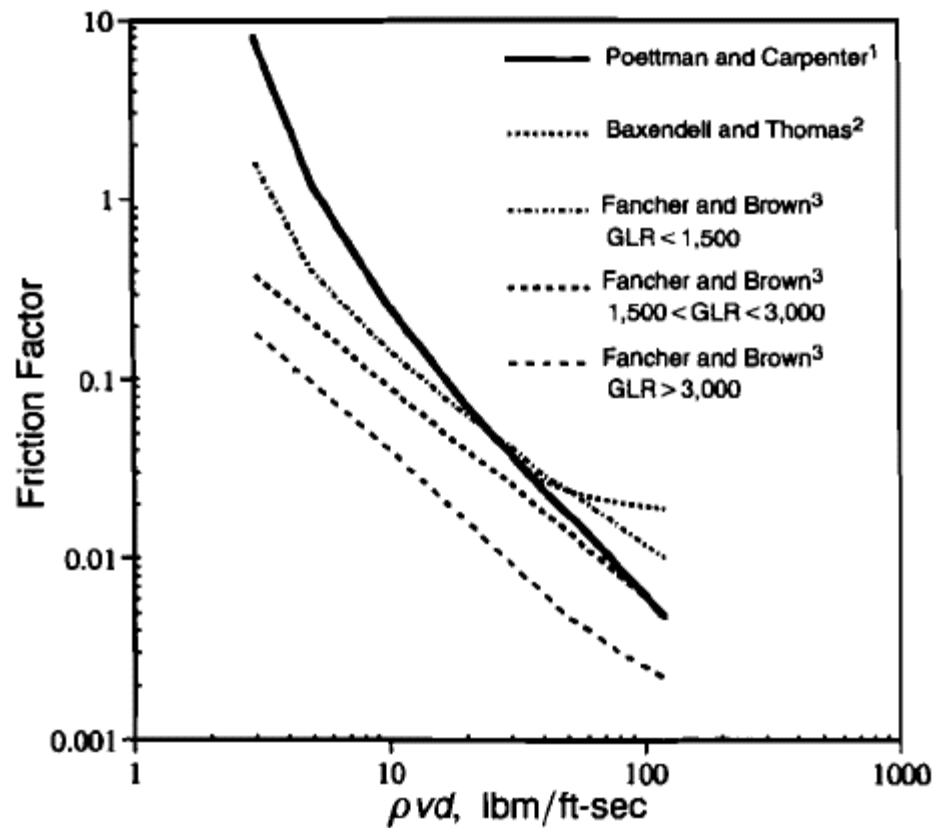


**Fig. 4.1—Category “a” friction-factor correlations.**

Category “a” methods no longer should be used to predict multi-phase-flow pressure gradients in wells. They can yield satisfactory results only for high-flow-rate wells for which the flow pattern would be dispersed-bubble flow. A no-slip condition characterizes the dispersed-bubble-flow pattern.

**Example 4.1—Using the Poettmann and Carpenter Method, Calculate the Vertical, Multiphase-Flow Pressure Gradient for Example 3.2.**

Given:  $\rho_L = 47.61 \text{ lbm/ft}^3$  and  $\rho_g = 5.88 \text{ lbm/ft}^3$ .

1. Determine no-slip mixture density:

$$\begin{aligned}\rho_n &= \rho_L \lambda_L + \rho_g (1 - \lambda_L) \\ &= (47.61)(0.507) + (5.88)(0.493) \\ &= 27.04 \text{ lbm/ft}^3.\end{aligned}$$

2. Determine friction factor:

$$\rho_n v_m d = (27.04)(7.83)(0.5) = 105.86 \text{ lbm/(ft-sec)}.$$

From Fig. 4.1,  $f = 0.0068$ .

3. Determine total pressure gradient:

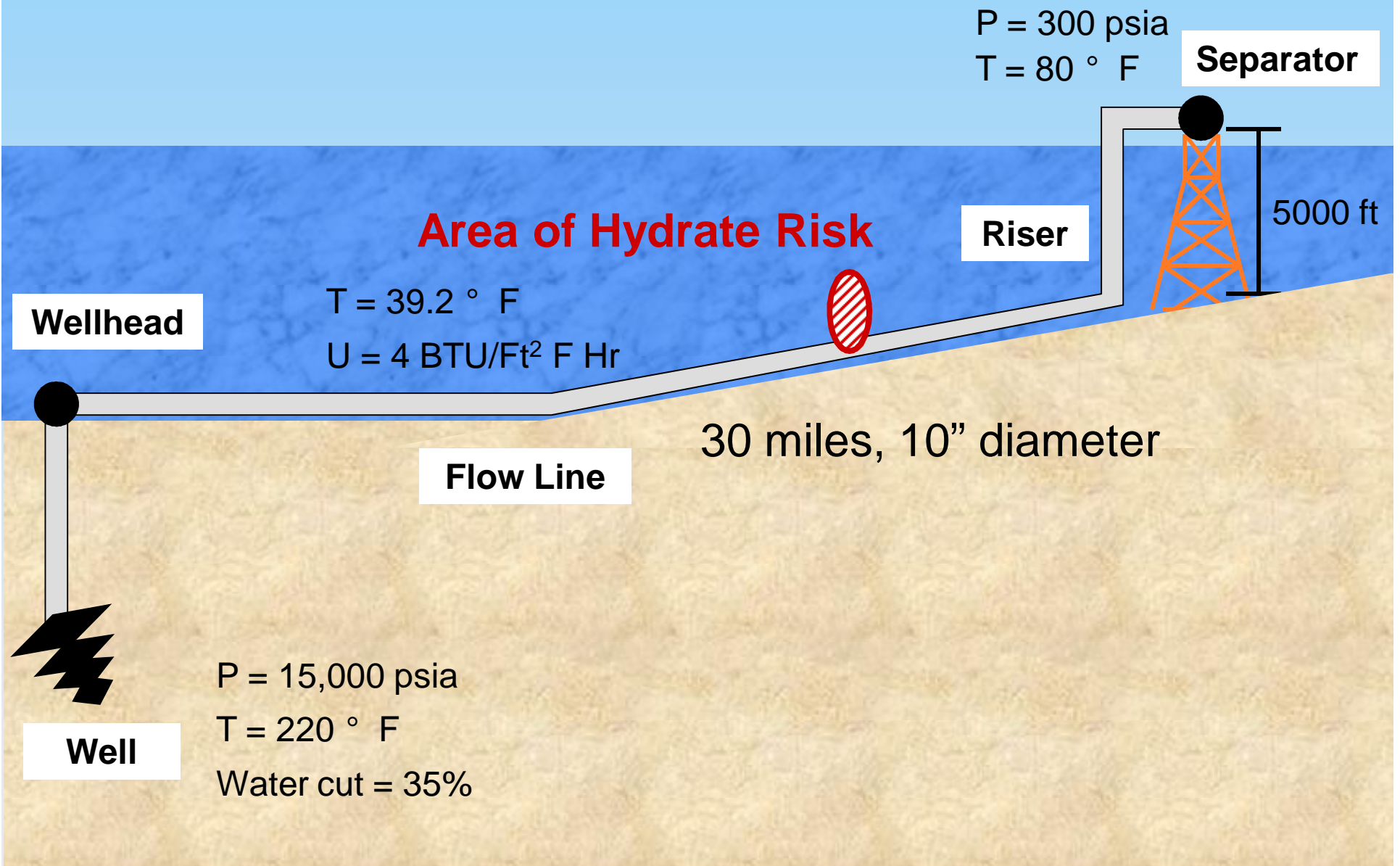
$$\begin{aligned}\frac{dp}{dZ} &= \rho_n + \frac{f \rho_n v_m^2}{2g_c d} = 27.04 + \frac{(0.0068)(27.04)(7.83)^2}{2(32.174)(0.5)} \\ &= 27.04 + 0.35 = 27.39 \text{ psf/ft} \\ &= 0.190 \text{ psi/ft}.\end{aligned}$$

**Category “b.”** Three methods are presented in this category. Hagedorn and Brown<sup>4</sup> is a generalized method developed for a broad range of vertical two-phase-flow conditions. The Gray method<sup>5</sup> is

a specialized one developed for use with vertical gas wells that also produce condensate fluids and/or free water. The Asheim<sup>6</sup> method uses MONA, a computer program based on a method that incorporates some basic mechanisms but also permits the adjustment of empirical parameters to fit available pressure measurements.

# The Beggs and Brill Method

# The Jomon Field Flow Line Schematic





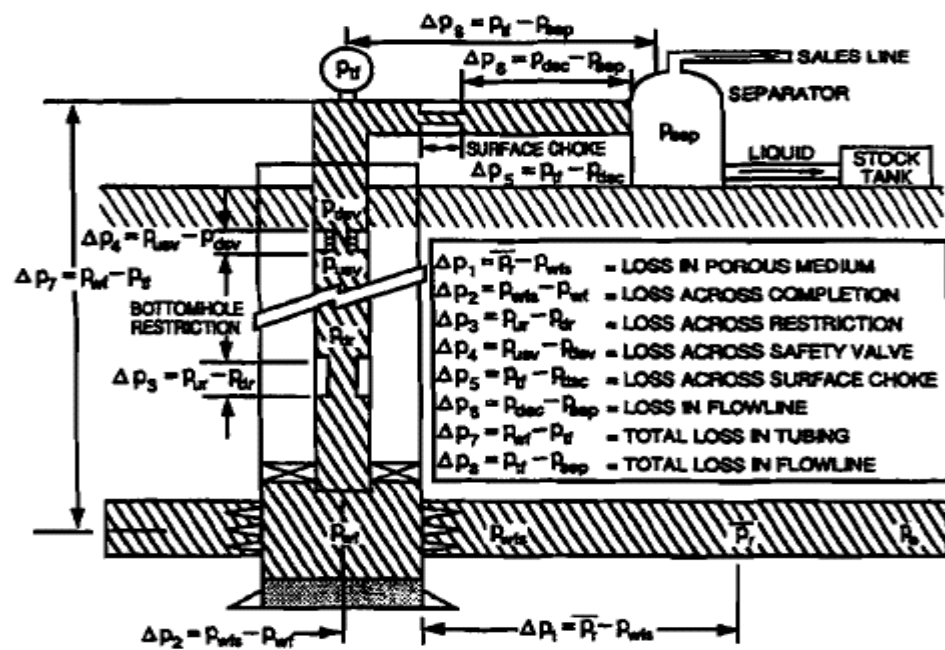
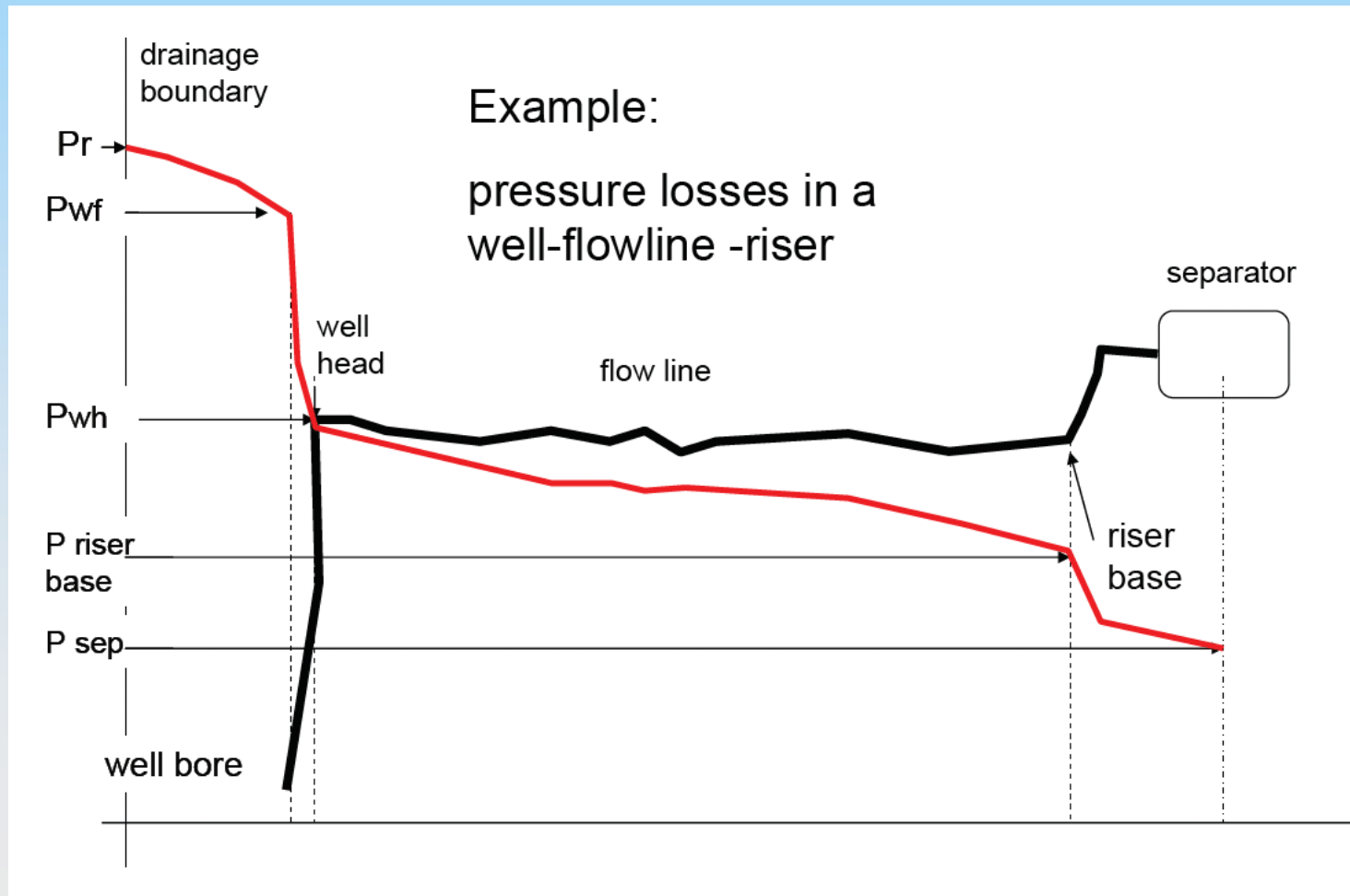


Fig. 6.1—Possible pressure losses in the producing system of a flowing well.<sup>6</sup>

$$p_{wf} = p_{sep} + \Delta p_h + (\Delta p_{fl} + \Delta p_t + \Delta p_{ch})_f + \Delta p_{acc},$$



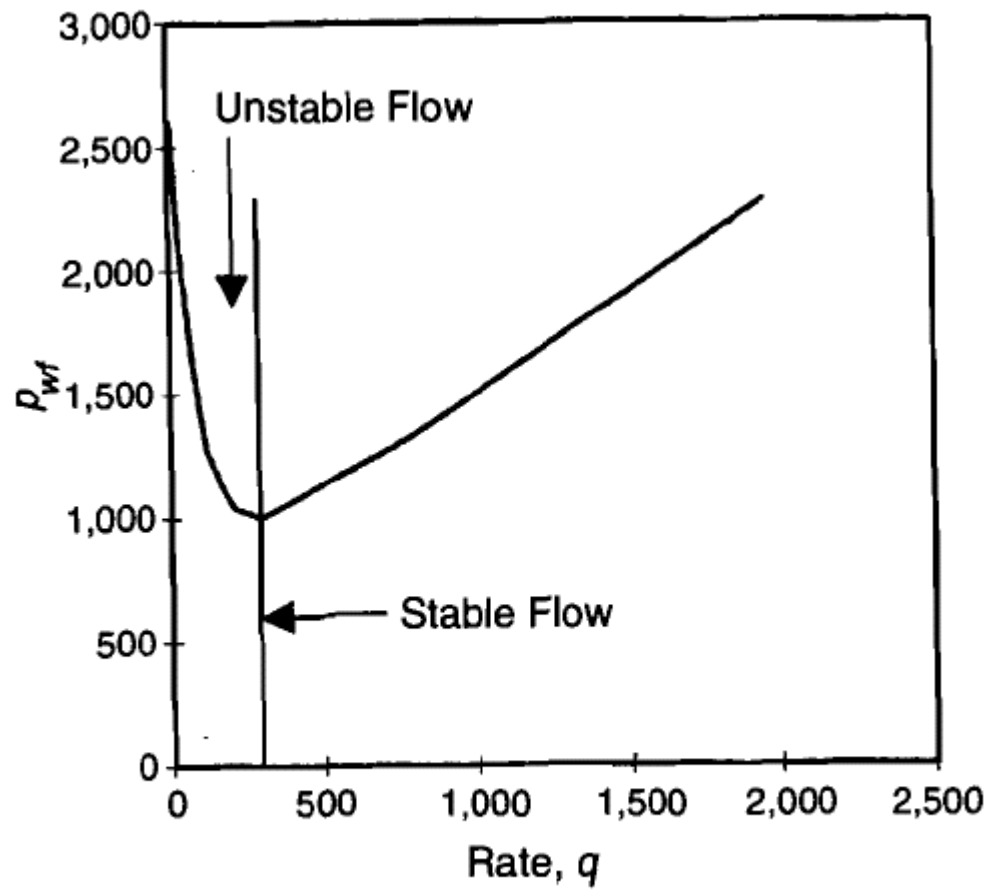
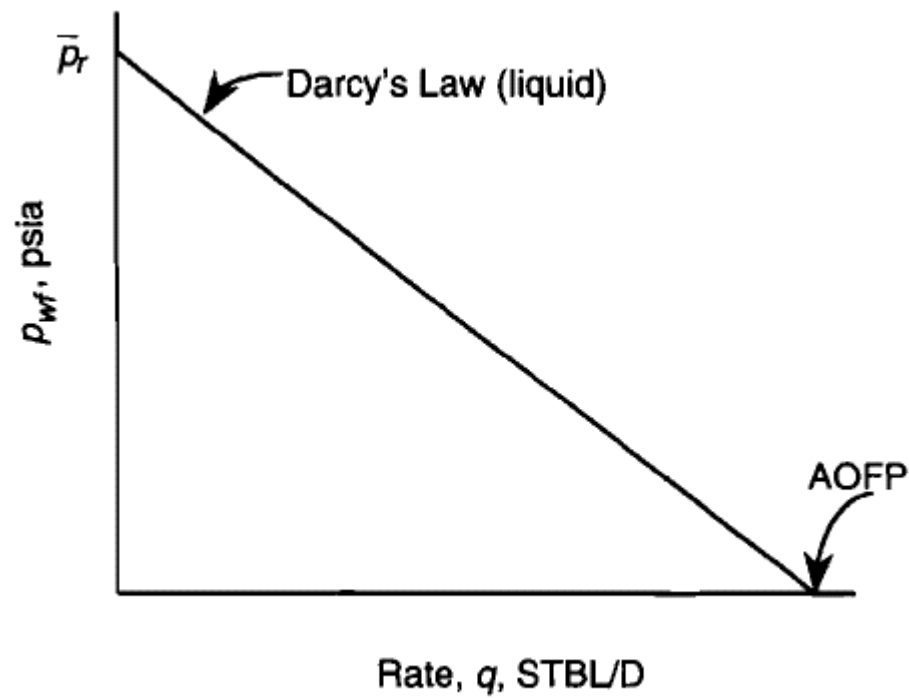


Fig. 6.3—Typical tubing-intake curve for producing wells.



**Fig. 6.6—Typical IPR curve.**

Category "c." Slip considered, flow pattern considered. Not only are correlations required to predict liquid holdup and friction factor, but methods to predict which flow pattern exists are necessary. Once the flow pattern is established, the appropriate holdup and friction-factor correlations are determined. The method used to calculate the acceleration pressure gradient also depends on flow pattern.

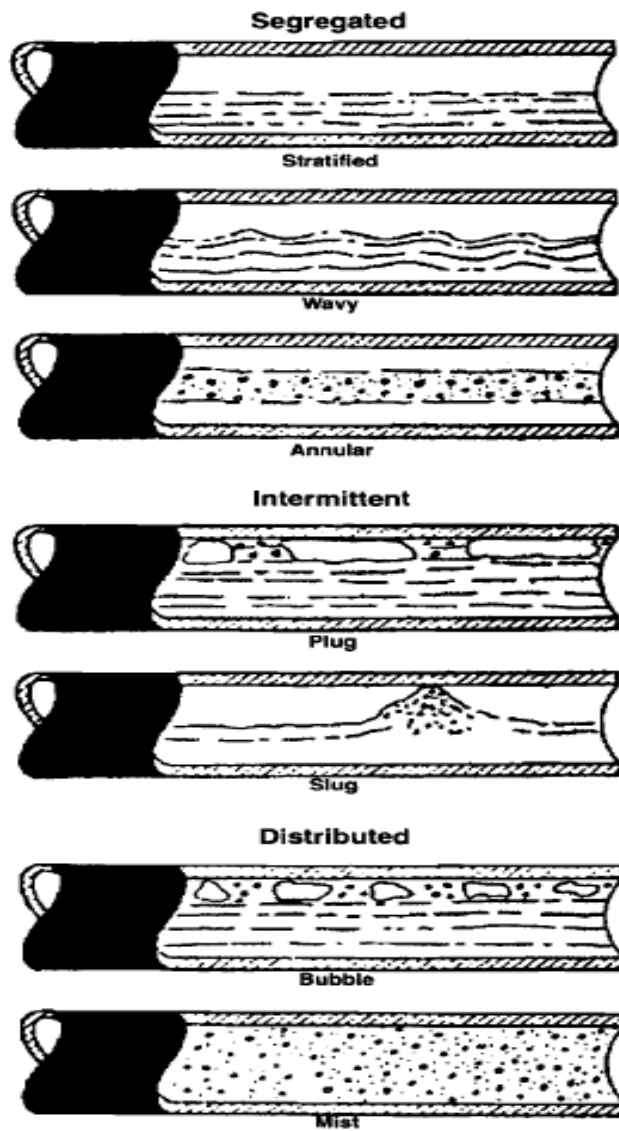


Fig. 4.16—Beggs and Brill<sup>11</sup> horizontal-flow patterns.

FIG. 17-14  
Two Phase Flow Regimes

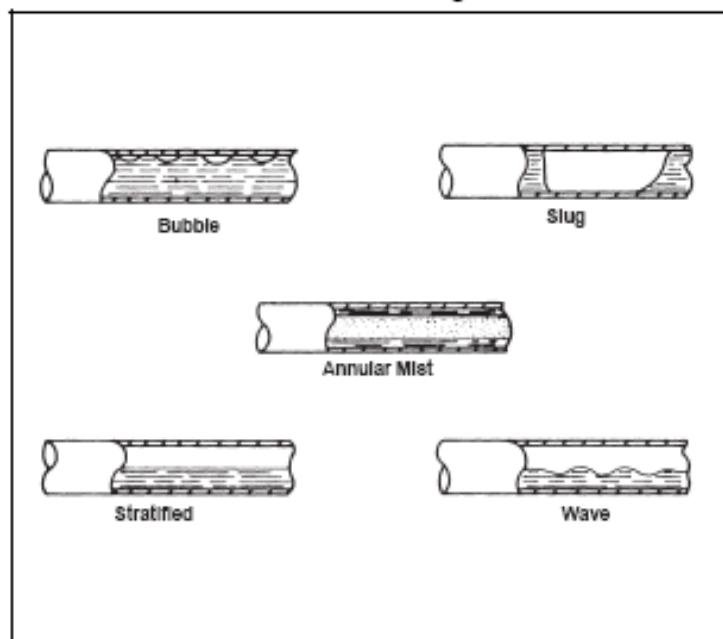
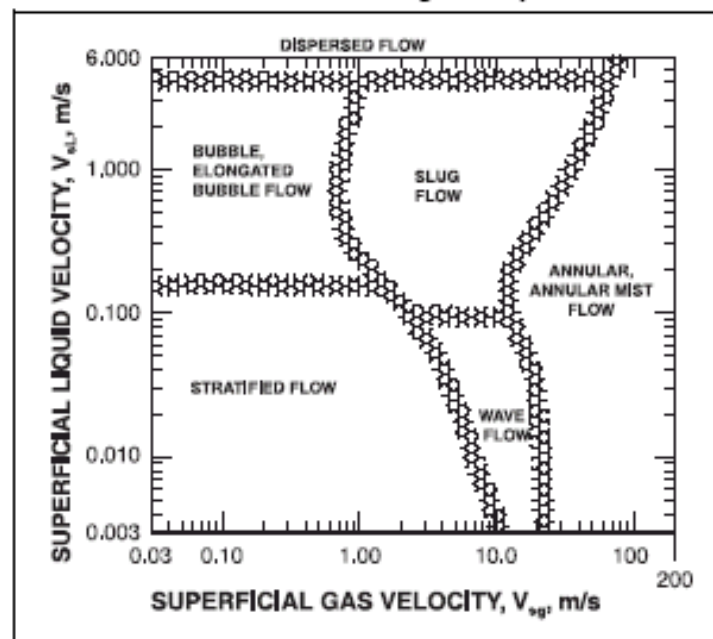


FIG. 17-15  
Horizontal Flow Regime Map<sup>12</sup>



17-16

The equations for the modified flow-pattern transition boundaries are

$$L_1 = 316\lambda_L^{0.302}, \dots\dots\dots (4.110)$$

$$L_2 = 0.000925\lambda_L^{-2.468}, \dots\dots\dots (4.111)$$

$$L_3 = 0.10\lambda_L^{-1.452}, \dots\dots\dots (4.112)$$

and

$$L_4 = 0.5\lambda_L^{-6.738}. \dots\dots\dots (4.113)$$



Segregated.

$$\lambda_L < 0.01 \text{ and } N_{Fr} < L_1$$

or

$$\lambda_L \geq 0.01 \text{ and } N_{Fr} < L_2$$

Transition.

$$\lambda_L \geq 0.01 \text{ and } L_2 \leq N_{Fr} \leq L_3$$

Intermittent.

$$0.01 \leq \lambda_L < 0.4 \text{ and } L_3 < N_{Fr} \leq L_4$$

or

$$\lambda_L \geq 0.4 \text{ and } L_3 < N_{Fr} \leq L_4$$

Distributed.

$$\lambda_L < 0.4 \text{ and } N_{Fr} \geq L_4$$

or

$$\lambda_L \geq 0.4 \text{ and } N_{Fr} > L_4$$

$$N_{Fr} = \frac{v_m^2}{gd} \dots \dots \dots (4.109)$$

$$H_{L(0)} = \frac{a\lambda_L^b}{N_{Fr}^c}, \dots\dots\dots (4.114)$$

<b>TABLE 4.2—BEGGS AND BRILL<sup>11</sup> EMPIRICAL COEFFICIENTS FOR HORIZONTAL LIQUID HOLDUP</b>			
<u>Flow Pattern</u>	<u>a</u>	<u>b</u>	<u>c</u>
Segregated	0.980	0.4846	0.0868
Intermittent	0.845	0.5351	0.0173
Distributed	1.065	0.5824	0.0609

$$H_{L(\theta)} = H_{L(0)}\Psi. \dots\dots\dots (4.115)$$

$$\Psi = 1.0 + C[\sin(1.8\theta) - 0.333 \sin^3(1.8\theta)], \dots\dots\dots (4.116)$$

$$C = (1.0 - \lambda_L) \ln(e\lambda_L^f N_{Lv}^g N_{Fr}^h), \dots\dots\dots (4.117)$$

**TABLE 4.3—BEGGS AND BRILL<sup>11</sup> EMPIRICAL COEFFICIENTS FOR C**

Flow Pattern	<i>e</i>	<i>f</i>	<i>g</i>	<i>h</i>
Segregated uphill	0.011	-3.7680	3.5390	-1.6140
Intermittent uphill	2.960	0.3050	-0.4473	0.0978
Distributed uphill	No correction: $C=0$ ; $\Psi=1$			
All patterns downhill	4.700	-0.3692	0.1244	-0.5056

When the flow pattern falls in the transition region, the liquid holdup must be interpolated between the segregated and intermittent liquid-holdup values as

$$H_{L(\theta)_{Tr}} = AH_{L(\theta)_{Seg}} + (1 - A)H_{L(\theta)_{Int}}, \dots\dots\dots (4.118)$$

where

$$A = \frac{L_3 - N_{Fr}}{L_3 - L_2} \dots\dots\dots (4.119)$$

$$f = f_n(f/f_n). \quad \dots\dots\dots (4.120)$$

The normalizing friction factor,  $f_n$ , is determined from the smooth pipe curve on the Moody diagram (Fig. 2.2) or from Eqs. 2.12 or 2.13 by use of a Reynolds number defined as

$$N_{Re} = \frac{\rho_n v_m d}{\mu_n} \quad \dots\dots\dots (4.121)$$

and  $\mu_n$  is obtained from Eq. 3.21.

The ratio of the two-phase friction factor to the normalizing friction factor was correlated with the Beggs and Brill experimental data, resulting in

$$f/f_n = e^s, \quad \dots\dots\dots (4.122)$$

where

$$s = \frac{\ln y}{-0.0523 + 3.182 \ln y - 0.8725(\ln y)^2 + 0.01853(\ln y)^4} \quad \dots\dots\dots (4.123)$$

and

$$y = \frac{\lambda_L}{[H_{L(\theta)}]^2} \quad \dots\dots\dots (4.124)$$

**Example 4.7—Using the Beggs and Brill Method, Calculate the Vertical, Multiphase-Flow Pressure Gradient for Example 3.2.**

Given:  $\mu_o = 0.97$  cp,  $\mu_g = 0.016$  cp,  $\sigma_o = 8.41$  dynes/cm, and  $\varepsilon = 0.00006$  ft.

1. Determine flow pattern:

From Eq. 4.109,

$$N_{Fr} = \frac{(7.83)^2}{(32.174)(0.5)} = 3.81.$$

From Fig 4.17 for  $\lambda_L = 0.507$ , the horizontal-flow pattern is intermittent.

2. Determine liquid holdup:

From Eq. 4.114,

$$H_{L(0)} = \frac{(0.845)(0.507)^{0.5351}}{(3.81)^{0.0173}} = 0.574.$$

From Eq. 4.117,

$$C = (0.493) \ln \left[ 2.96(0.507)^{0.305} (11.87)^{-0.4473} (3.81)^{0.0978} \right]$$
$$= -0.048 < 0.$$

Therefore,

$$C = 0, \Psi = 1.0, \text{ and } H_{L(90)} = H_{L(0)} = 0.574.$$

Apply Payne *et al.* correction factor:

$$H_{L(90)} = (0.924)(0.574) = 0.530.$$

3. Determine friction factor:

From Eq. 3.21,

$$\mu_n = (0.97)(0.507) + (0.016)(0.493) = 0.50 \text{ cp.}$$

From Eq. 4.121,

$$N_{Re} = \frac{(1,488)(27.04)(7.83)(0.5)}{(0.50)} = 3.15 \times 10^5.$$

From Fig. 2.2 for  $\epsilon/d = 0.00012$ ,  $f_n = 0.0155$ .

From Eq. 4.124,

$$y = \frac{(0.507)}{(0.530)^2} = 1.805.$$

From Eq. 4.123,

$$s = (0.591) / \left[ -0.0523 + 3.182(0.591) \right. \\ \left. - 0.8725(0.591)^2 + 0.01853(0.591)^4 \right]$$
$$= 0.3873.$$

From Eq. 4.122,

$$\frac{f}{f_n} = e^{(0.3873)} = 1.473.$$

Therefore,  $f = (1.473)(0.0155) = 0.0228$ .

4. Determine pressure gradient:

$$\begin{aligned} \frac{dp}{dL} &= \frac{(0.0228)(27.04)(7.83)^2}{(2)(32.174)(0.5)} \\ &+ [(47.61)(0.53) + (5.88)(0.47)] \frac{(32.174)}{(32.174)} \sin(90^\circ) \\ &= 1.17 + 28.00 = 29.17 \text{ psf/ft} \\ &= 0.203 \text{ psi/ft.} \end{aligned}$$

## Beggs & Brill Correlation

The Beggs & Brill correlation is developed for tubing strings in inclined wells and pipelines for hilly terrain. This correlation resulted from experiments using air and water as test fluids over a wide range of parameters. The performance of the correlation is given below.

- **Tubing Size.** For the range in which the experimental investigation was conducted (i.e., tubing sizes between 1 and 1.5 in.), the pressure losses are accurately estimated. Any further increase in tubing size tends to result in an over prediction in the pressure loss.
- **Oil Gravity.** A reasonably good performance is obtained over a broad spectrum of oil gravities.
- **Gas-Liquid Ratio (GLR).** In general, an over predicted pressure drop is obtained with increasing GLR. The errors become especially large for GLR above 5000.
- **Water-Cut.** The accuracy of the pressure profile predictions is generally good up to about 10% water-cut.



Payne *et al.* found that the Beggs and Brill method underpredicted friction factors. Because the Beggs and Brill method was based on data obtained in smooth pipe, Payne *et al.* recommended that the normalizing friction factor,  $f_n$ , be obtained from the Moody diagram (Fig. 2.2) or from Eq. 2.17 for an appropriate value of relative roughness. This change improved the pressure-drop predictions for the Beggs and Brill method for rough pipes.

$$\frac{1}{\sqrt{f}} = 1.74 - 2 \log \left( \frac{2\varepsilon}{d} + \frac{18.7}{N_{Re} \sqrt{f}} \right) \dots\dots\dots (2.17)$$

Payne *et al.* also found that the Beggs and Brill method overpredicted liquid holdup in both uphill and downhill flow. On the basis of their limited data, Payne *et al.* recommended these constant correction factors to improve liquid-holdup values.

If  $\theta > 0$ ,

$$H_{L(\theta)} = 0.924H_{L(\theta)} \dots \dots \dots (4.126)$$

If  $\theta < 0$ ,

$$H_{L(\theta)} = 0.685H_{L(\theta)} \dots \dots \dots (4.127)$$

However, the resulting liquid holdup for  $\theta > 0^\circ$  should not be less than  $\lambda_L$ . The original Beggs and Brill method has been found to overpredict pressure drops in producing wells. Consequently, improved results should be obtained if the Payne *et al.* liquid-holdup correction factor is applied for wells.

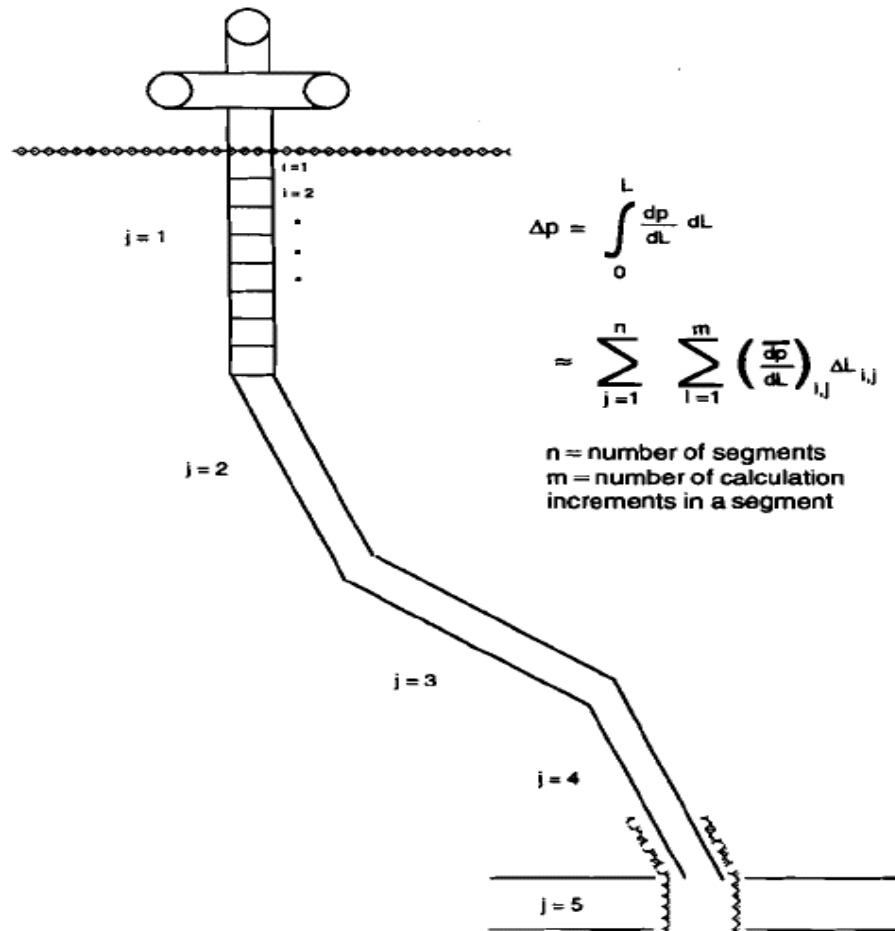


**Fig. 3.9—Segmenting typical wellbore.**

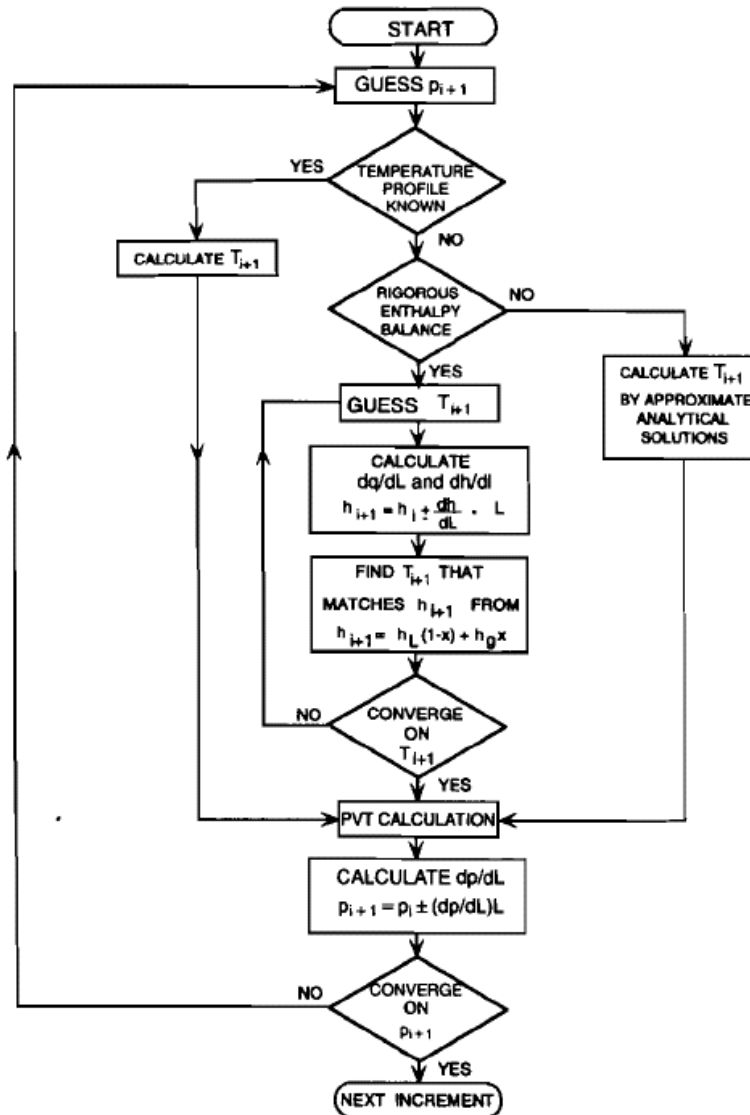


Fig. 3.10—Marching algorithm for a calculation increment.

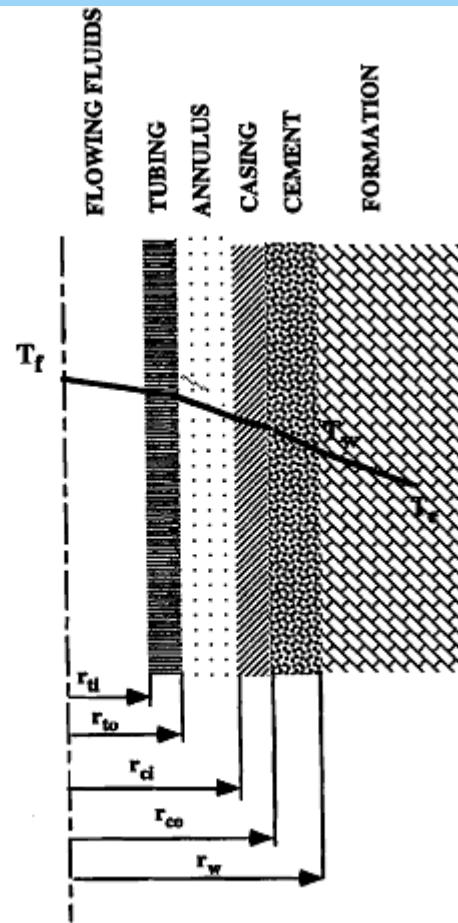


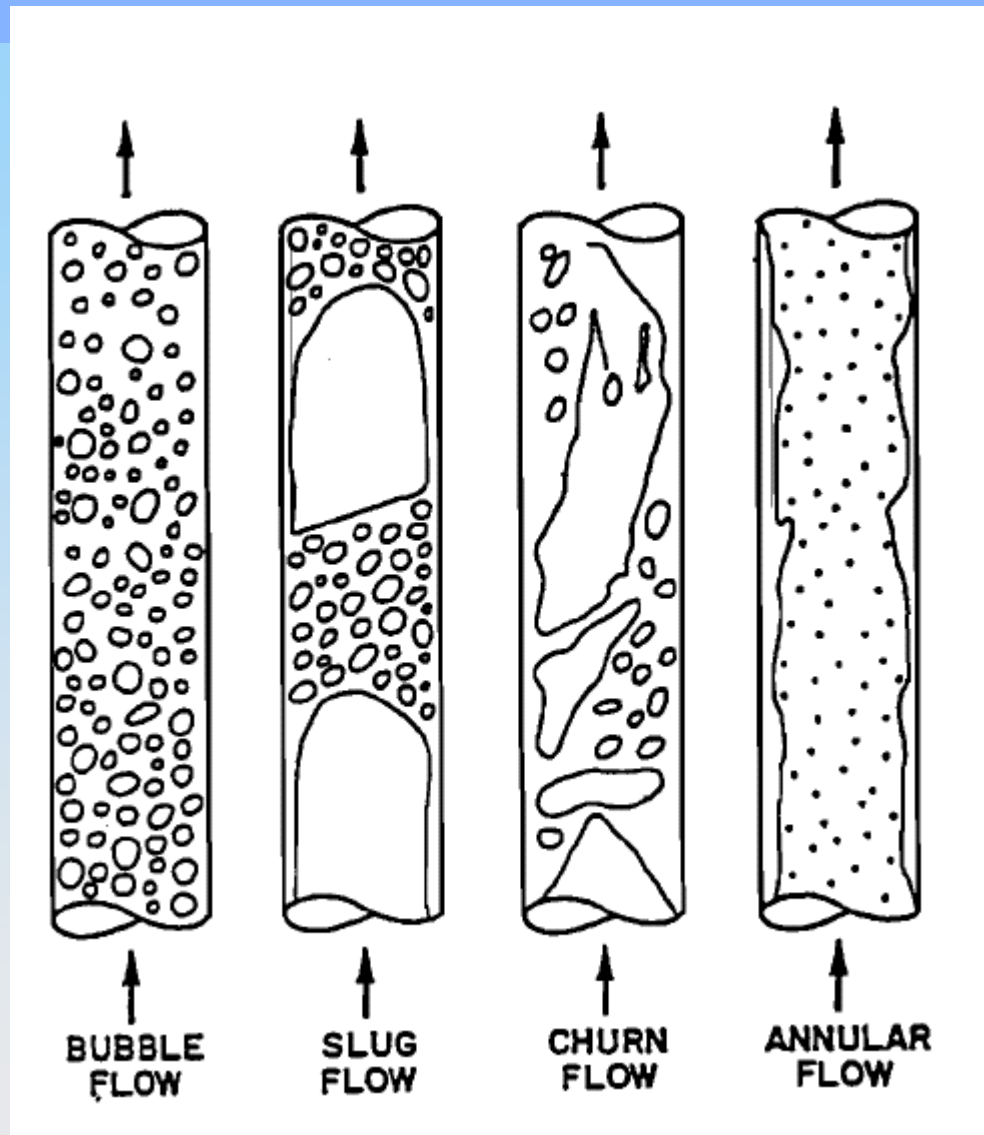
Fig. 2.7—Cross section of typical wellbore.<sup>3</sup> (Reproduced with permission of the McGraw-Hill Cos.)

# Hagedorn and Brown Model

## Hagedorn & Brown Correlation

This correlation was developed using data obtained from a 1500-ft vertical well. Tubing diameters ranging from 1-2 in. were considered in the experimental analysis along with 5 different fluid types, namely: water and four types of oil with viscosities ranging between 10 and 110 cp (@ 80°F) The correlation developed is independent of flow patterns and its performance is briefly outlined below.

- **Tubing Size.** The pressure losses are accurately predicted for tubing sizes between 1 and 1.5 in., the range in which the experimental investigation was conducted. A further increase in tubing size causes the pressure drop to be over predicted.
- **Oil Gravity.** The Hagedorn-Brown method is seen to over predict the pressure loss for heavier oils (13-25 °API) and under predict the pressure profile for lighter oils (40-56 °API)
- **Gas-Liquid Ratio (GLR).** The pressure drop is over predicted for GLR greater than 5000.
- **Water-Cut.** The accuracy of the pressure profile predictions is generally good for a wide range of water-cuts.





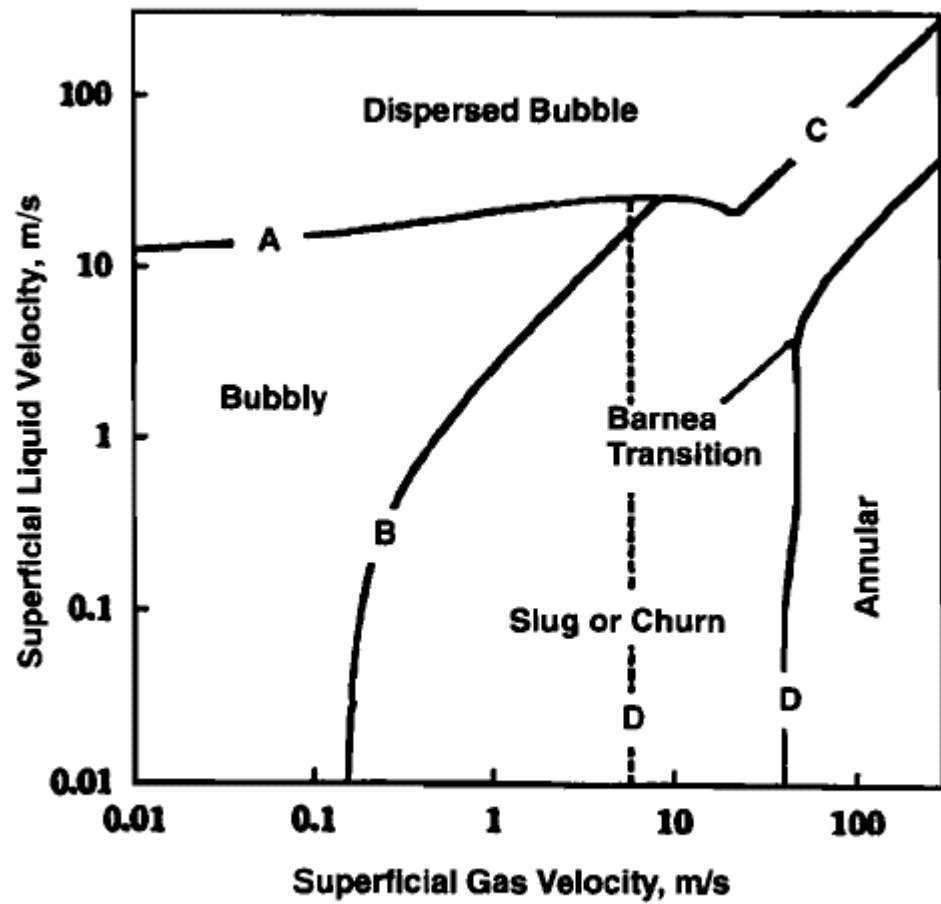
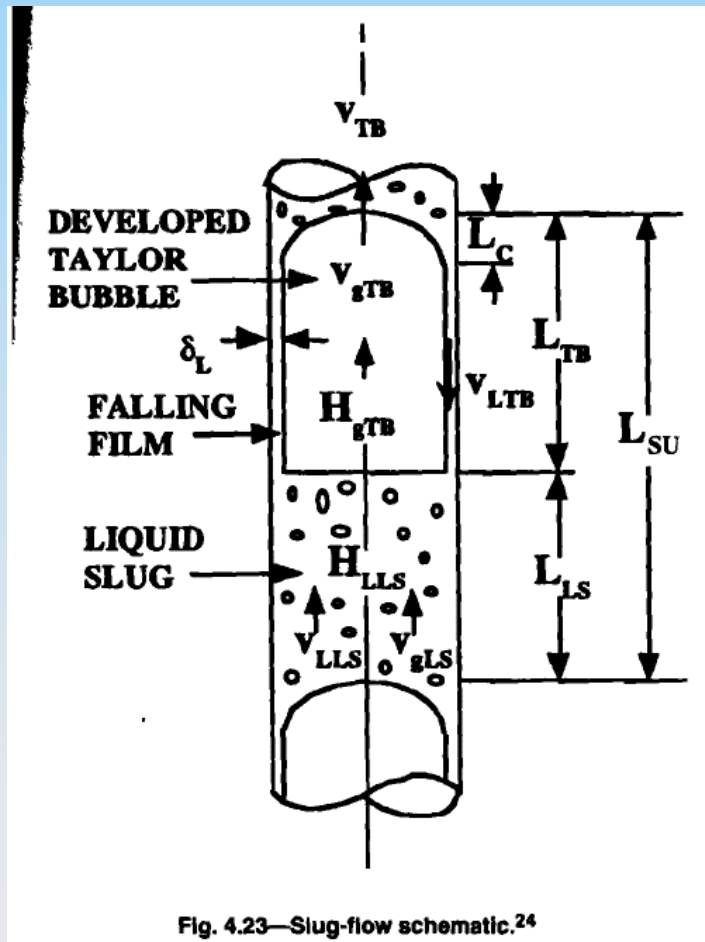


Fig. 4.22—Typical flow-pattern map for wellbores.<sup>24</sup>



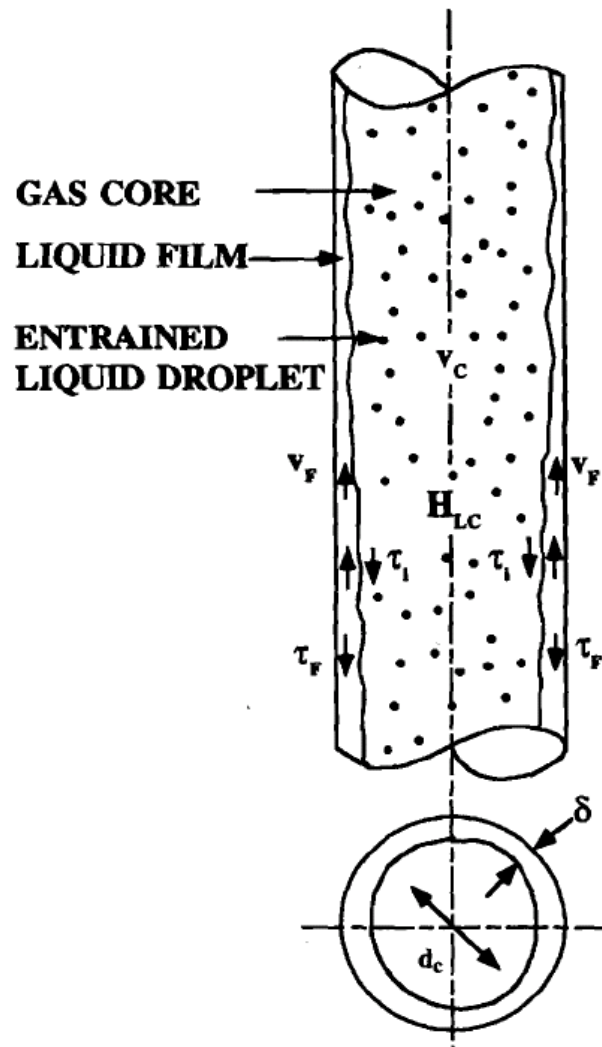
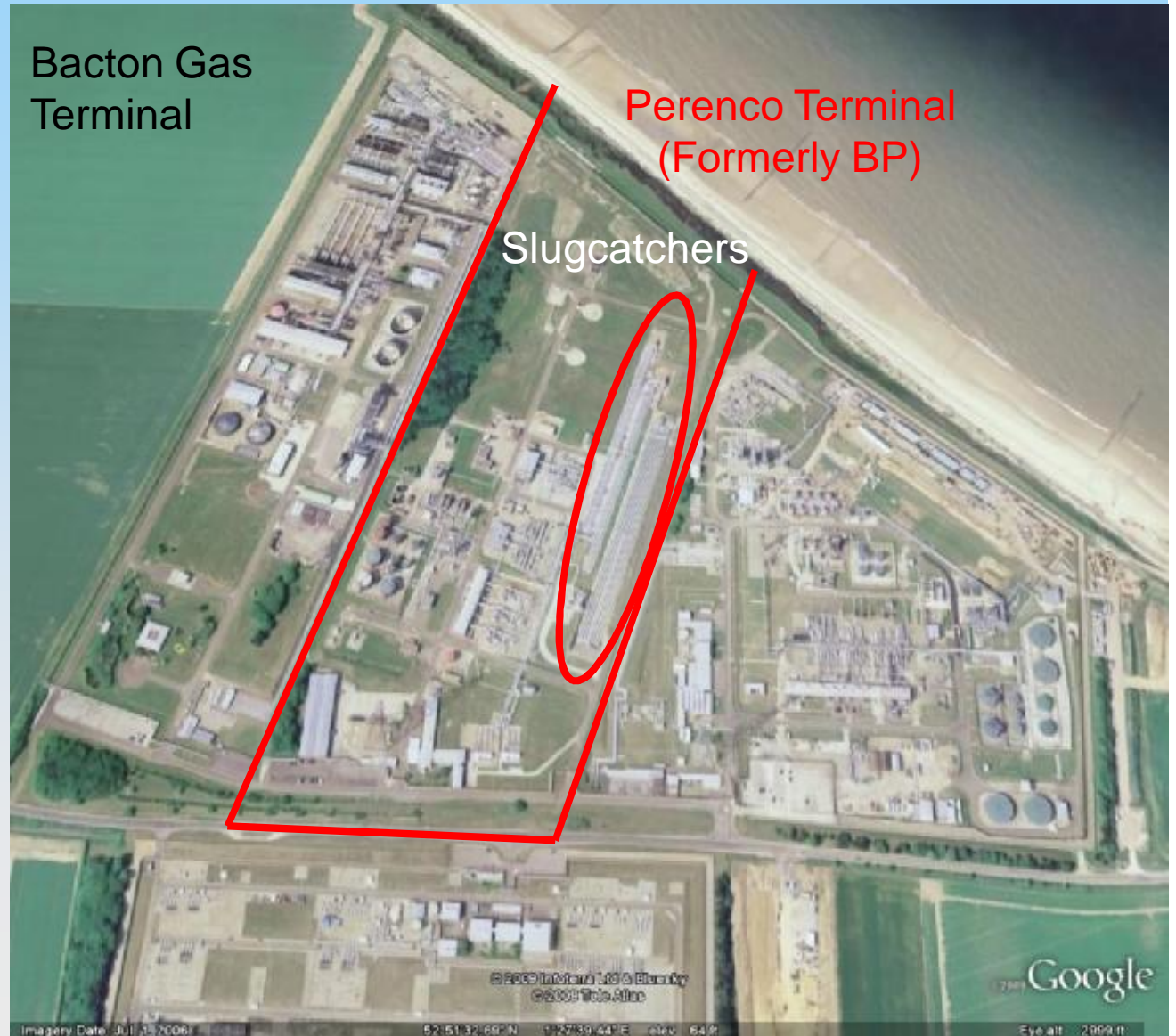
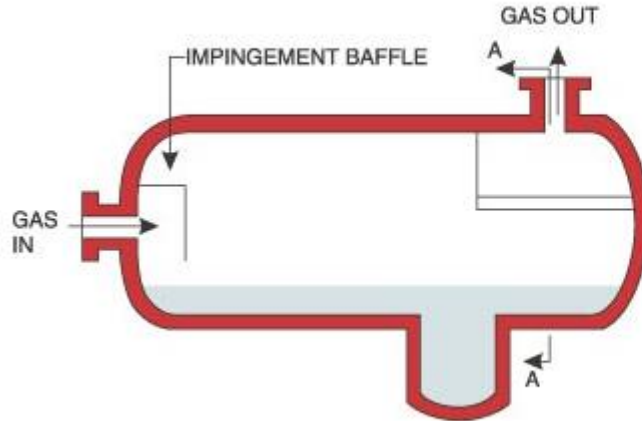


Fig. 4.24—Annular-flow schematic.<sup>24</sup>

## Slug Catchers Can be Huge

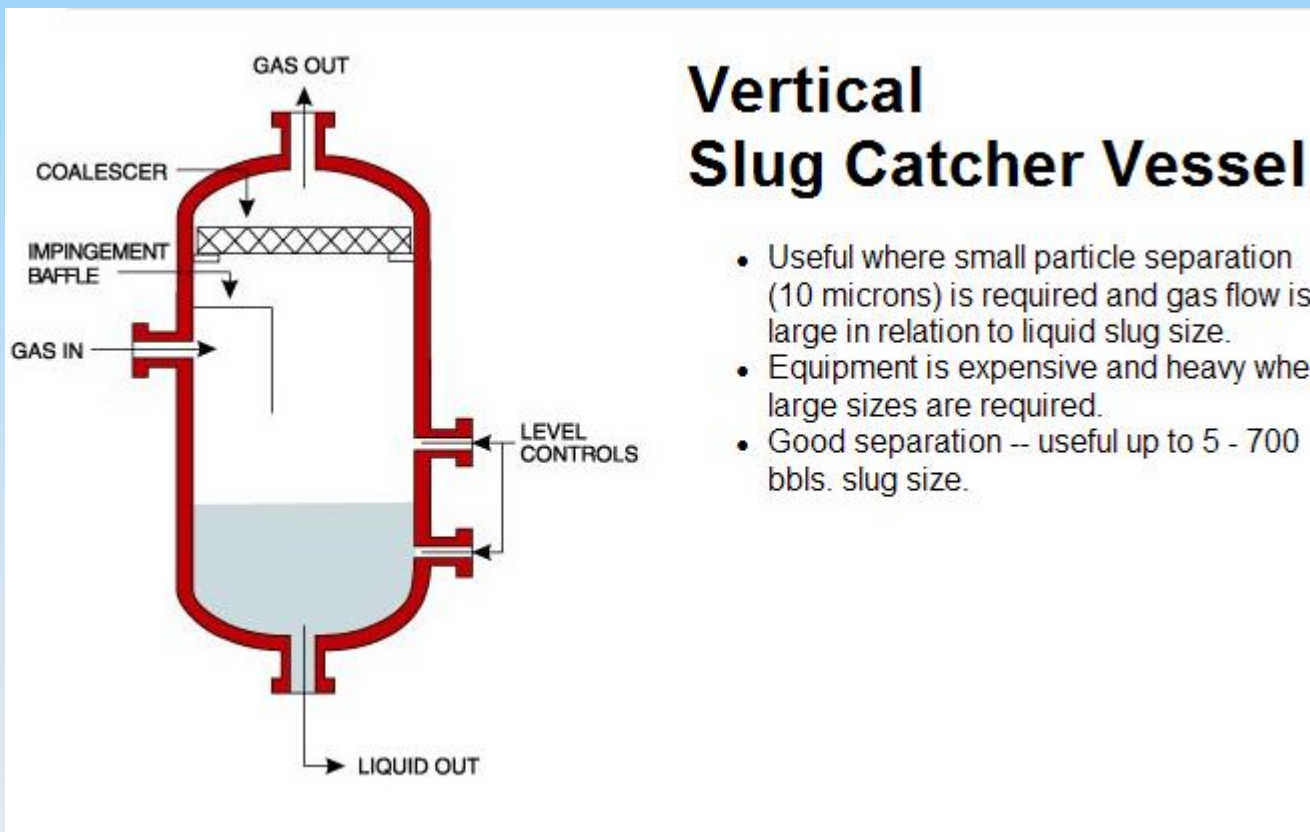
- Often the largest part of a gas terminal.
- Must be able to catch the largest slugs from the pipeline and allow time for the liquid to be processed.



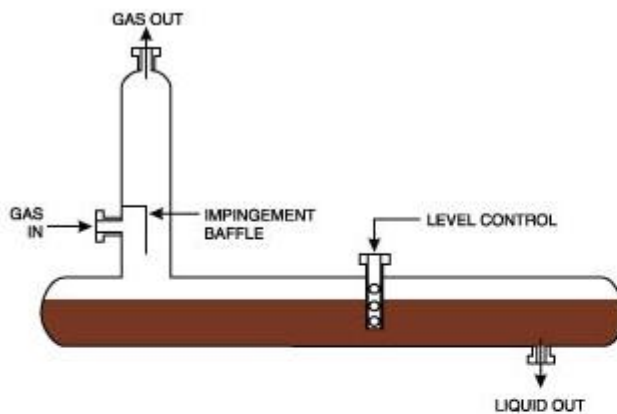


## Horizontal Slug Catcher Vessel

- Can give small particle separation (10 microns) where there is more liquid and lower gas flow.
- Useful as three phase separator.
- Becomes expensive and heavy when large sizes are required.
- Good separation up to 5 - 700 bbls. slug size.







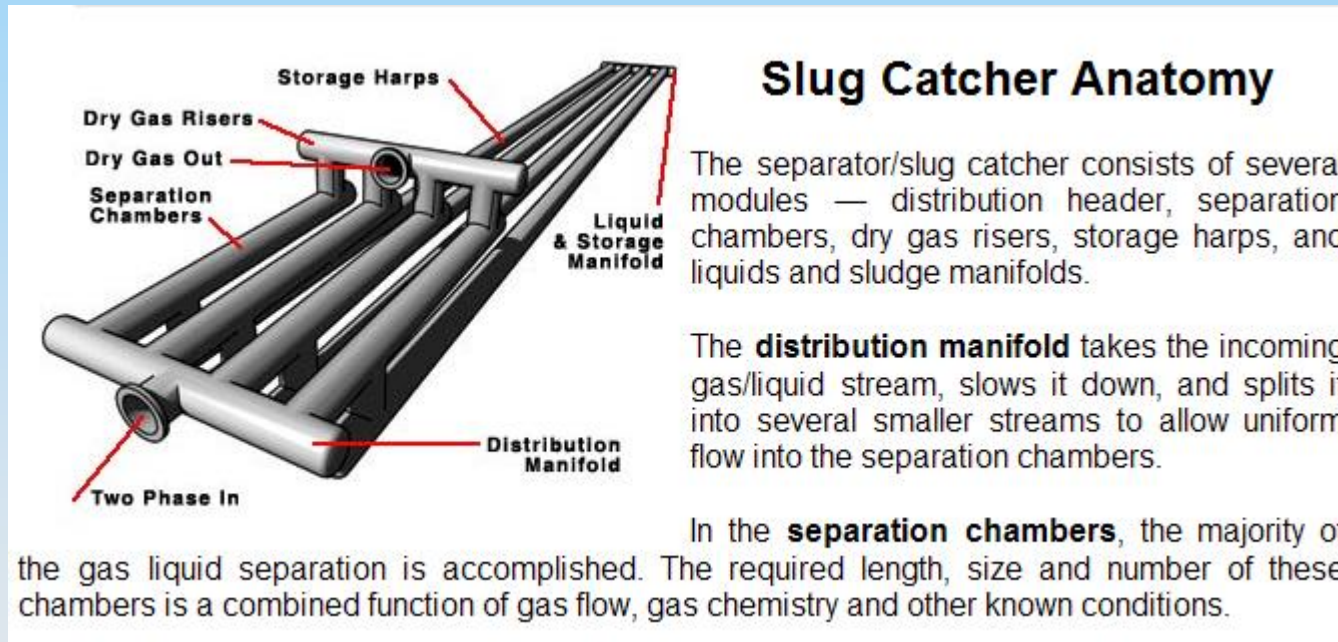
- Very economical where small liquid slugs are to be caught.
- Particle separation is poor and relatively unpredictable.
- Catches slugs up to 150 - 200 bbls.

## Pipe Fitting Type Slug Catcher

This type of separation equipment typically has an impingement plate to knock out bulk liquids and a vertical column to form a gravity type separator, but it usually has insufficient area to effectively remove small particles. Normally, it is just used to catch the slugs of liquid and hold them. For economic reasons, these slug catchers are usually designed as pipe and fittings, rather than as pressure vessels.

The pipe fitting type slug catcher provides good slug separation and slug storage volume at a reasonable cost. Small particle separation is poor, but it improves at low flow rates. A slug catcher of this type can be used to protect a centrifugal type separator and the combination will give separation and slug storage capacity.

# Harp type slug catcher





The Slug catcher for Troll has a Capacity of 2400 m<sup>3</sup>



Hagedorn and Brown developed this pressure-gradient equation for vertical multiphase flow

$$\frac{dp}{dZ} = \frac{f\rho_n^2 v_m^2}{2\rho_s d} + \rho_s g + \frac{\rho_s \Delta(v_m^2)}{2dZ} \dots \dots \dots (4.2)$$

*Liquid-Holdup Prediction.* A liquid-holdup value must be determined to calculate the pressure-gradient component that results from a change in elevation. To correlate the pseudo liquid-holdup values, Hagedorn and Brown used four dimensionless groups proposed by Duns and Ros.<sup>7</sup>

Liquid velocity number:

Liquid velocity number:

$$N_{Lv} = v_{SL} \sqrt[4]{\frac{\rho_L}{g\sigma_L}} \dots\dots\dots (4.3)$$

Gas velocity number:

$$N_{gv} = v_{Sg} \sqrt[4]{\frac{\rho_L}{g\sigma_L}} \dots\dots\dots (4.4)$$

Pipe diameter number:

$$N_d = d \sqrt{\frac{\rho_L g}{\sigma_L}} \dots\dots\dots (4.5)$$

Liquid viscosity number:

$$N_L = \mu_L \sqrt[4]{\frac{g}{\rho_L \sigma_L^3}} \dots\dots\dots (4.6)$$

age-

If constants are included:

$$N_{Lv} = 1.938v_{SL} \sqrt[4]{\frac{\rho_L}{\sigma_L}},$$

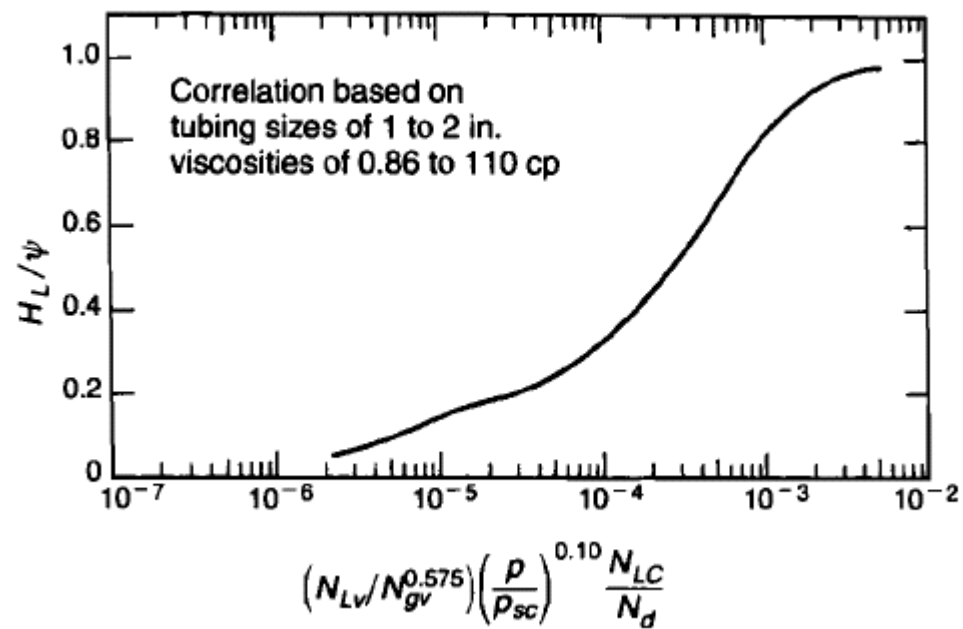
$$N_{gv} = 1.938v_{Sg} \sqrt[4]{\frac{\rho_L}{\sigma_L}},$$

$$N_d = 120.872d \sqrt{\frac{\rho_L}{\sigma_L}},$$

and

$$N_L = 0.15726\mu_L \sqrt[4]{\frac{1}{\rho_L\sigma_L^3}},$$

where  $v_{SL}$  is in feet per second,  $v_{Sg}$  is in feet per second,  $\rho_L$  is in pounds per cubic foot,  $\sigma$  is in dynes per centimeter,  $\mu_L$  centipoise, and  $d$  is in feet.



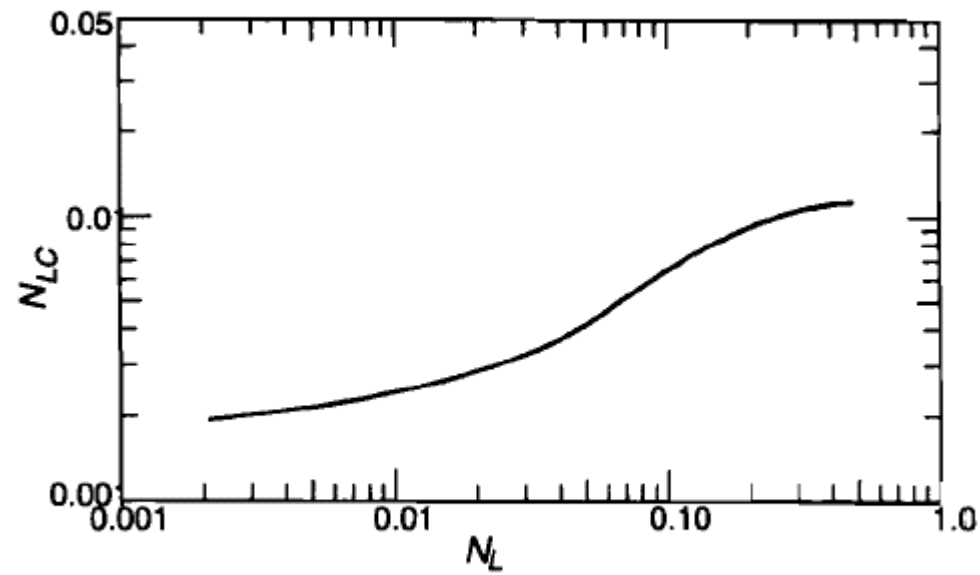
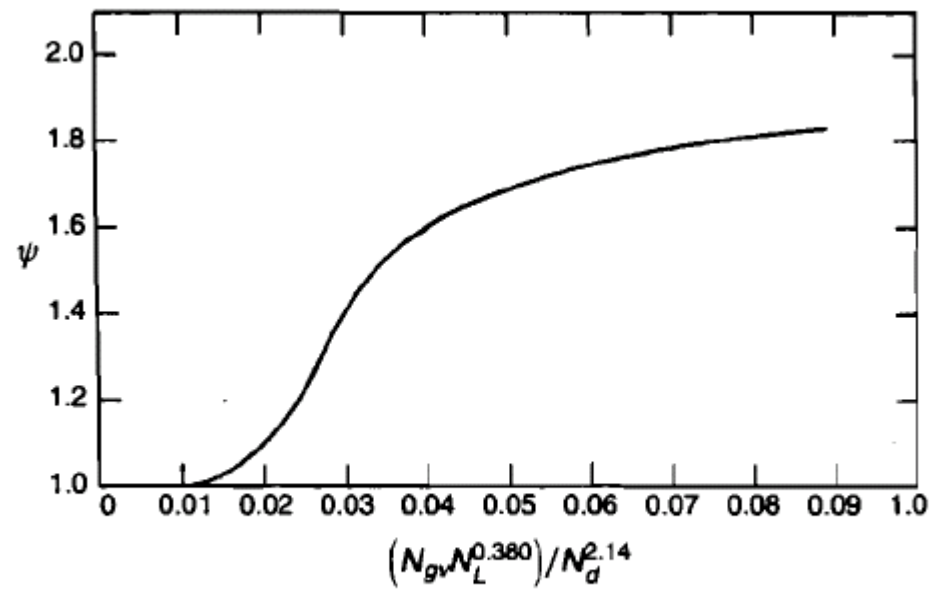


Fig. 4.3—Hagedorn and Brown<sup>4</sup> correlation for  $N_{LC}$ .



**Fig. 4.4—Hagedorn and Brown<sup>4</sup> correlation for  $\psi$ .**

***Friction-Factor Prediction.*** Hagedorn and Brown assumed that two-phase friction factors could be predicted in the same way as single-phase friction factors. Thus,  $f$  is obtained from the single-phase Moody diagram in Fig. 2.2 for a given relative roughness and a two-phase Reynolds number defined as

$$N_{Re} = \frac{\rho_n v_m d}{\mu_s}, \dots \dots \dots (4.7)$$



**Acceleration Term.** The pressure gradient resulting from acceleration is given by

$$\left(\frac{dp}{dZ}\right)_{acc} = \frac{\rho_s \Delta(v_m^2)}{2dZ}, \dots\dots\dots (4.8)$$

where

$$\Delta(v_m^2) = v_{m1}^2 - v_{m2}^2.$$

and 1, 2 designate downstream and upstream ends of a calculation increment, respectively.

If  $E_k$  is defined as

$$E_k = \frac{dZ}{dp} \left(\frac{dp}{dZ}\right)_{acc} = \frac{\rho_s \Delta(v_m^2)}{2dp}, \dots\dots\dots (4.9)$$

$$\frac{dp}{dZ} = \frac{\left(\frac{dp}{dZ}\right)_{el} + \left(\frac{dp}{dZ}\right)_f}{1 - E_k} \dots\dots\dots (4.10)$$

**Example 4.2—Using the Modified Hagedorn and Brown Method, Calculate the Vertical, Multiphase-Flow Pressure Gradient for Example 3.2.**

Given:  $\mu_o = 0.97$  cp,  $\sigma_o = 8.41$  dynes/cm,  $\mu_g = 0.016$  cp, and  $\varepsilon = 0.00006$  ft.

**3.2.3 Volumetric Flow Rates.** After mass transfer calculations are completed, it is possible to calculate the in-situ volumetric flow rates of each phase. For the black-oil model, volumetric flow rates are determined from

$$q_o = q_{o_{sc}} B_o, \dots\dots\dots (3.1)$$

$$q_w = q_{w_{sc}} B_w, \dots\dots\dots (3.2)$$

and

$$q_g = (q_{g_{sc}} - q_{o_{sc}} R_s - q_{w_{sc}} R_{sw}) B_g, \dots\dots\dots (3.3)$$

where  $B_g$  is derived from the engineering equation of state to be

$$B_g = p_{sc} ZT / pZ_{sc} T_{sc} \dots\dots\dots (3.4)$$

Appendix B gives methods to predict gas compressibility,  $Z$ .

For the compositional model, volumetric flow rates are calculated from

$$q_L = \frac{w_l(1 - x_g)}{\rho_L} \dots\dots\dots (3.5)$$

and

$$q_g = w_l x_g / \rho_g, \dots\dots\dots (3.6)$$

where  $x_g$  is the no-slip quality or gas mass fraction and is obtained from the results of a VLE calculation as follows,

$$x_g = \frac{VM_g}{VM_g + LM_L} \dots\dots\dots (3.7)$$

**Example 3.2—Superficial Velocities: Black-Oil Model.** An oil well is flowing 10,000 STBO/D with a producing gas/oil ratio of 1,000 scf/STBO or a gas-production rate of 10 MMscf/D. At a location in the tubing where the pressure and temperature are 1,700 psia and 180°F, calculate the in-situ volumetric flow rates and superficial velocities of the liquid and gas phases. Also calculate the mixture velocity and the no-slip liquid holdup. The following is known from the pressure/volume/temperature (PVT) example problem given in Appendix B.

$$\begin{aligned} B_o &= 1.197 \text{ bbl/STBO} \\ B_g &= 0.0091 \text{ ft}^3/\text{scf} \\ R_s &= 281 \text{ scf/STBO} \\ d &= 6.0 \text{ in.} \end{aligned}$$

$$A_p = \frac{\pi}{4} d^2 = \frac{\pi}{4} \left( \frac{6}{12} \right)^2 = 0.196 \text{ ft}^2.$$

With Eq. 3.1,

$$\begin{aligned} q_o &= \frac{(10,000 \text{ STBO/D})(1.197 \text{ bbl/STBO})(5.614 \text{ ft}^3/\text{bbl})}{86,400 \text{ sec/D}} \\ &= 0.778 \text{ ft}^3/\text{sec.} \end{aligned}$$

With Eq. 3.10,

$$v_{SL} = \frac{q_L}{A_p} = \frac{0.778}{0.196} = 3.97 \text{ ft/sec.}$$

With Eq. 3.3,

$$q_g = \frac{[10 \times 10^6 - (10,000)(281)](0.0091)}{86,400} = 0.757 \text{ ft}^3/\text{sec.}$$

With Eq. 3.11,

$$v_{Sg} = q_g/A_p = 0.757/0.196 = 3.86 \text{ ft/sec.}$$

With Eq. 3.12,

$$v_m = v_{SL} + v_{Sg} = 3.97 + 3.86 = 7.83 \text{ ft/sec.}$$

With Eq. 3.8,

$$\lambda_L = \frac{q_L}{q_L + q_g} = \frac{0.778}{0.778 + 0.757} = 0.507.$$

1. Determine Duns and Ros dimensionless groups:

$$\begin{aligned} N_{Lv} &= 1.938 v_{SL} \left( \frac{\rho_L}{\sigma_L} \right)^{1/4} \\ &= (1.938)(3.97) \left( \frac{47.61}{8.41} \right)^{0.25} = 11.87, \end{aligned}$$

$$\begin{aligned} N_{gv} &= 1.938 v_{Sg} \left( \frac{\rho_L}{\sigma_L} \right)^{1/4} \\ &= (1.938)(3.86) \left( \frac{47.61}{8.41} \right)^{0.25} = 11.54, \end{aligned}$$

$$\begin{aligned} N_d &= 120.872 d \sqrt{\frac{\rho_L}{\sigma_L}} \\ &= (120.872) \left( \frac{6}{12} \right) \sqrt{\left( \frac{47.61}{8.41} \right)} = 143.8, \end{aligned}$$

and

$$\begin{aligned} N_L &= 0.15726 \mu_L \left( \frac{1}{\rho_L \sigma_L^3} \right)^{1/4} \\ &= (0.15726)(0.97) \left[ \frac{1}{(47.61)(8.41)^3} \right]^{0.25} = 0.0118. \end{aligned}$$

2. Determine liquid holdup:

From Fig. 4.3,  $N_{LC} = 0.0024$ .

From Fig 4.2, the abscissa,  $a$ , is

$$\begin{aligned} a &= \frac{N_{Lv} N_{LC}}{N_{gV}^{0.575} N_d} \left( \frac{p}{p_{sc}} \right)^{0.1} \\ &= \frac{(11.87)(0.0024)}{(11.54)^{0.575} (143.8)} \left( \frac{1,700}{14.7} \right)^{0.1} \\ &= 7.81 \times 10^{-5} \end{aligned}$$

$$\therefore \frac{H_L}{\psi} = 0.3.$$

From Fig. 4.4, the abscissa,  $a$ , is

$$\begin{aligned} a &= \frac{N_{gv} N_L^{0.380}}{N_d^{2.14}} \\ &= \frac{(11.42)(0.0118)^{0.380}}{(143.8)^{2.14}} \\ &= 5.1 \times 10^{-5} \end{aligned}$$

$$\therefore \psi = 1.0$$

and

$$H_L = \frac{H_L}{\psi} \psi = (0.3)(1.0) = 0.3.$$

3. Check validity of  $H_L$ :  
Because  $H_L < \lambda_L$ , set  $H_L = \lambda_L = 0.507$ .

4. Calculate slip density:

$$\begin{aligned}\rho_s &= \rho_L H_L + \rho_g (1 - H_L) \\ &= (47.61)(0.507) + (5.88)(1 - 0.507) \\ &= 27.04 \text{ lbm/ft}^3.\end{aligned}$$

5. Determine friction factor:

From Eq. 3.19,

$$\begin{aligned}\mu_s &= (0.97)^{0.507}(0.016)^{(1-0.507)} \\ &= 0.13 \text{ cp.}\end{aligned}$$

From Eq. 4.7,

$$\begin{aligned}N_{Re} &= \frac{(1,488)(27.04)(7.83)(0.5)}{0.13} \\ &= 1.21 \times 10^6\end{aligned}$$

and

$$\frac{\varepsilon}{d} = \left(\frac{0.00006}{0.5}\right) = 0.00012.$$

From Fig. 2.2 or Eq. 2.17,  $f = 0.0135$ .

6. Determine pressure gradient, neglecting kinetic energy effects:

From Eq. 4.2,

$$\begin{aligned}\frac{dp}{dZ} &= \frac{(0.0135)(27.04)^2(7.83)^2}{(2)(27.04)(32.174)(0.5)} + (27.04)\frac{(32.174)}{(32.174)} \\ &= 0.70 + 27.04 = 27.74 \text{ psf/ft} \\ &= 0.193 \text{ psi/ft.}\end{aligned}$$

7. If calculations had been made with the incorrect liquid-holdup value of 0.3, the pressure gradient would have been 0.14 psi/ft.



*Modifications.* Over the years, several modifications have been proposed to improve the Hagedorn and Brown pressure-gradient predictions.

In conversations with Hagedorn, he suggested the first modification when he found that the correlation did not predict accurate pressure gradients for bubble flow. He suggested that, if the Griffith and Wallis<sup>13</sup> criteria predicted the occurrence of bubble flow, the Griffith<sup>14</sup> bubble-flow method should be used to predict pressure gradient. This approach is part of the Orkiszewski<sup>8</sup> method, presented later.

The second modification is much more significant and is possibly a result of Hagedorn and Brown correlating pseudo liquid-holdup values rather than measured ones. Liquid-holdup values obtained from Figs. 4.2 through 4.4 are often less than no-slip holdup values. This is physically impossible because, for upward multiphase flow, liquid cannot travel faster than the gas phase. When this incorrect prediction occurs, the liquid-holdup value must be replaced with one that is physically possible. The approach normally used is to proceed with the no-slip liquid holdup. No attempt has been made to investigate whether this problem is peculiar to a specific range of variables.

## **General Recommendations**

In general, the Orkiszewski and Hagedorn & Brown model are found to perform satisfactorily for vertical wells with or without water-cut, and should therefore be considered equally as the first choice in such wells. As mentioned earlier, the Duns & Ros correlation is not applicable for wells with water-cut and should be avoided for such cases. The Beggs & Brill method is applicable for inclined wells with or without water-cut and is currently the best choice available for deviated wells. However, the method can also be utilized for vertical wells as the last choice. Finally, it should be noted that the performance of the multiphase flow models may not always be affected entirely by the particular flow variable against which the performance trend is indicated. In most cases, the performance of these models may be dependent on a combination of several of these flow variables considered. Therefore, keeping these limitations in mind, the above discussion could be used as a guide to eliminate or select a particular correlation in the absence of other relevant information.

Example Problem by Hagedorn - Brown Method

Given:

$$v_{sg} = 4.09 \text{ ft/sec}$$

$$p = 720 \text{ psia}$$

$$v_{sL} = 2.65 \text{ ft/sec}$$

$$T = 128^\circ \text{ F}$$

$$d = 0.249 \text{ ft} = 3.00 \text{ in.}$$

$$\mu_o = 18 \text{ cp}$$

$$N_{Lv} = 6.02$$

$$\mu_g = .018 \text{ cp}$$

$$N_{gv} = 9.29$$

$$\rho_L = 56.6 \text{ lbm/cu ft}$$

$$N_L = 0.08$$

$$\rho_g = 2.84 \text{ lbm/cu ft}$$

$$N_d = 41.34$$

$$e/d = .0006$$

Neglecting acceleration, calculate the flowing pressure gradient at these conditions.

### Lockhart and Martinelli Correlation

The Lockhart and Martinelli<sup>32</sup> correlation does not follow the friction factor analogy but presents the two-phase pressure gradient in terms of a single-phase gradient multiplied by a correction factor. The single-phase gradients are calculated as if each phase flowed in the pipe alone. Although a correlation is given for liquid holdup, it is not required for pressure drop calculations. Acceleration was ignored in the Lockhart and Martinelli method.

$$\frac{dp}{dX} = \phi_g^2 \left( \frac{dp}{dX} \right)_g = \phi_L^2 \left( \frac{dp}{dX} \right)_L \dots\dots\dots 4.21$$

where  $\left( \frac{dp}{dX} \right)_g = \frac{f_g \rho_g v_{sg}^2}{2 g_c d}$ ,

and  $\left( \frac{dp}{dX} \right)_L = \frac{f_L \rho_L v_{sL}^2}{2 g_c d}$

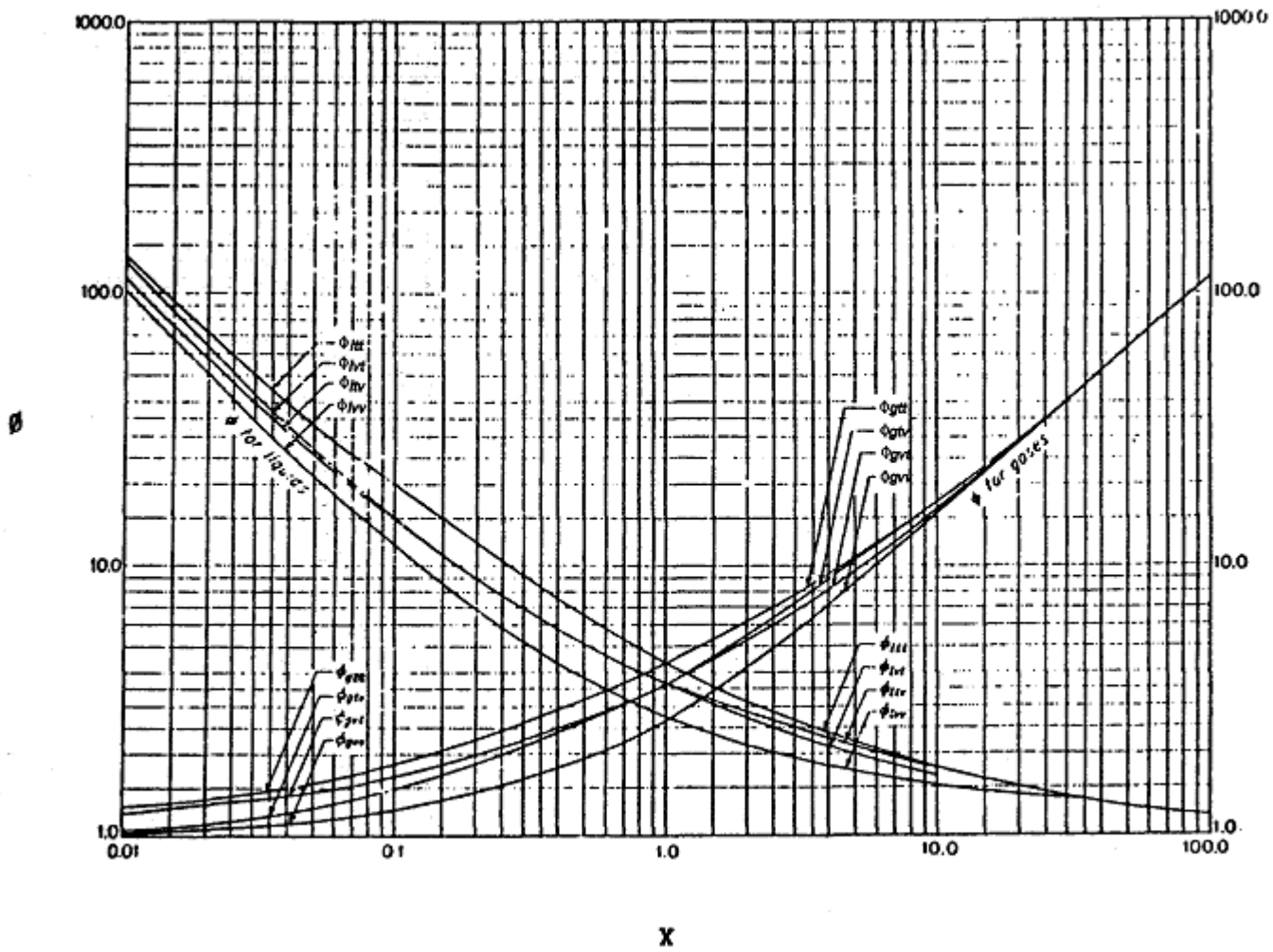
The friction factors  $f_g$  and  $f_L$  are determined from Fig. 3.9 for values of the Reynolds numbers.

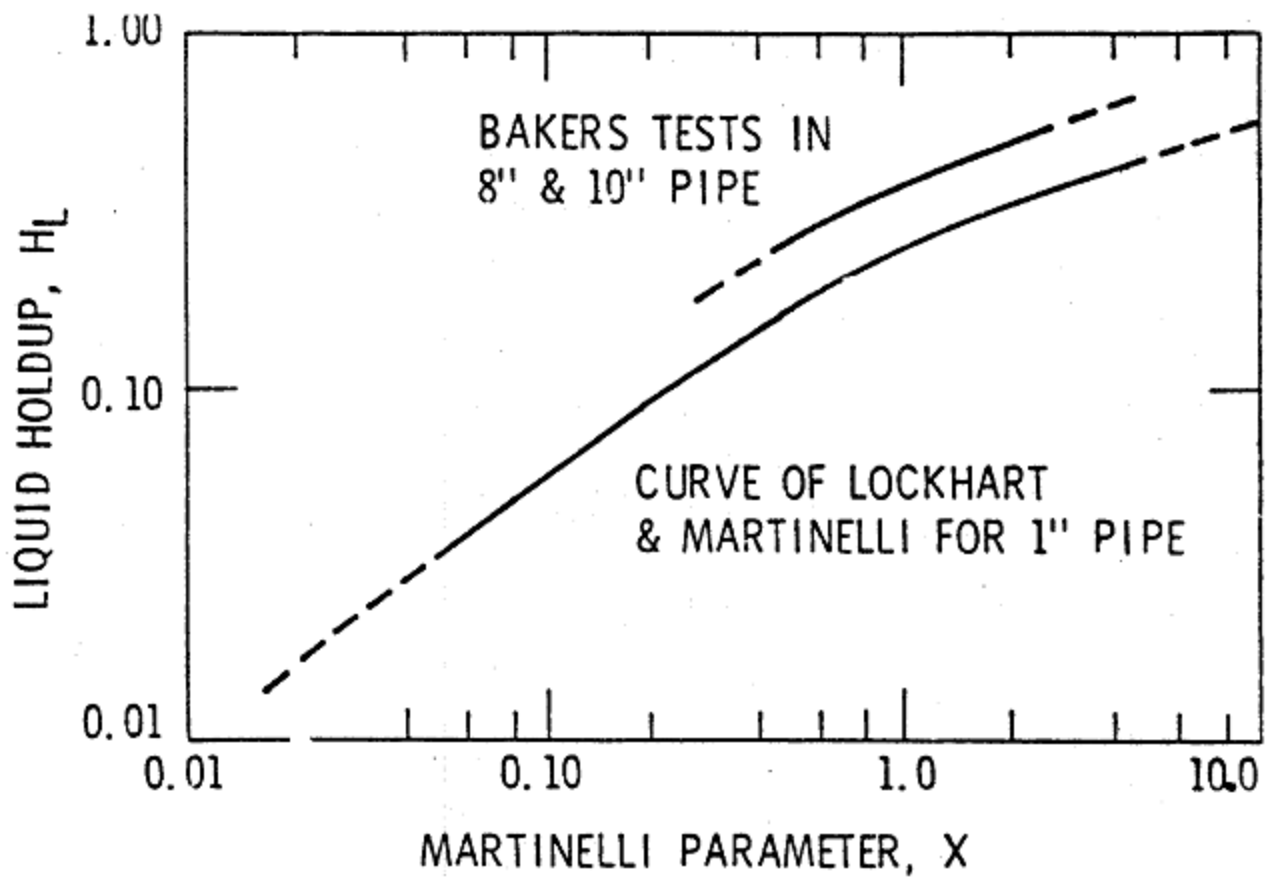
$$N_{\text{Reg}} = \frac{\rho_g v_{sg} d}{\mu_g} \quad \text{and} \quad N_{\text{ReL}} = \frac{\rho_L v_{sL} d}{\mu_L}$$

The two-phase correction factors are correlated with a parameter defined as

$$X = \left[ \left( \frac{dp}{dX} \right)_L / \left( \frac{dp}{dX} \right)_g \right]^{0.5} \dots\dots\dots 4.22$$

The correlation is shown graphically in Fig. 4.7. They found that different curves existed for each  $\phi$  depending on the Reynolds number of each phase. They considered that laminar flow existed in a phase if the Reynolds number for that phase was less than 1000. The subscripts on the  $\phi$  terms represent turbulent or laminar flow, with the first subscript representing the liquid phase. For example,  $\phi_{\text{LtL}}$  is the correction factor applied to the single-phase liquid pressure gradient when the liquid phase is turbulent and the gas phase is laminar.







Sessions 9 and 10:  
two phase flow through restrictions

Three restrictions commonly found in oil and gas production operations are chokes (or choke beans or positive-flow beans), velocity-controlled subsurface safety valves, and conventional valves and fittings, often called piping components.

Chokes are installed in wells to control flow rates or pressures. They normally have slightly rounded entrances and can be several inches long. For example, the Thornhill-Craver choke beans are about 6 in. long with diameters from  $\frac{1}{8}$  to  $\frac{3}{4}$  in.<sup>1</sup> Fig. 5.1 shows a typical choke schematic.

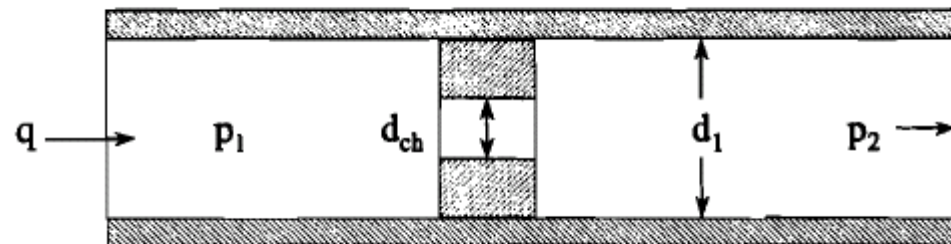


Fig. 5.1—Choke schematic.

The Willis choke<sup>2</sup> shown in Fig. 5.2 is an example of an MOV. This choke consists of a stationary ceramic disk and a movable ceramic disk, each with two holes. The size of the opening can be changed by rotating the movable disk relative to the stationary disk, as shown in Fig. 5.3. When changing the opening size, the resulting flow path can cause the fluids to impact on the pipe wall downstream of the valve, potentially causing erosion problems. Erosion concepts are described in Chap. 6.

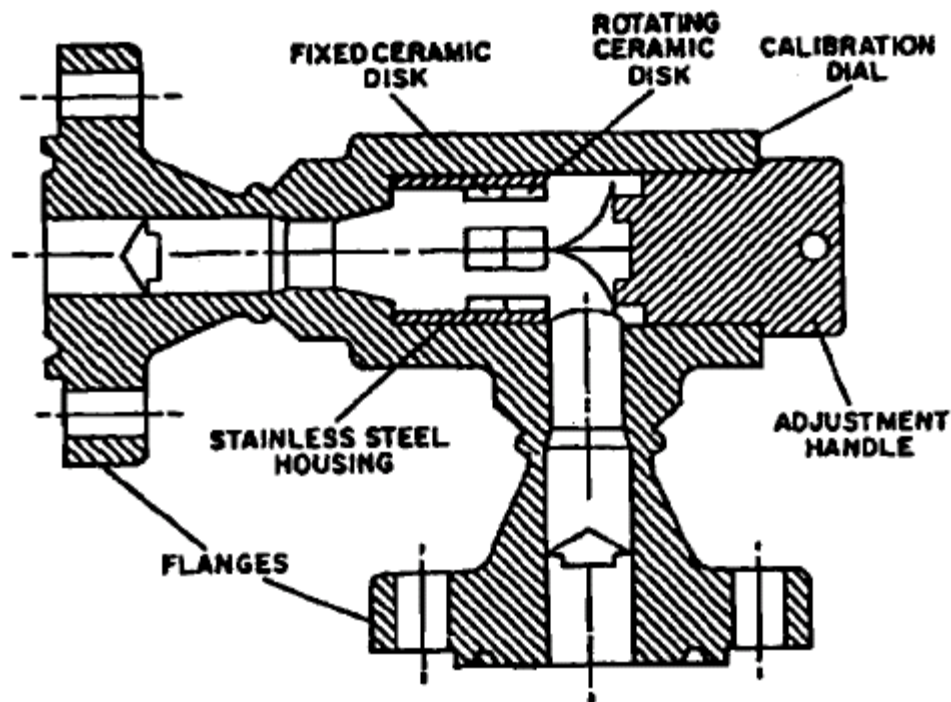


Fig. 5.2—Multiple orifice valve wellhead choke design (after Willis Oil Tool Co.<sup>2</sup>).

**5.3.1 Single-Phase Liquid Flow.** Single-phase liquid flow seldom occurs in wellhead chokes because wellhead pressures are almost always below the bubblepoint pressure of the produced fluids. Because sonic velocities are high for single-phase liquids, flow behavior is always subcritical. Eq. 5.1, which can be developed from a combination of Bernoulli's equation<sup>4</sup> and conservation of mass, describes single-phase flow of an incompressible liquid through a choke.

$$q = CA \sqrt{\frac{2g_c \Delta p}{\rho}} \dots \dots \dots (5.1)$$

In oil field units, this equation becomes

$$q = 22,800Cd_{ch}^2 \sqrt{\frac{\Delta p}{\rho}} \dots \dots \dots (5.2)$$

where  $q$  is in B/D and  $d_{ch}$  = the choke diameter in inches. Choke diameter is frequently called "bean" size and is measured in 64ths of an inch.

The flow coefficient,  $C$ , in Eqs. 5.1 and 5.2 accounts for all irreversibilities, such as friction.  $C$  can be determined experimentally and depends primarily on the type of restriction (i.e., venturi, nozzle, orifice, or choke), the ratio of the restriction diameter to the pipe diameter, and the Reynolds number. **Fig. 5.6** shows the flow-coefficient behavior for a nozzle.

**5.3.2 Single-Phase Gas Flow.** For gases, Bernoulli's equation can be combined with an isentropic (adiabatic-frictionless) equation of state. All irreversible losses are accounted for through a discharge coefficient. The resulting Eq. 5.3<sup>7</sup> is applicable for both critical and subcritical flow. However, for critical flow, the pressure ratio  $y = p_2/p_1$  is replaced by the critical-pressure ratio,  $y_c$ .

$$q_{sc} = \frac{C_n p_1 d_{ch}^2}{\sqrt{\gamma_g T_1 Z_1}} \sqrt{\left(\frac{k}{k-1}\right) \left(y^{\frac{2}{k}} - y^{\frac{k+1}{k}}\right)} \dots \dots \dots (5.3)$$

where

$$C_n = \frac{C_s C_D T_{sc}}{p_{sc}} \dots \dots \dots (5.4)$$

**Table 5.1** gives values for the constants in Eqs. 5.3 and 5.4 for both customary and SI units.

The critical-pressure ratio for a gas with a ratio of specific heats  $k = C_p/C_v$  is given by

$$y_c = \left(\frac{p_2}{p_1}\right)_c = \left(\frac{2}{k+1}\right)^{\frac{k}{k-1}} \dots \dots \dots (5.5)$$

**TABLE 5.1—CONSTANTS AND UNITS FOR EQS. 5.3<sup>7</sup> AND 5.4**

Symbol	Customary	SI Metric
$q_{sc}$	Mscf/D	m <sup>3</sup> /d
$d_{ch}$	in.	mm
$p$	psia	kPa
$T$	°R	K
$C_s$	27.611	1.6259
$C_D$	0.865	0.865
$p_{sc}$	14.696 psia	101.325 kPa
$T_{sc}$	519.68 °R	273.16 K
$C_n$	844.57	3.7915

**Critical-Flow Boundary.** Several authors have developed methods to predict the critical-flow boundary in multiphase flow.

*Ashford and Pierce.* Ashford and Pierce<sup>8</sup> developed an expression for total-mass flow rate of a multiphase mixture. They assumed isentropic flow through the restriction, an incompressible liquid, no liquid flashing in the choke, and a homogeneous mixture. Eq. 5.6 assumes the derivative of the flow rate with respect to pressure ratio is zero at the critical boundary.

$$y_c = \frac{\frac{2R_1}{k\left(1 + R_1 y_c^{-\frac{1}{k}}\right)} \left[ \left(\frac{R_1}{b}\right) (1 - y_c^b) - y_c + 1 \right] y_c^{-e} - 1}{R_1}, \quad \dots \dots \dots (5.6)$$

where

$$b = \frac{k - 1}{k}$$

and

$$e = \frac{k + 1}{k}.$$

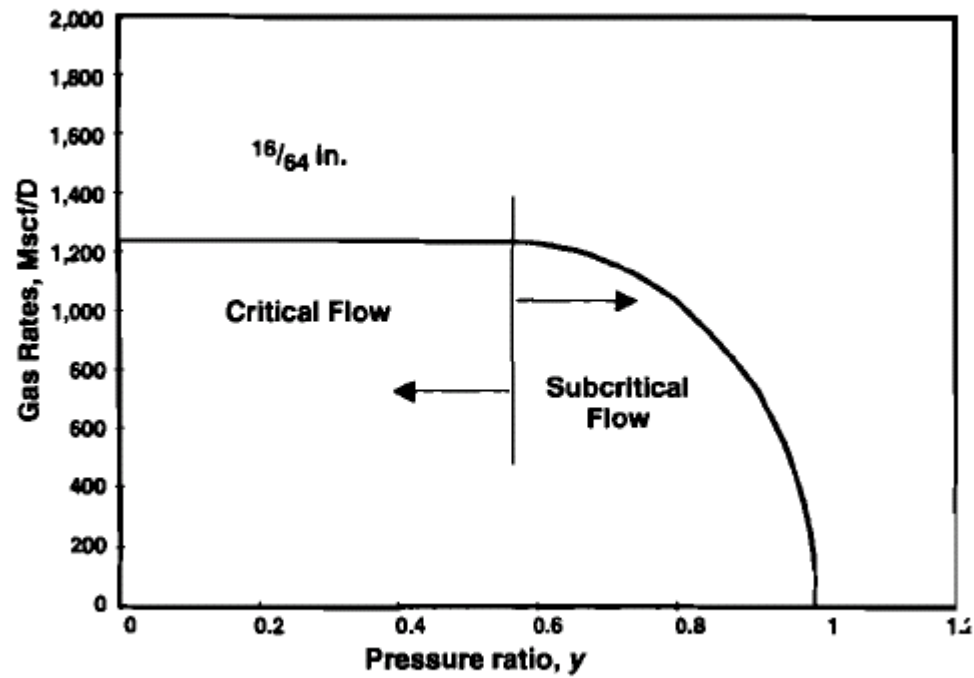


Fig. 5.5—Dependence of choke flow rate on  $y$ .







## Pipeline inspection gauge

---

A pipeline inspection gauge or pig in the [pipeline](#) industry is a tool that is sent down a pipeline and propelled by the [pressure](#) of the product in the pipeline itself. There are four main uses for pigs:

1. physical separation between different liquids being transported in pipelines;
2. internal cleaning of pipelines;
3. inspection of the condition of pipeline walls (also known as an Inline Inspection (ILI) tool);
4. capturing and recording geometric information relating to pipelines (e.g. size, position).



# Session 11: Mechanistic models



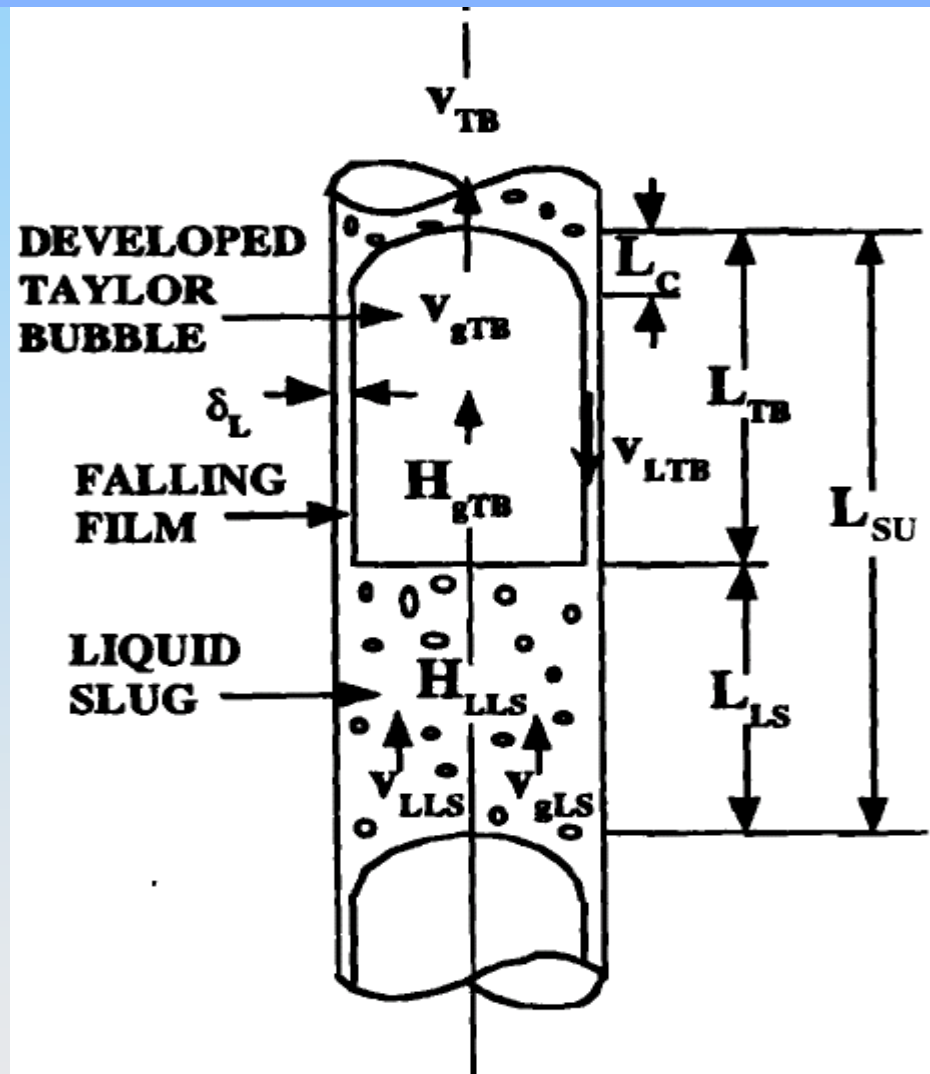


Fig. 4.23—Slug-flow schematic.<sup>24</sup>

The Taylor-bubble-rise velocity is equal to the centerline velocity plus the Taylor-bubble-rise velocity in a stagnant liquid column.

$$v_{TB} = 1.2v_m + 0.35 \left[ \frac{gd(\rho_L - \rho_g)}{\rho_L} \right]^{1/2} \dots \dots \dots (4.190)$$

$$v_{gLS} = 1.2v_m + 1.53 \left[ \frac{g\sigma_L(\rho_L - \rho_g)}{\rho_L^2} \right]^{1/4} H_{LLS}^{0.5} \dots \dots \dots (4.191)$$

$$H_{gLS} = \frac{v_{Sg}}{0.425 + 2.65v_m} \dots \dots \dots (4.194)$$

$$\bar{A} = H_{gLS}(v_{TB} - v_{gLS}) + v_m. \quad (4.196)$$

With  $v_{TB}$  and  $H_{gLS}$  given by Eqs. 4.190 and 4.194, respectively,  $\bar{A}$  can be determined readily from Eq. 4.196. Eq. 4.195 can be solved for  $H_{LTB}$  by use of an iterative-solution method. Defining the left side of Eq. 4.195 as  $F(H_{LTB})$ ,

$$F(H_{LTB}) = (9.916 \sqrt{gd}) (1 - \sqrt{1 - H_{LTB}})^{0.5} H_{LTB} - v_{TB}(1 - H_{LTB}) + \bar{A}. \quad (4.197)$$

The derivative of Eq. 4.197 with respect to  $H_{LTB}$  yields

$$F'(H_{LTB}) = v_{TB} + (9.916 \sqrt{gd}) \times (1 - \sqrt{1 - H_{LTB}})^{0.5} + \frac{H_{LTB}}{4 \sqrt{1 - H_{LTB}}(1 - \sqrt{1 - H_{LTB}})} \quad (4.198)$$

Eqs. 4.197 and 4.198 suggest that the Newton-Raphson approach can be incorporated easily to determine  $H_{LTB}$ , the root of Eq. 4.197. Vo and Shoham also showed that, if a root exists in the interval of (0,1), the root is unique. Thus,

$$H_{LTB_{j+1}} = H_{LTB_j} - \frac{F(H_{LTB_j})}{F'(H_{LTB_j})} \quad (4.199)$$



The velocity  $v_{LTB}$  of the falling film around the Taylor bubble can be correlated with the film thickness,  $\delta_L$  by use of the Brotz<sup>41</sup> expression,

$$v_{LTB} = \sqrt{196.7g\delta_L}, \dots\dots\dots (4.192)$$

where  $\delta_L$  is the constant film thickness for fully developed slug flow. From geometrical considerations,  $v_{LTB}$  can be expressed in terms of the Taylor-bubble void fraction to give

$$v_{LTB} = 9.916 \left[ gd \left( 1 - \sqrt{H_{gTB}} \right) \right]^{1/2} \dots\dots\dots (4.193)$$

The liquid-slug void fraction can be obtained from the correlation developed by Sylvester,<sup>40</sup> who used data from Fernandes *et al.*<sup>39</sup> and Schmidt.<sup>42</sup>

Mass balances for steady-state liquid and gas transfer between the liquid slug and the Taylor bubble, respectively, are

$$(v_{TB} - v_{LLS})H_{LLS} = [v_{TB} - (-v_{LTB})]H_{LTB} \dots\dots\dots (4.188)$$

and

$$(v_{TB} - v_{gLS})(1 - H_{LLS}) = (v_{TB} - v_{gTB})(1 - H_{LTB}).$$

\dots\dots\dots (4.189)

For fully developed slug flow, the elevation component of the pressure gradient occurring across a slug unit is given by

$$\left(\frac{dp}{dL}\right)_{el} = [(1 - \beta)\rho_{LS} + \beta\rho_g]g \sin \theta, \dots\dots\dots (4.200)$$

where

$$\rho_{LS} = \rho_L H_{LS} + \rho_g(1 - H_{LS}). \dots\dots\dots (4.201)$$

Eq. 4.200 assumes that the liquid film around the Taylor bubble does not contribute to the elevation component. Friction losses were assumed to occur only across the liquid slug and are neglected along the Taylor bubble. Therefore, the friction component of the pressure gradient is

$$\left(\frac{dp}{dL}\right)_f = \frac{f_{LS}\rho_{LS}v_m^2}{2d}(1 - \beta), \dots\dots\dots (4.202)$$

where  $f_{LS}$  is obtained from a Moody diagram (Fig. 2.2) for a Reynolds number defined by

$$N_{Re_{LS}} = \frac{\rho_{LS}v_m d}{\mu_{LS}}. \dots\dots\dots (4.203)$$

# Session 12: slug and pigs

# Session 13:

## Heat Transfer in Multiphase flow

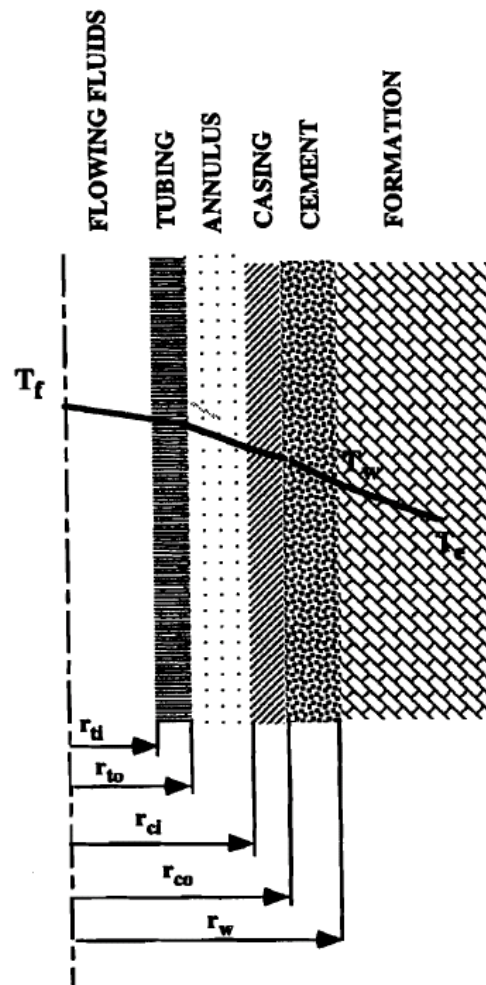


Fig. 2.7—Cross section of typical wellbore.<sup>3</sup> (Reproduced with permission of the McGraw-Hill Cos.)

### 2.6 Conservation of Energy

Application of energy conservation to fluid flow in pipes requires that in a given pipe segment the energy in, minus the energy out, plus the heat energy transferred to or from the surroundings must equal the rate of energy accumulation.<sup>15</sup>

$$\frac{\partial}{\partial t}(\rho e) = \frac{\partial}{\partial L} \left[ \rho v \left( e + \frac{p}{\rho g_c J} \right) \right] + \frac{Q \pi d}{A} \dots \dots \dots (2.65)$$

For steady-state flow, Eq. 2.65 reduces to

$$\frac{d}{dL} \left[ \rho v \left( e + \frac{p}{\rho g_c J} \right) \right] = \frac{-Q \pi d}{A} \dots \dots \dots (2.66)$$

The parameter  $J$  is the mechanical equivalent of heat and is necessary when dealing with customary units where mechanical energy and thermal energy have different units.

Expanding the left side of Eq. 2.66 yields

$$\rho v \frac{d}{dL} \left( e + \frac{p}{\rho g_c J} \right) + \left( e + \frac{p}{\rho g_c J} \right) \frac{d(\rho v)}{dL} = \frac{-Q\pi d}{A}.$$

..... (2.67)

In Eqs. 2.66 and 2.67,  $e$  is the intrinsic specific energy and is defined by

$$e = \frac{gL \sin \theta}{g_c J} + \frac{1}{2} \frac{v^2}{g_c J} + u. \quad \text{..... (2.68)}$$

Combining Eqs. 2.67 and 2.68 with Eq. 2.2 from conservation of mass principles yields

$$\rho v \frac{d}{dL} \left( \frac{gL \sin \theta}{g_c J} + \frac{1}{2} \frac{v^2}{g_c J} + u + \frac{p}{\rho g_c J} \right) = \frac{-Q\pi d}{A}.$$

..... (2.69)



Because specific enthalpy is defined as

$$h = u + \frac{P}{\rho g_c J} \dots \dots \dots (2.70)$$

Eq. 2.69 can be expressed as

$$\rho v \frac{g \sin \theta}{g_c J} + \frac{\rho v v}{g_c J} \frac{dv}{dL} + \rho v \frac{dh}{dL} = \frac{-Q \pi d}{A} \dots \dots \dots (2.71)$$

Finally, solving for the enthalpy gradient yields

$$\frac{dh}{dL} = \frac{-Q \pi d}{w} - \frac{v}{g_c J} \frac{dv}{dL} - \frac{g \sin \theta}{g_c J} \dots \dots \dots (2.72)$$

The heat flux,  $Q$ , is defined in terms of overall heat-transfer coefficient and temperature difference between the fluids and the surroundings. Thus,

$$Q = U(T_f - T_e). \dots\dots\dots (2.73)$$

Eq. 2.72 clearly shows that the steady-state enthalpy-gradient equation is made up of three components. Thus,

$$\left(\frac{dh}{dL}\right)_t = \left(\frac{dh}{dL}\right)_{HT} + \left(\frac{dh}{dL}\right)_{acc} + \left(\frac{dh}{dL}\right)_{el}, \dots\dots\dots (2.74)$$

where

$$\left(\frac{dh}{dL}\right)_{HT} = - \frac{U\pi d(T_f - T_e)}{w}. \dots\dots\dots (2.75)$$

**2.6.1 Wellbore Heat Transfer.** When hot reservoir fluids enter a wellbore and begin to flow to the surface, they immediately begin losing heat to the cooler surrounding rock. The surrounding rock gradually heats up, reducing the temperature difference and the heat transfer between the fluids and the rock. Eventually, for a constant-mass flow rate, the earth surrounding the well reaches a steady-state temperature distribution. Prediction of fluid temperatures in the wellbore as a function of depth and time is necessary to determine the fluid's physical properties and calculate pressure gradients.

Because of the high thermal conductivity and relatively small radial distance between the flowing fluids and the borehole wall, heat transfer in this region normally can be considered steady state. All heat lost by the fluids instantaneously flows through the wellbore and into the surrounding rock. An axial cross section of a typical wellbore is shown in **Fig. 2.7**. The following description of steady-state heat transfer in a wellbore would have to be modified for other types of completions.

Heat transfer within the tubing and in a fluid-filled annulus is primarily a result of convection. Heat transfer through the tubing and casing walls and through a cement-filled annulus between the casing and borehole wall primarily results from conduction.

Heat transfer resulting from conduction can be described by Fourier's equation in radial coordinates<sup>15</sup>

$$q = -2\pi r \Delta L k \frac{\partial T}{\partial r}, \dots\dots\dots (2.76)$$

where  $q$  is the amount of heat flowing radially through a solid with thermal conductivity,  $k$ . Integration of Eq. 2.76 gives

$$T_2 - T_1 = \frac{q}{2\pi \Delta L} \frac{\ln\left(\frac{r_1}{r_2}\right)}{k_{1-2}} \dots\dots\dots (2.77)$$

Heat transfer resulting from radial convection can be described by<sup>15</sup>

$$q = 2\pi r \Delta L h \Delta T, \dots\dots\dots (2.78)$$

where  $h$  = local convective-film coefficient.

If steady-state heat transfer occurs in the wellbore,  $q$  is constant. Expressions for temperature change through the wellbore can be developed from Eqs. 2.77 and 2.78 as follows.

For convection in the tubing,

$$T_f - T_{ti} = \frac{q}{2\pi \Delta L} \frac{1}{r_i h_f} \dots\dots\dots (2.79)$$

For conduction through the tubing wall,

$$T_{ti} - T_{to} = \frac{q}{2\pi \Delta L} \frac{\ln\left(\frac{r_{to}}{r_{ti}}\right)}{k_t} \dots\dots\dots (2.80)$$

For convection through the casing/tubing annulus,

$$T_{to} - T_{ci} = \frac{q}{2\pi \Delta L} \frac{1}{r_{ci} h_{an}} \dots\dots\dots (2.81)$$

For conduction through the casing,

$$T_{ci} - T_{co} = \frac{q}{2\pi \Delta L} \frac{\ln\left(\frac{r_{co}}{r_{ci}}\right)}{k_c} \dots\dots\dots (2.82)$$

For conduction through the cement in the casing/borehole annulus,

$$T_{co} - T_w = \frac{q}{2\pi \Delta L} \frac{\ln\left(\frac{r_w}{r_{co}}\right)}{k_{cem}} \dots\dots\dots (2.83)$$

$$T_{co} - T_w = \frac{q}{2\pi\Delta L} \frac{\ln\left(\frac{r_w}{r_{co}}\right)}{k_{cem}} \quad (2.83)$$

Heat transfer into the surrounding rock is by heat conduction and is a transient process. The transient radial-heat-conduction equation is identical to the diffusivity equation encountered in transient well-test analysis.<sup>31</sup> The infinite-reservoir, line-source solution is

$$T_w - T_e = \frac{q}{2\pi\Delta L} \frac{f(t)}{k_e} \quad (2.84)$$

where  $T_e$  = the undisturbed geothermal earth temperature,  $f(t)$ , is given by

$$f(t) = \frac{1}{2} E_i\left(\frac{-r_w^2}{4\alpha t}\right) \quad (2.85)$$

and  $\alpha$  = the earth thermal diffusivity defined as

$$\alpha = \frac{k_e}{\rho C} \quad (2.86)$$

To monitor temperatures at the wellbore, the logarithmic approximation to the  $E_i$  solution is valid for times greater than 1 week.<sup>32</sup> Thus, for  $x < 0.0025$

$$E_i(-x) \approx \ln(x) + 0.5772 \quad (2.87)$$

and

$$f(t) = 0.405 + 0.5 \ln(t_{Dw}), \quad (2.88)$$

where

$$t_{Dw} = \frac{\alpha t}{r_w^2} \quad (2.89)$$

Hasan and Kabir<sup>33</sup> showed that for typical reservoirs Eq. 2.88 can cause significant errors if applied to times less than 250 hours. They presented Eqs. 2.90 and 2.91 as simplified equations that, when used together, are valid for all times.

If  $t_{Dw} \leq 1.5$ ,

$$f(t) = 1.1281 \sqrt{t_{Dw}} (1 - 0.3 \sqrt{t_{Dw}}) \quad (2.90)$$

If  $t_{Dw} > 1.5$ ,

$$f(t) = [0.4063 + 0.5 \ln(t_{Dw})] \left(1 + \frac{0.6}{t_{Dw}}\right) \dots \dots \dots (2.91)$$

Hasan and Kabir<sup>34</sup> also stated that, in most cases of oil production, the temperature difference across the annulus is usually small and convective (natural) heat transfer becomes important. Unfortunately, the literature reports no work on natural convection in vertical annular geometry. Hasan and Kabir recommended using

$$h_{an} = \frac{0.049(N_{Gr}N_{Pr})^{1/3} N_{Pr}^{0.074} k_{an}}{r_{to} \ln\left(\frac{r_{ci}}{r_{to}}\right)} \dots \dots \dots (2.92)$$

where the Grashof number,  $N_{Gr}$ , reflects the extent of motion of the annulus fluid resulting from natural convection:

$$N_{Gr} = \frac{(r_{ci} - r_{to})^3 g \rho_{an}^2 \beta (T_{to} - T_{ci})}{\mu_{an}^2} \dots \dots \dots (2.93)$$

The density of the heated fluid next to the tubing wall is less than the fluid next to the casing, creating a buoyancy force. The product of  $\beta$  (coefficient of thermal expansion) and the temperature difference is a measure of the density difference. The viscous force working against the buoyancy generates a circular motion of the fluid in the annulus. The Prandtl number,  $N_{Pr}$ , is a measure of the interaction between the hydrodynamic boundary layer and the thermal boundary layer and is defined as

Combining Eqs. 2.79 through 2.84 determines the total temperature change between the fluids and the undisturbed geothermal temperature of the surrounding rock.

$$T_f - T_e = \frac{q}{2\pi\Delta L} \left[ \frac{1}{r_o h_f} + \frac{\ln\left(\frac{r_{io}}{r_{ii}}\right)}{k_t} + \frac{1}{r_{ci} h_{an}} + \frac{\ln\left(\frac{r_{co}}{r_{ci}}\right)}{k_c} + \frac{\ln\left(\frac{r_w}{r_{co}}\right)}{k_{cem}} + \frac{f(t)}{k_e} \right] \dots \dots \dots (2.95)$$

A simple expression for the total heat loss from the fluids in the tubing can be estimated from Newton's law of cooling,<sup>15</sup>

$$q = 2\pi r_o \Delta L U \Delta T, \dots \dots \dots (2.96)$$

where  $U$  = an overall heat-transfer coefficient. Comparing Eqs. 2.95 and 2.96, it is evident that  $(r_o U)^{-1}$  is the bracketed term in Eq. 2.95.



# Temperature profile

Because enthalpy is a state property,  $h = h(p, T)$ , a change in enthalpy can be calculated by considering effects of temperature and pressure separately. Thus,

$$\begin{aligned} dh &= \left(\frac{\partial h}{\partial T}\right)_p dT + \left(\frac{\partial h}{\partial p}\right)_T dp \\ &= C_p dT + \left(\frac{\partial h}{\partial p}\right)_T dp. \dots\dots\dots (2.97) \end{aligned}$$

Consider an isenthalpic process so that

$$dh = 0 = C_p dT + \left(\frac{\partial h}{\partial p}\right)_T dp,$$

or

$$\left(\frac{\partial h}{\partial p}\right)_T = -C_p \left(\frac{dT}{dp}\right)_h = -C_p \eta, \dots\dots\dots (2.98)$$

where  $\eta$  = the Joule-Thompson coefficient and represents isenthalpic cooling (or heating) by expansion. Combining Eqs. 2.97 and 2.98 gives

$$dh = C_p dT - C_p \eta dp. \dots\dots\dots (2.99)$$

Combining Eqs. 2.99 and 2.72 gives

$$\begin{aligned} C_p \frac{dT_f}{dL} - C_p \eta \frac{dp}{dL} = \\ -\frac{g \sin \theta}{g_c J} - \frac{v}{g_c J} \frac{dv}{dL} - \frac{U \pi d}{w} (T_f - T_e). \dots\dots\dots (2.100) \end{aligned}$$

Eq. 2.100 can be simplified to this differential equation.

$$\frac{dT_f}{dL} + \frac{T_f}{A} = \frac{T_e}{A} + \frac{1}{J \rho C_p} \frac{dp}{dL} \phi, \dots\dots\dots (2.101)$$

where

$$A = \frac{C_p w}{U \pi d} \dots \dots \dots (2.102)$$

and

$$\phi = \left[ \frac{J \rho \eta C_p \frac{dp}{dL} - \frac{\rho g \sin \theta}{g_c} - \frac{\rho v}{g_c} \frac{dv}{dL}}{\frac{dp}{dL}} \right] \dots \dots \dots (2.103)$$

If the surrounding temperature varies linearly with depth,

$$T_e = T_{ei} - g_G L \sin \theta, \dots \dots \dots (2.104)$$

where  $T_{ei}$  = surrounding temperature at the inlet of the pipe and is often taken as the reservoir temperature. The geothermal temperature gradient,  $g_G$ , typically varies from approximately 1.0 to 2.0°F/100 ft of vertical depth, depending on the thickness of the earth crust, presence of volcanic activity, and other such factors.

Combining Eqs. 2.101 and 2.104 yields a generalized differential equation that incorporates both the enthalpy- and pressure-gradient equations with no limiting assumptions. Thus,

$$\frac{dT_f}{dL} + \frac{T_f}{A} = \frac{T_{ei}}{A} - \frac{g_G L \sin \theta}{A} + \frac{1}{J \rho C_p} \frac{dp}{dL} \phi. \dots \dots \dots (2.105)$$

Eq. 2.106 degenerates to all the more restrictive approximate analytical expressions to predict temperatures of fluids flowing in pipes.

For the case of horizontal flow, where  $\theta = 0^\circ$ , and neglecting acceleration effects, Eq. 2.103 simplifies to

$$\phi = J\rho\eta C_p \dots\dots\dots (2.107)$$

and Eq. 2.106 degenerates to

$$T_f = T_{ei} + (T_i - T_{ei})e^{-L/\Lambda} + \eta \frac{dp}{dL} A(1 - e^{-L/\Lambda}) \dots\dots\dots (2.108)$$

Eq. 2.108 is equivalent to the Coulter and Bardon<sup>37</sup> equation to predict temperatures in horizontal pipelines.

For an ideal gas,  $\eta = 0$ , and neglecting acceleration effects, Eq. 2.103 simplifies to

$$\phi = \left[ \frac{-\frac{\rho g \sin \theta}{g_c}}{\frac{dp}{dL}} \right] \dots\dots\dots (2.109)$$

and Eq. 2.106 degenerates to

$$T_f = (T_{ei} - g_G L \sin \theta) + (T_i - T_{ei})e^{-L/\Lambda} + g_G \sin \theta A(1 - e^{-L/\Lambda}) - \frac{g \sin \theta}{Jg_c C_p} A(1 - e^{-L/\Lambda}),$$

For the case of an incompressible liquid,

$$\eta = -\frac{1}{JC_p\rho} \dots\dots\dots (2.111)$$

and

$$\phi = \left[ \frac{-\frac{dp}{dL} - \frac{\rho g \sin\theta}{g_c} - \frac{\rho v}{g_c} \frac{dv}{dL}}{\frac{dp}{dL}} \right] = \left[ \frac{\frac{\tau\pi d}{A}}{\frac{dp}{dL}} \right] \dots\dots\dots (2.112)$$

Neglecting friction,  $\phi = 0$ , and Eq. 2.106 degenerates to

$$T_f = (T_{ei} - g_C L \sin\theta) + (T_i - T_{ei})e^{-L/A} + g_C \sin\theta A(1 - e^{-L/A}), \dots\dots\dots (2.113)$$

which is equivalent to the Ramey expression for incompressible-liquid flow.

Comparison of Eqs. 2.106 and 2.113 shows that the Alves *et al.*<sup>36</sup> solution is actually the Ramey equation for single-phase liquid, plus a correction term. The correction term is a function of the total pressure gradient and the dimensionless parameter,  $\phi$ . Analysis of this dimensionless coefficient can show when consideration of the correction term becomes important.

Calculation of flowing temperatures as a function of depth and time can be very tedious because of the complexity of the overall heat-transfer coefficient in Eq. 2.96. Shiu and Beggs<sup>38</sup> proposed an empirical correlation for  $A$  that was developed from a broad set of flowing-temperature surveys. The resulting equation is independent of time

$$A = 0.0149(w)^{0.5253} (d_{ti})^{-0.2904} (\gamma_{APi})^{0.2608} (\gamma_g)^{4.4146} (\rho_L)^{2.9303}, \dots\dots\dots (2.114)$$

where  $w$  is in pounds per second,  $d_{ti}$  is in inches, and  $\rho_L$  is in pounds per cubic foot

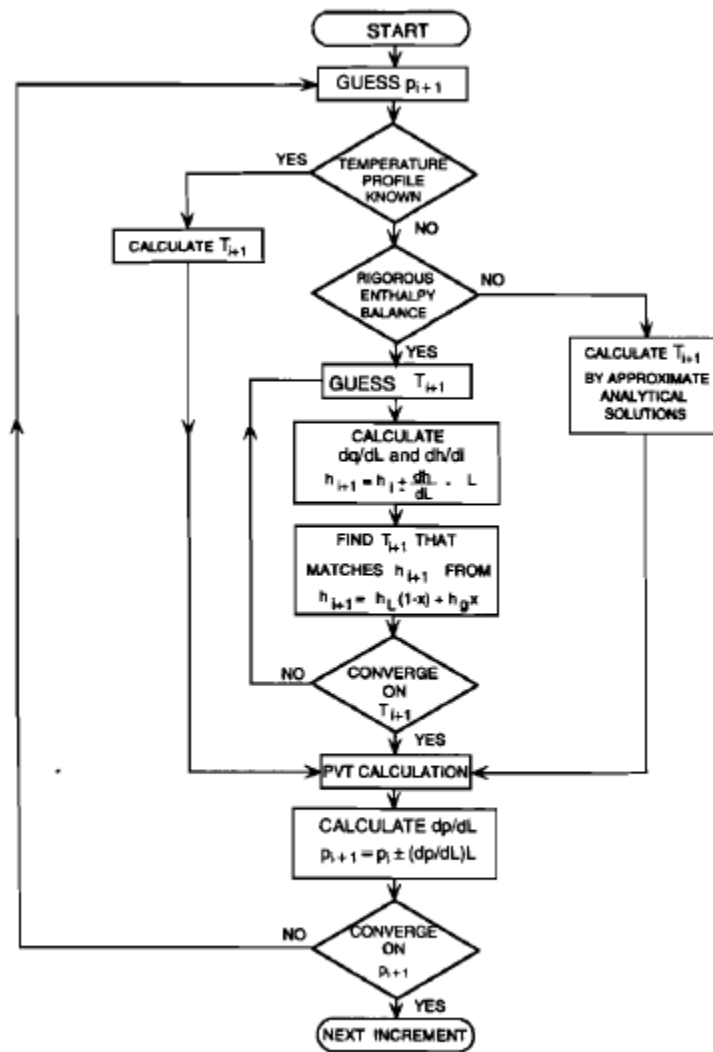


Fig. 3.10—Marching algorithm for a calculation increment.

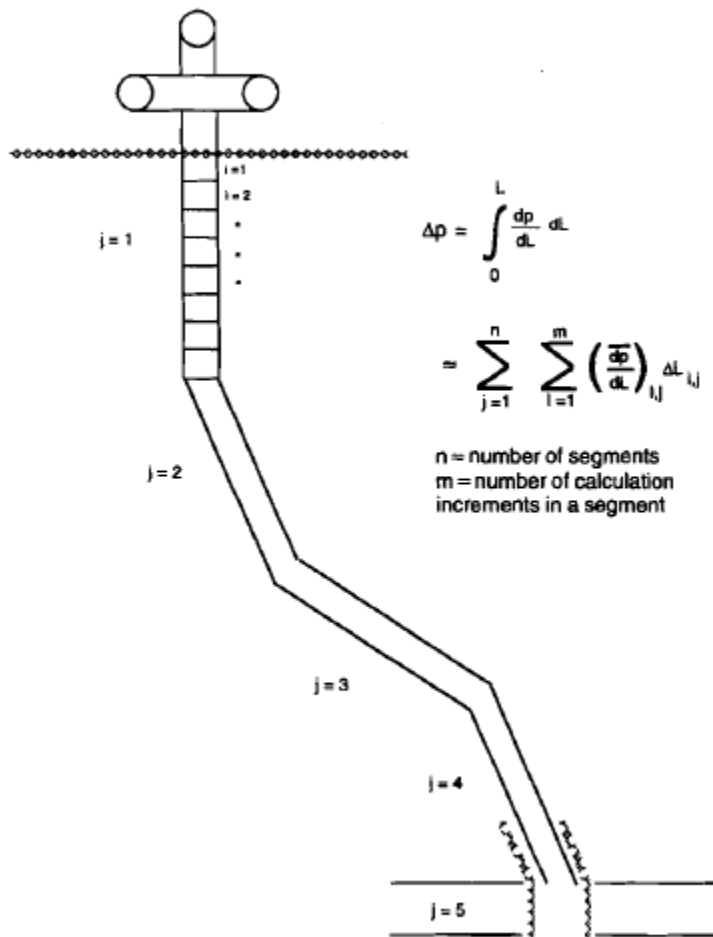


Fig. 3.9—Segmenting typical wellbore.

Session 14:  
Two phase flow and wells design application



# objective

The mechanics of fluid flow in every component in a well's plumbing system affects the flow rate. Accurate well design is the key to achieving optimum flow rate. Consequently, understanding the mechanics of fluid flow through each component, from the reservoir to the first stage of separation, is imperative for accurate well design. The overall objective of this chapter is to present example applications of multiphase-flow theories to well design and optimization. It also provides a brief discussion of the reservoir flow into the wellbore to enable well design calculations.

The well design methods presented in this chapter also are used to troubleshoot well problems. In this context, some of the key constraining phenomena in well design, such as gas-well loading, erosion, and formation of natural gas hydrates, are also discussed.

The plumbing system is an interfacing conduit between the reservoir and the surface handling facilities. Without it, the hydrocarbons cannot become a tangible asset. For optimal production, a well design requires complex engineering considerations that depend on well components. Optimal production yields a maximum return on investment, not a maximum production rate. **Fig. 6.1** shows the major components with substantial pressure losses in a typical well. A production system consists of the following major components.<sup>1-9</sup>

- Porous medium.
- Completion (stimulation, perforations, and gravel pack).
- Tubing with safety valve and choke.
- Artificial lift system (pump and gas-lift valves among others).
- Flowline with choke and other piping components (valves, elbows, and other such elements) from the wellhead to the first-stage separator.

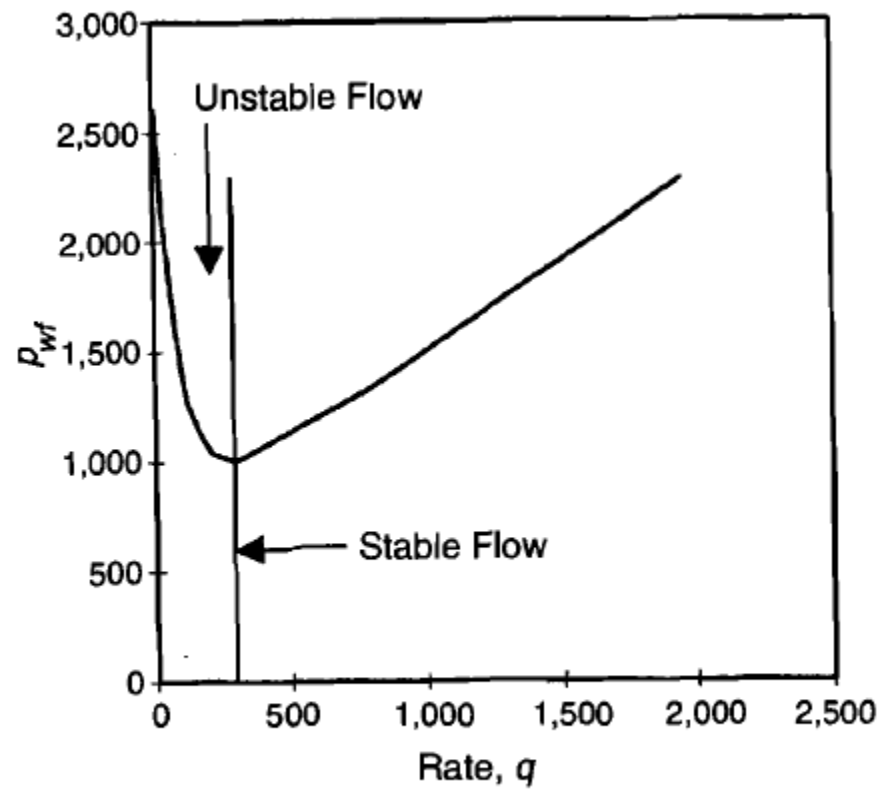


Fig. 6.3—Typical tubing-intake curve for producing wells.

### 6.3 Inflow Performance

Inflow performance relationship (IPR) is defined as the functional relationship between the production rate from the reservoir and the bottomhole flowing pressure. Gilbert<sup>2</sup> first proposed well analysis using this relationship. IPR is defined in the pressure range between the average reservoir pressure and atmospheric pressure. The flow rate corresponding to atmospheric bottomhole flowing pressure is defined as the absolute open flow potential (AOFP) of the well, whereas the flow rate is always zero when the bottomhole pressure is the average reservoir pressure, representing a shut-in condition. **Fig. 6.6** presents a typical IPR based on Darcy's law for single-phase liquid flow. The actual flowing bottomhole pressure also depends on the separator pressure and the pressure loss in the flow conduits up to the depth of midperforation.

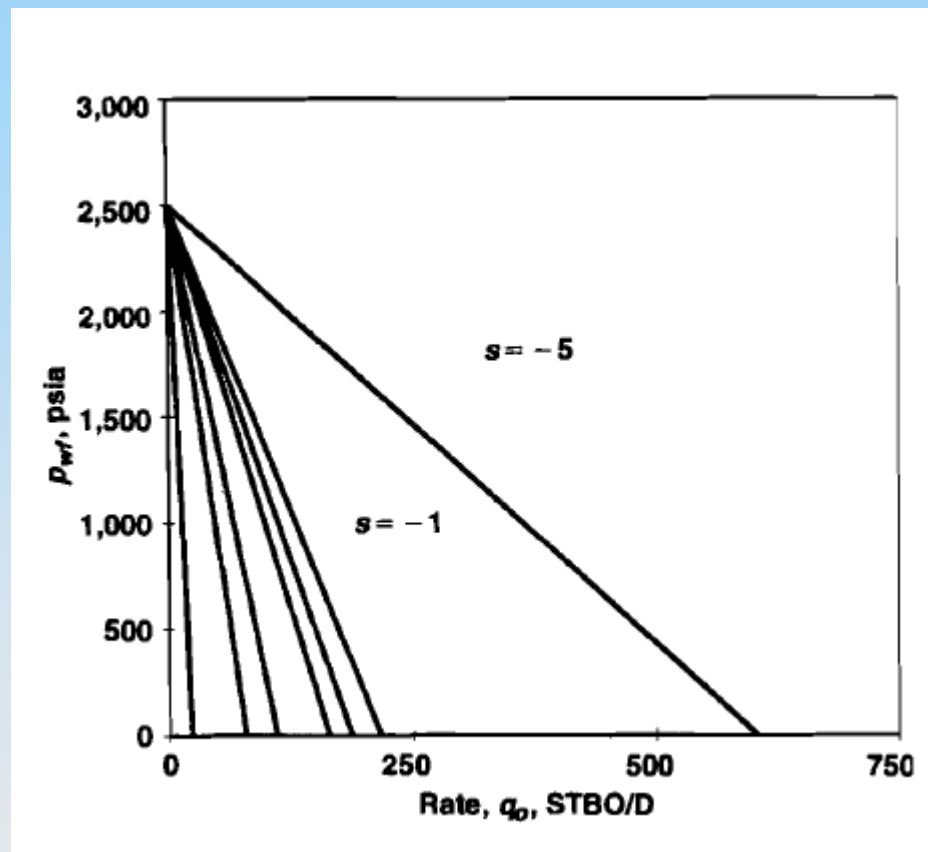
**6.3.1 Single-Phase Liquid Flow.** For single-phase oil or liquids, the IPR shown in Fig. 6.6 is stated by Darcy's law<sup>10,11</sup> for radial flow as

$$q_o = \frac{7.08 \times 10^{-3} k_o h (\bar{p}_r - p_{wf})}{\mu_o B_o \left[ \ln\left(\frac{r_e}{r_w}\right) - 0.75 + s_i + Dq_o \right]}, \dots\dots\dots (6.3)$$

where  $q_o$  = oil flow rate into the well, STBO/D;  $B_o$  = formation volume factor of oil, bbl/STBO, (see Appendix B);  $\mu_o$  = viscosity of oil, cp, (see Appendix B);  $k_o$  = effective permeability of the formation to oil, md;  $h$  = net thickness of the formation, ft;  $\bar{p}_r$  = average reservoir pressure, psia;  $p_{wf}$  = bottomhole flowing pressure, psia;  $r_e$  = radius of drainage, ft =  $\sqrt{A/\pi}$ , where  $A$  is area of circular drainage, ft<sup>2</sup>;  $r_w$  = wellbore radius, ft;  $s_i$  = total skin; and  $Dq_o$  = pseudo-skin caused by turbulence. In oil wells, this term is insignificant, especially for low-permeability reservoirs.

**TABLE 6.5—EXAMPLE OF SKIN FACTORS AND AAFP'S**

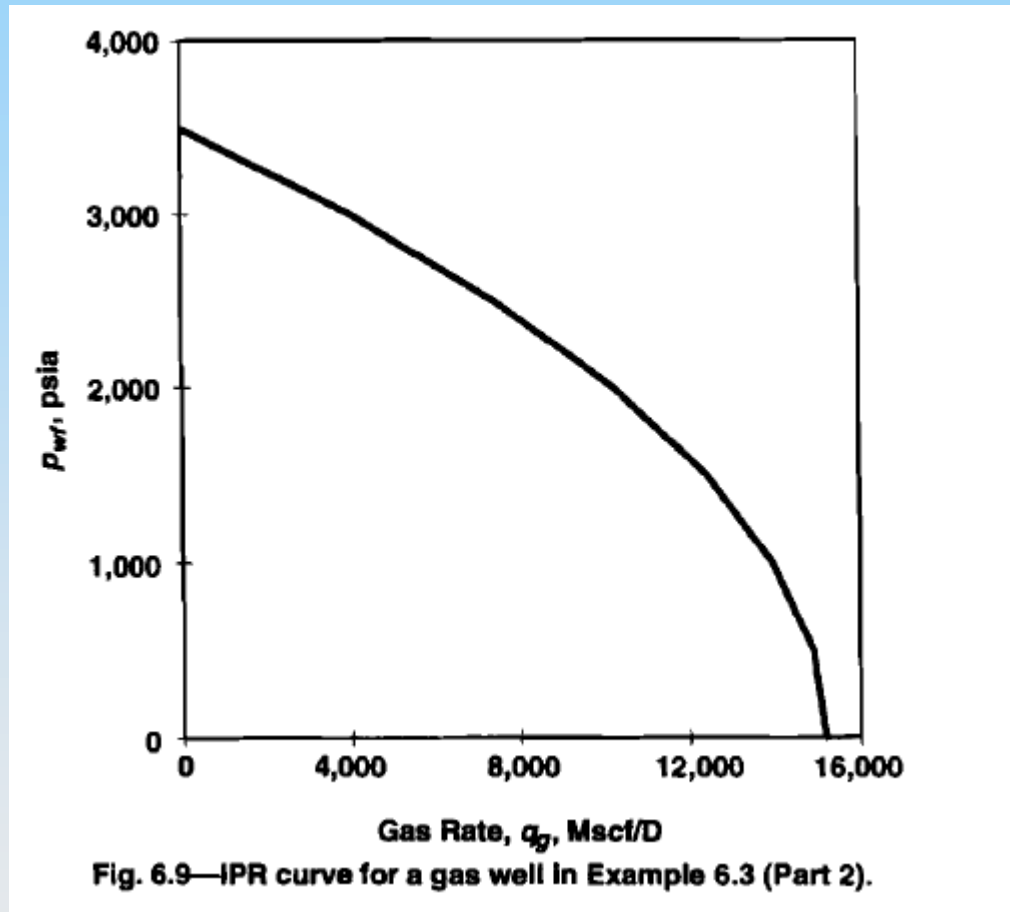
<u>Skin, <i>s</i></u>	<u>AAFP (STBO/D)</u>
-5	604
-1	216
0	186
1	163
5	110
10	78
50	23

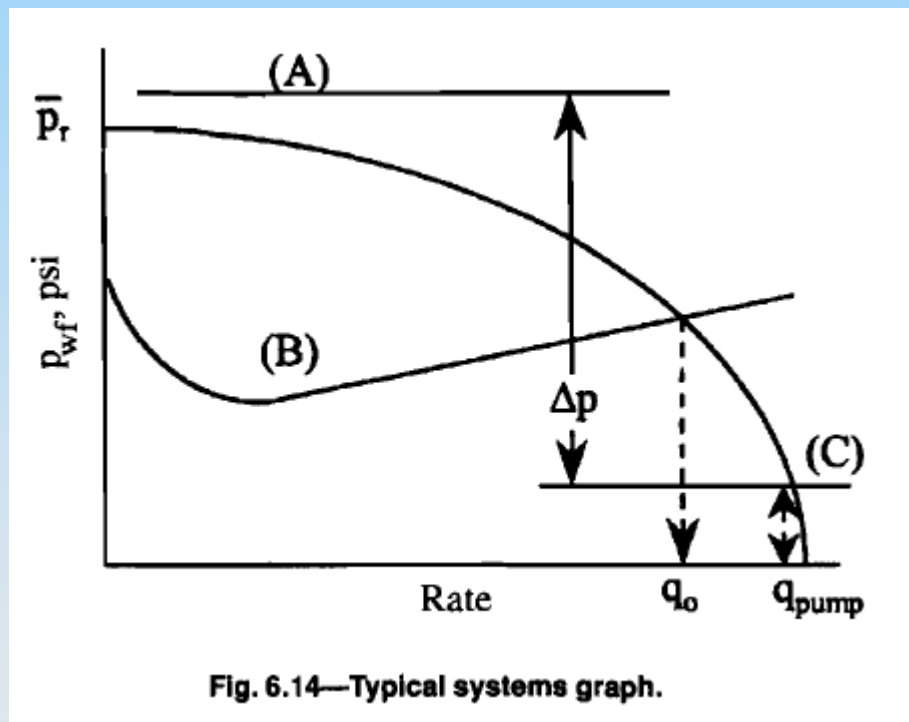


**6.3.3 Single-Phase Gas Flow.** Darcy's law for single-phase gas is

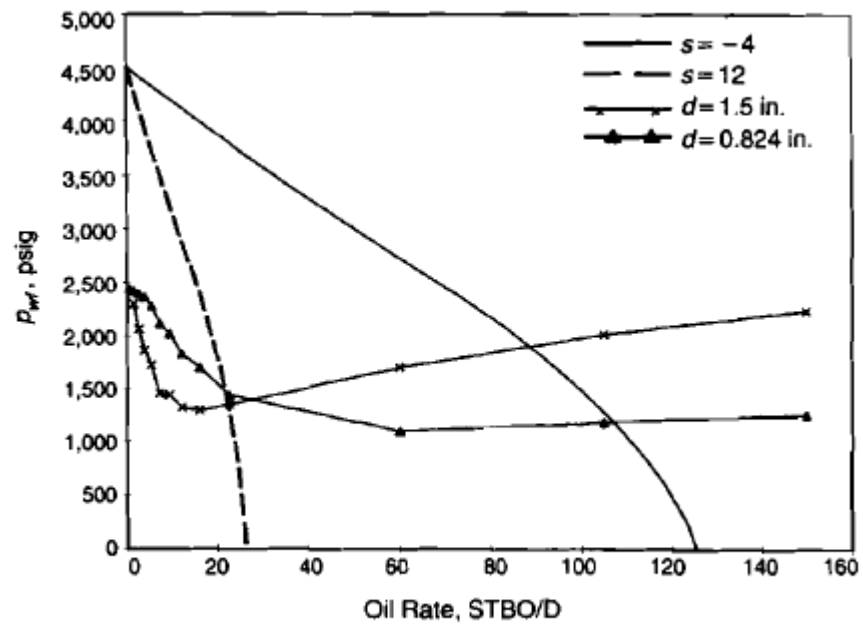
$$q_g = \frac{7.03 \times 10^{-4} k_g h (\bar{p}_r^2 - p_{wf}^2)}{\bar{\mu}_g \bar{Z} T_r \left[ \ln\left(\frac{r_e}{r_w}\right) - 0.75 + s_i + Dq_g \right]}, \dots\dots\dots (6.6)$$

where  $q_g$  = gas flow rate, Mscf/D;  $k_g$  = effective permeability to gas, md;  $\bar{Z}$  = gas compressibility factor determined at average temperature and average pressure, fraction;  $T_r$  = average reservoir temperature, °R; and  $\bar{\mu}_g$  = gas viscosity calculated at average pressure and average temperature, cp.

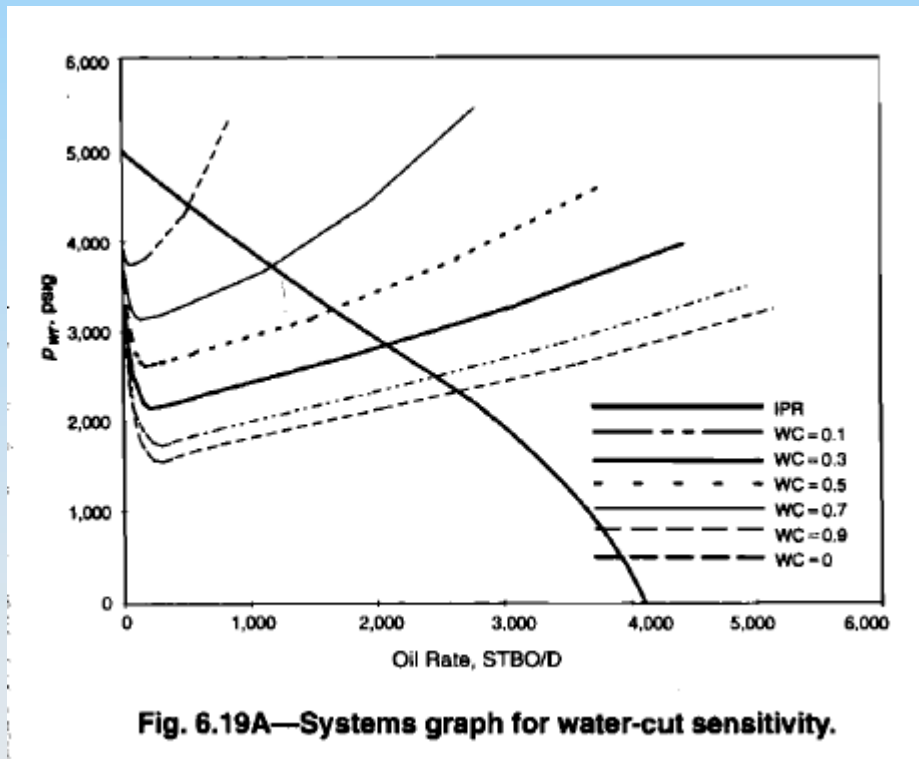








**Fig. 6.15—Effects of tubing ID and skin on production performance.**



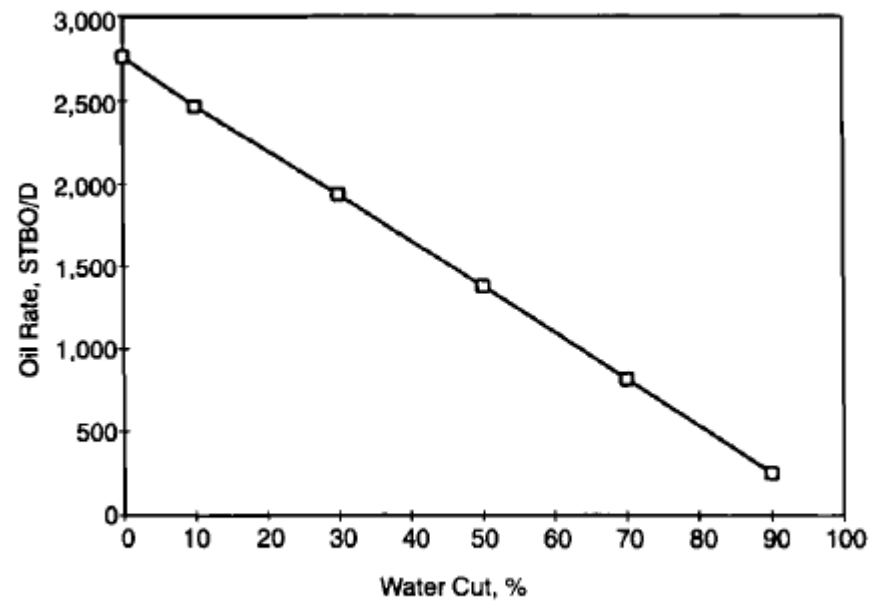


**Fig. 6.19B—Water-cut sensitivity.**

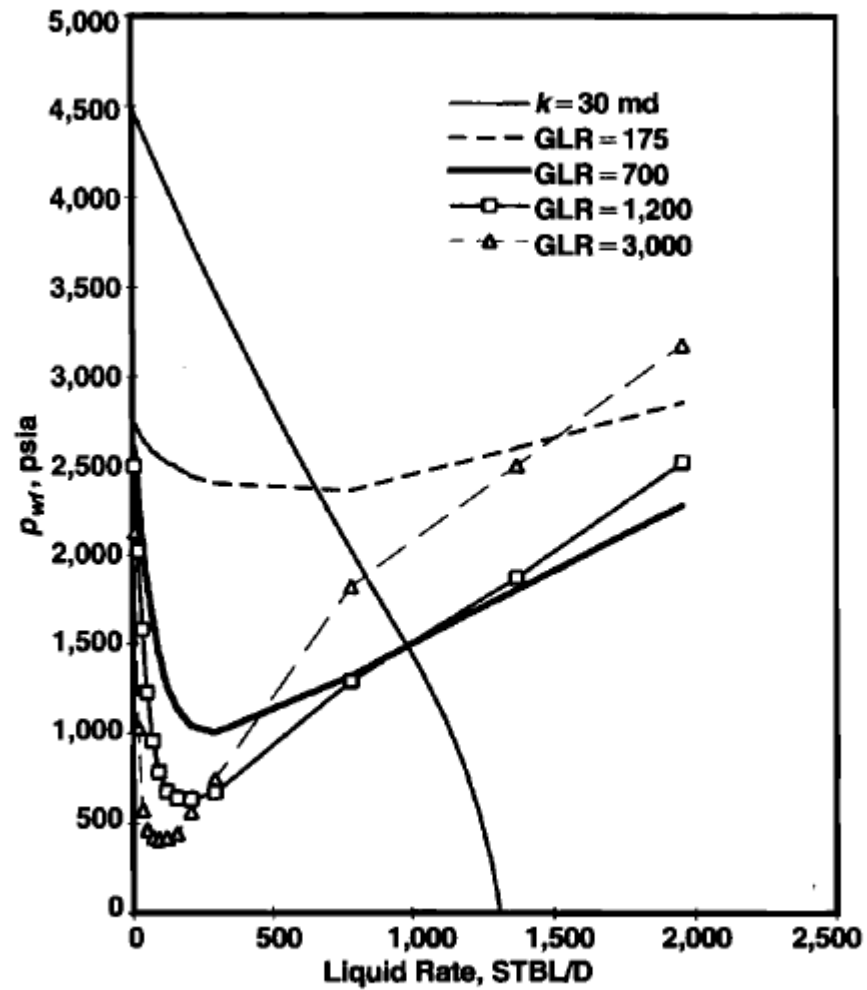
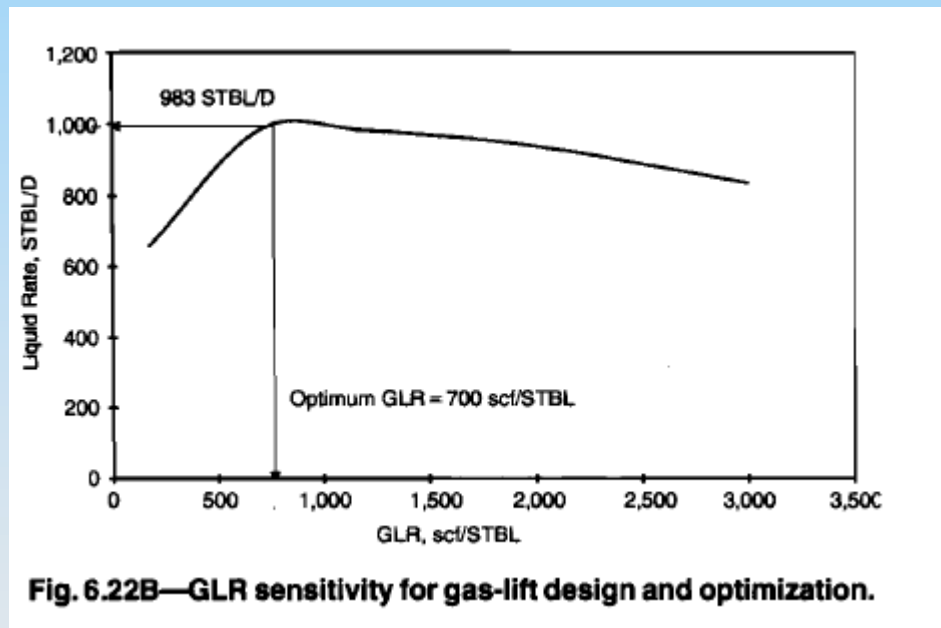


Fig. 6.22A—Production-systems graph for GLR sensitivity.



**Fig. 6.22B—GLR sensitivity for gas-lift design and optimization.**

## **6.6 Gas-Well Loading**

Gas wells often produce a liquid phase, such as oil, condensates, or even interstitial water. Depending on the phase behavior of the gas, it is even conceivable that a well producing dry gas may have liquid in the wellbore. This problem can be particularly severe in condensate or retrograde condensate reservoirs. If the velocity of the producing gas is sufficiently high, the wellbore liquids are produced to the surface and the well does not accumulate any liquids. However, in low-permeability gas wells, particularly with low reservoir pressures, the gas velocity may not be sufficient to lift the liquid phase to the surface unless the tubing diameter is reduced to attain the liquid unloading velocity. Lower velocities result in accumulation of liquid in the well. This liquid accumulation eventually can create enough hydrostatic pressure in the wellbore to curtail gas production severely, even completely stopping it with time. This phenomenon is called gas-well loading.<sup>34-42</sup> In oil wells with high liquid velocity this may not be a problem. Artificial-lift methods can be used to mitigate the problem. In gas-condensate reservoirs, particularly in the presence of a large retrograde envelope, the effective permeability to gas can be severely reduced if condensation occurs near the wellbore. This may drastically reduce the gas velocity in the wellbore, causing severe well-loading problems.

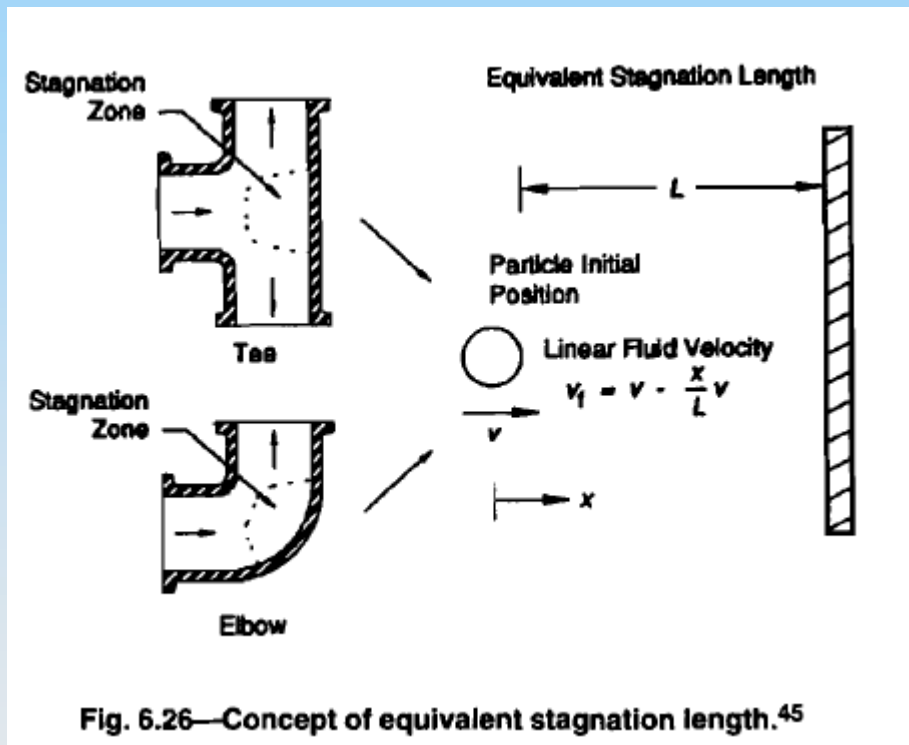
### 6.7 Erosional Velocity

Erosion is the physical removal of pipe material in contact with a flowing fluid. Erosion limits the life of flow strings. Continuous excessive erosion often leads to mechanical failure, leakage, or both. Erosion is caused by cavitation or bubble collapse and by the impingement of liquid or solid particles on the pipe wall. But this subject is very controversial and often not emphasized in design. The mitigation procedure used in this section should be used as guidelines for proper design.

To control erosion, the American Petroleum Inst. (API)<sup>43</sup> recommends limiting the maximum velocity in the flow string to a critical value called erosional velocity. To ensure a predesigned life of flow strings, erosional velocity can be calculated from this empirical equation.

$$v_e = \frac{C}{\sqrt{\rho}}, \dots\dots\dots (6.23)$$

where  $v_e$  is the erosional velocity in ft/sec,  $\rho$  is the density of the flowing fluid in lbm/ft<sup>3</sup>, and  $C$  is an empirical constant. For sand-free flow, the API study recommends  $C$  factors of 100 for continuous flow and 150 for intermittent flow. For sand-laden fluids, API





$$h = 496,920 \left[ \frac{q_{sd} v_p^2}{T d^2} \right], \dots\dots\dots (6.25)$$

where  $h$  = erosion penetration rate, mil/yr;  $q_{sd}$  = sand production rate, ft<sup>3</sup>/D;  $v_p$  = particle impact velocity, ft/sec;  $T$  = elbow metal hardness, psi; and  $d$  = elbow diameter, in.

Salama and Venkatesh obtained this expression for erosional velocity in ft/sec. Assuming particle impact velocity equals flow stream velocity in Eq. 6.25.

$$v_e = 1.73d / \sqrt{q_{sd}} \dots\dots\dots (6.26)$$

This equation assumes hardness  $T = 1.55 \times 10^5$  psi and an allowable penetration rate of  $h = 10$  mil/year.

**6.8.1 Permafrost/Marine Environment.** Permafrost is the frozen or semifrozen alluvial formation found in arctic climates. Depending on the geographical area, permafrost thickness may exceed 2,000 ft. Because of permafrost on Alaska's North Slope, some unusual production problems have been reported.<sup>57,58</sup> Many of them are related to the abnormal geothermal gradients in the area. The permafrost zone is abnormally cold with low geothermal gradients (0.8 to 3.1°F/100 ft, on the basis of a study of 34 wells by Godbole and Ehlig-Economides<sup>57</sup>), whereas the geothermal gradient below the base of permafrost was found by those authors and Lachenbruch *et al.*<sup>58</sup> to be in the range of 1.4 to 5.4°F/100 ft. There is also a significant difference in the flowing and static temperature gradients in these zones.

Similar problems<sup>60-62</sup> caused by abnormal temperature gradients also have been observed in marine pipelines, where a negative hydrothermal gradient<sup>60</sup> in sea water follows a positive geothermal gradient below the seabed. Thus, in a marine environment with sub-sea wells, wax deposition and hydrate problems<sup>62</sup> may be expected, depending on the characteristics of the produced fluid.

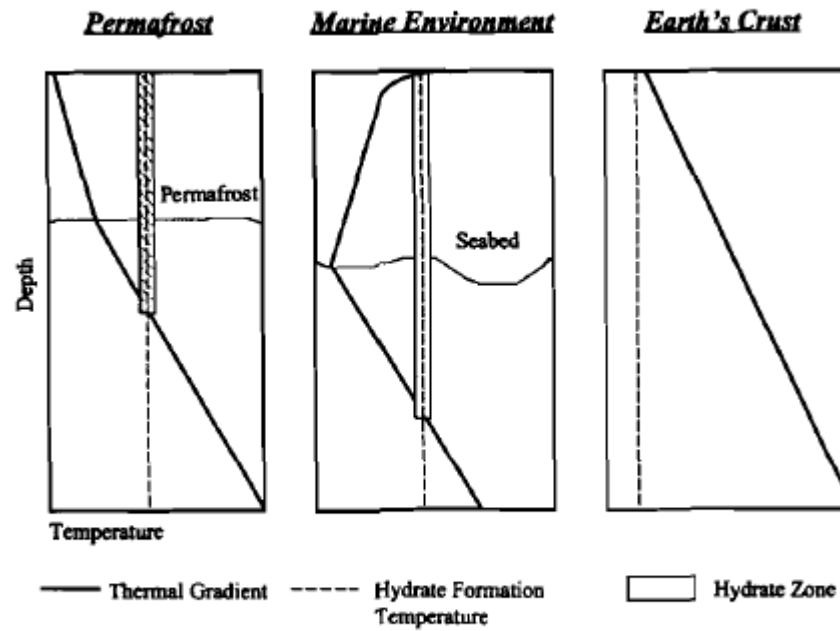
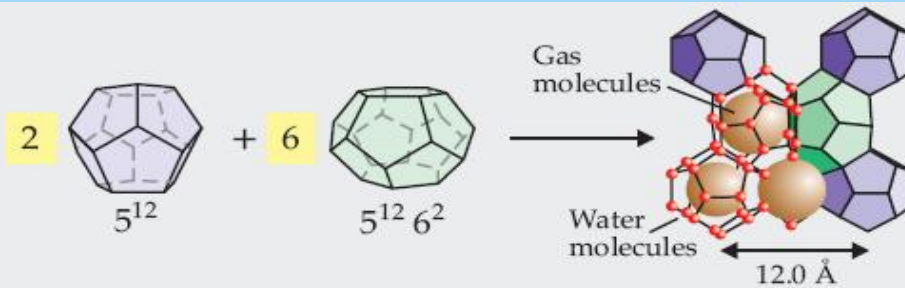


**Fig. 6.28—Geothermal and hydrothermal gradient in different environments.**

# Sessions 15: Gas Hydrates

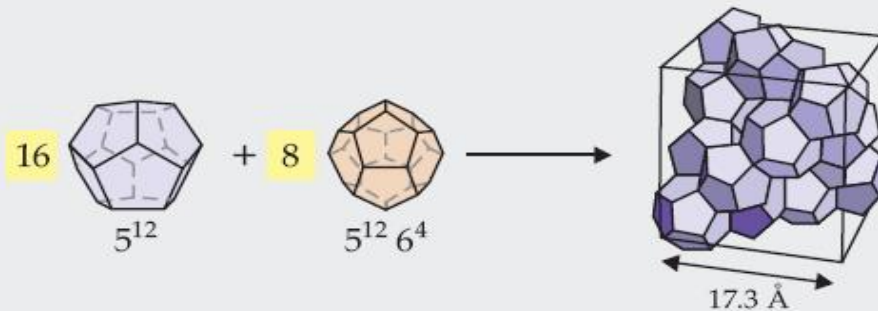
# Typical stable hydrate structures

sI



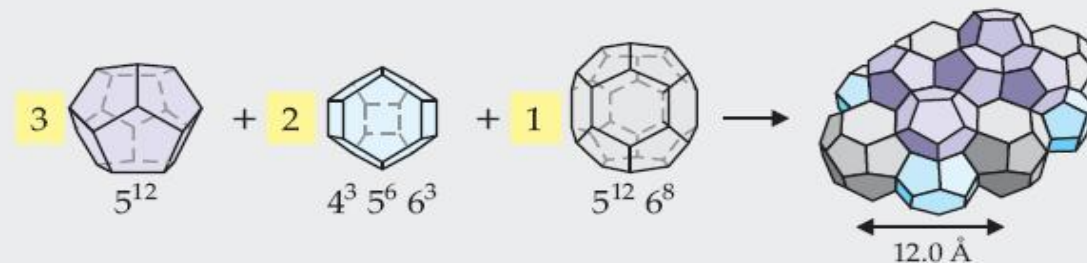
cubic

sII



cubic

sH



hexagonal

**Table 2-1**  
**Comparison Between Type I and Type II Hydrates**

	<b>Type I</b>	<b>Type II</b>
<b>Water Molecules per Unit Cell</b>	46	136
<b>Cages per Unit Cell</b>		
Small	2	16
Large	6	8
<b>Theoretical Formula<sup>†</sup></b>		
All cages filled	$X \times 5\frac{3}{4} \text{ H}_2\text{O}$	$X \times 5\frac{2}{3} \text{ H}_2\text{O}$
Mole fraction hydrate former	0.1481	0.1500
Only large cages filled	$X \times 7\frac{2}{3} \text{ H}_2\text{O}$	$X \times 17 \text{ H}_2\text{O}$
Mole fraction hydrate former	0.1154	0.0556
<b>Cavity Diameter (Å)</b>		
Small	7.9	7.8
Large	8.6	9.5
<b>Volume of Unit Cell (m<sup>3</sup>)</b>	$1.728 \times 10^{-27}$	$5.178 \times 10^{-27}$
<b>Typical Formers</b>	CH <sub>4</sub> , C <sub>2</sub> H <sub>6</sub> , H <sub>2</sub> S, CO <sub>2</sub>	C <sub>3</sub> H <sub>8</sub> , i-C <sub>4</sub> H <sub>10</sub> , N <sub>2</sub>
† = where X is the hydrate former.		

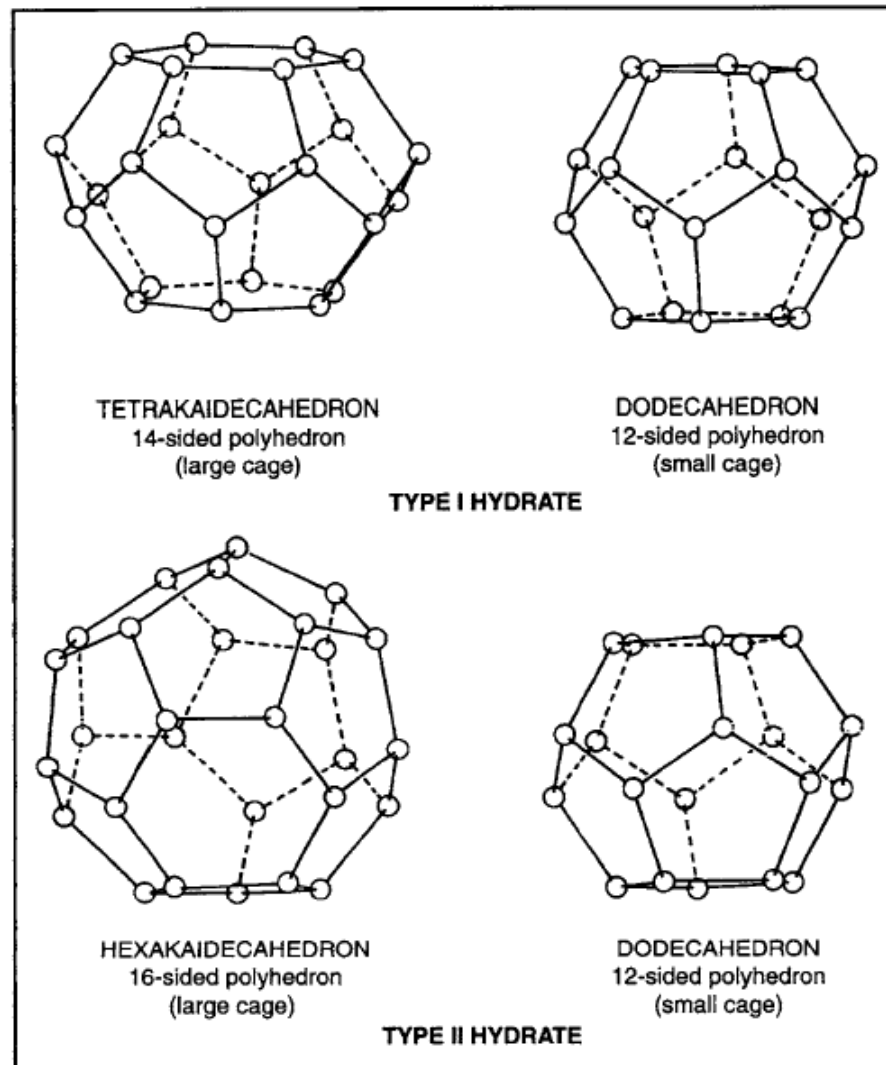


**Figure 2-1. The polyhedral cages of Type I and Type II hydrates**

# Effect of guest molecule size

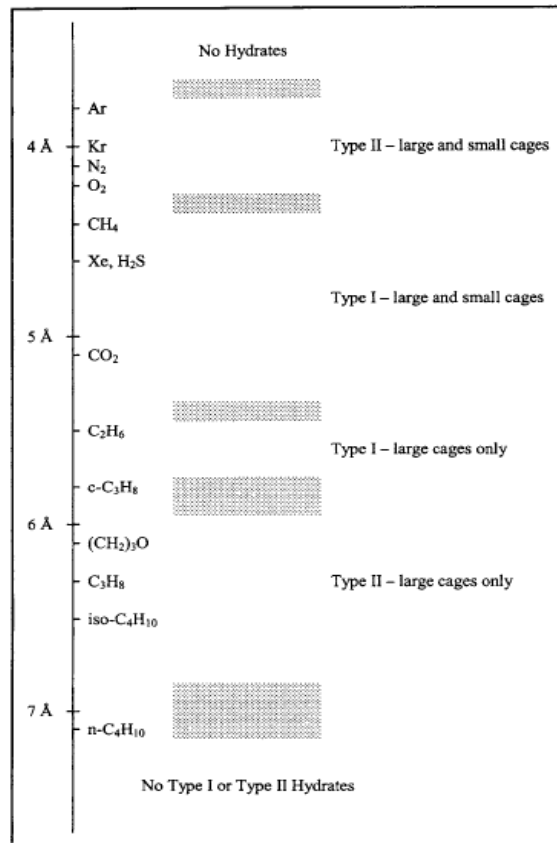


**Figure 2-2. Comparison of guest size, hydrate type, and cavities occupied for various hydrate formers. Modified from original by von Stackelberg, 1949**



# Typical Hydrate Equilibrium Curve

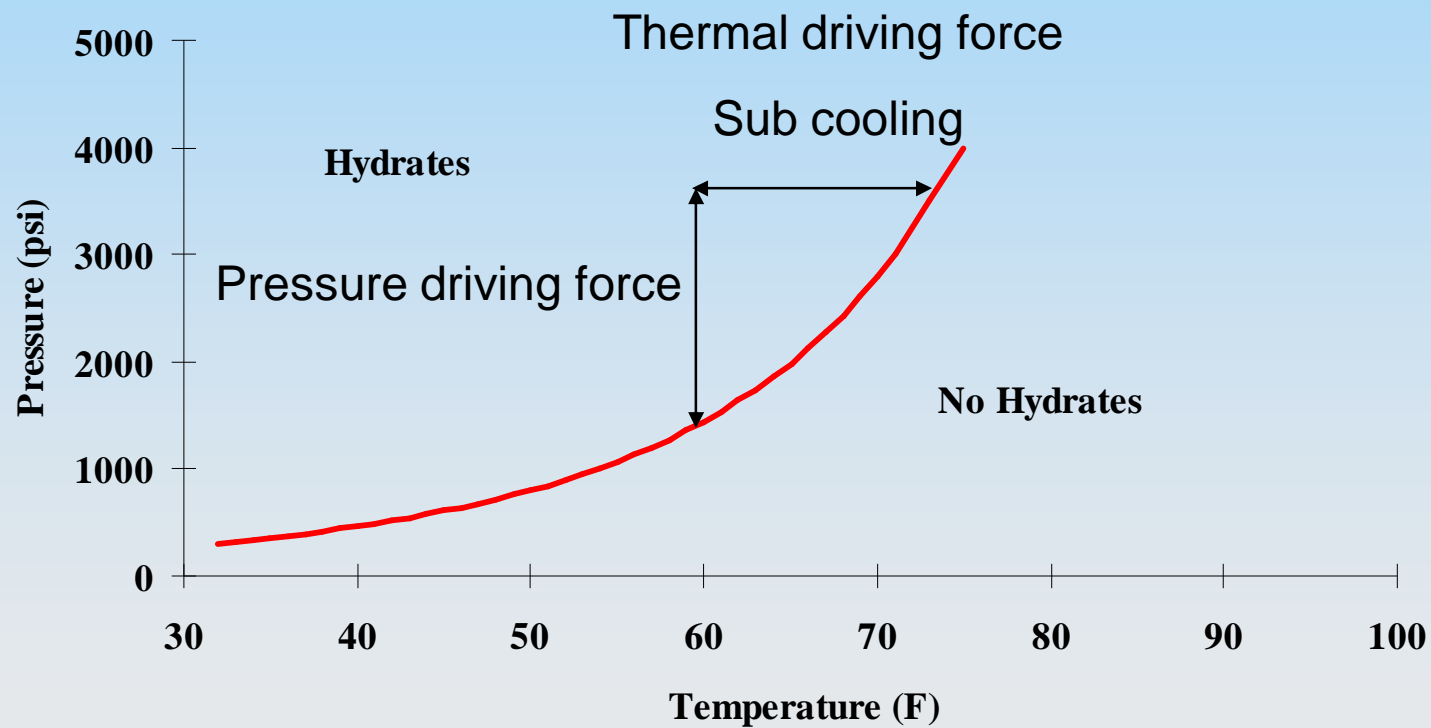


**Table 2-2**  
**Hydrate-Forming Conditions for Methane**

Temp. (°C)	Press. (MPa)	Phases	Composition (mol %)		
			Aqueous	Vapor	Hydrate
0.0	2.60	L <sub>A</sub> -H-V	0.10	0.027	14.1
2.5	3.31	L <sub>A</sub> -H-V	0.12	0.026	14.2
5.0	4.26	L <sub>A</sub> -H-V	0.14	0.026	14.3
7.5	5.53	L <sub>A</sub> -H-V	0.16	0.025	14.4
10.0	7.25	L <sub>A</sub> -H-V	0.18	0.024	14.4
12.5	9.59	L <sub>A</sub> -H-V	0.21	0.024	14.5
15.0	12.79	L <sub>A</sub> -H-V	0.24	0.025	14.5
17.5	17.22	L <sub>A</sub> -H-V	0.27	0.025	14.5
20.0	23.4	L <sub>A</sub> -H-V	0.30	0.027	14.6
22.5	32.0	L <sub>A</sub> -H-V	0.34	0.028	14.6
25.0	44.1	L <sub>A</sub> -H-V	0.37	0.029	14.7
27.5	61.3	L <sub>A</sub> -H-V	0.41	0.029	14.7
30.0	85.9	L <sub>A</sub> -H-V	0.45	0.029	14.7

**Notes:** Composition for the aqueous phase and for the hydrate is the mole percent of the hydrate former (CH<sub>4</sub>). For the vapor the composition is the mole percent water.

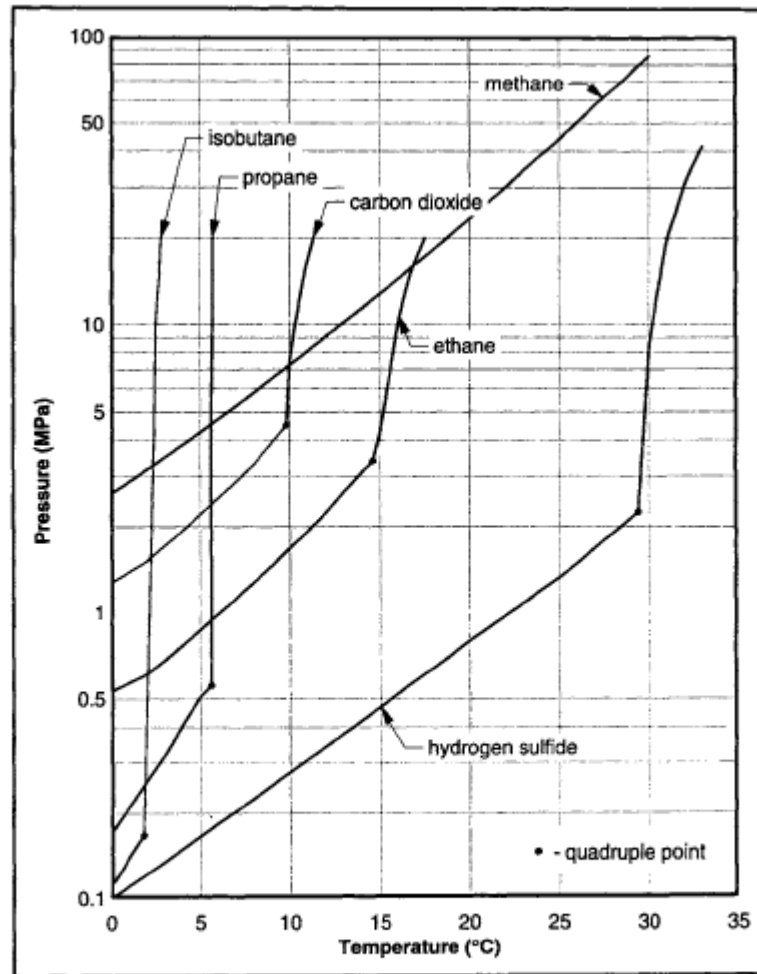


**Figure 2-3. The hydrate loci for several components found in natural gas**

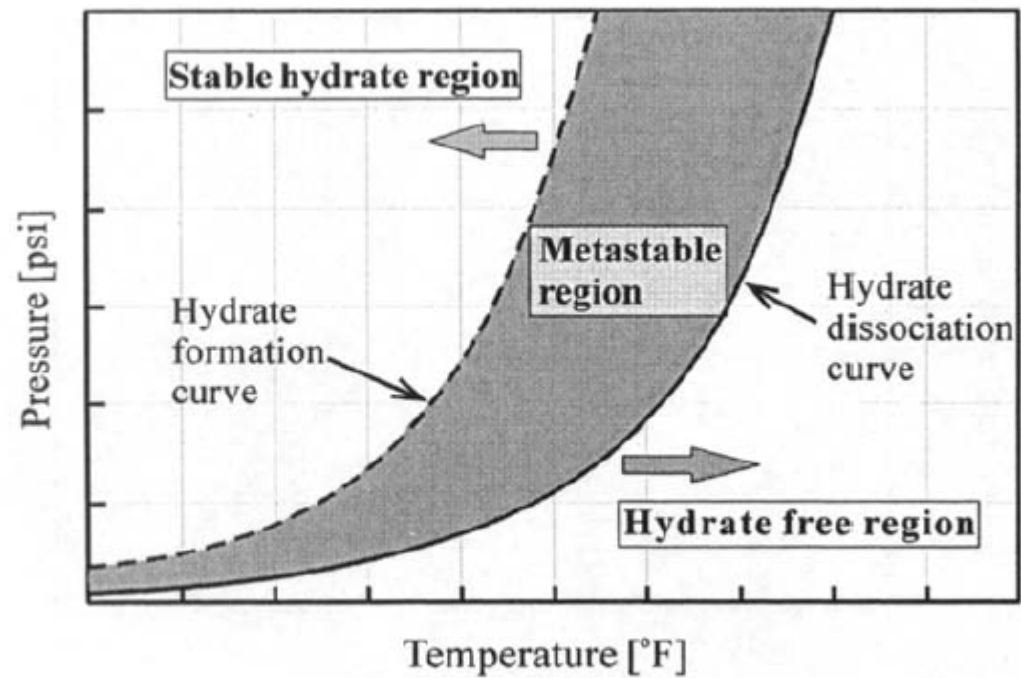


**Figure 20.4 Hydrate formation and dissociation regions.**

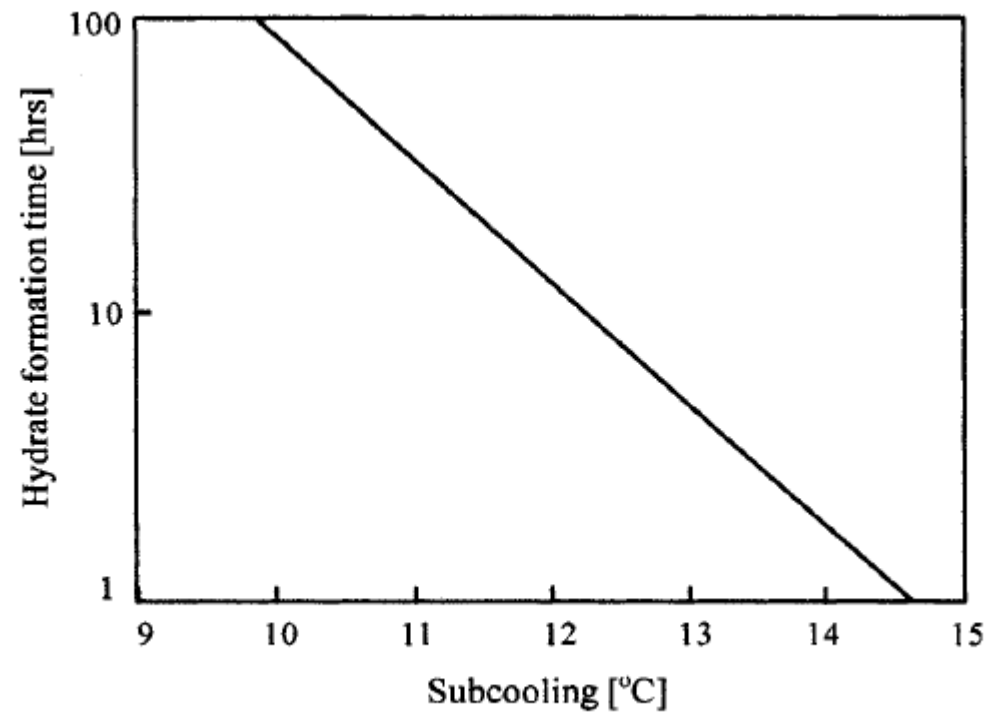


**Figure 20.5** Variation of hydrate formation time with subcooling (Ellision and Gallagher, 2001).

### Gas Gravity Method

The gas gravity method was developed by Professor Katz and co-workers in the 1940s. The beauty of this method is its simplicity, involving only a single chart. The chart is simply a plot of pressure and temperature, with the specific gravity of the gas as a third parameter. Two such charts, one in SI Units and the other in Engineering Units, are given here in Figures 3-1 and 3-2.

The first curve on these plots (i.e., the one at the highest pressure) is for pure methane. This is the same pressure-temperature locus presented in Chapter 2.

The chart is very simple to use. First you must know the specific gravity of the gas, which is also called the relative density. Given the molar mass

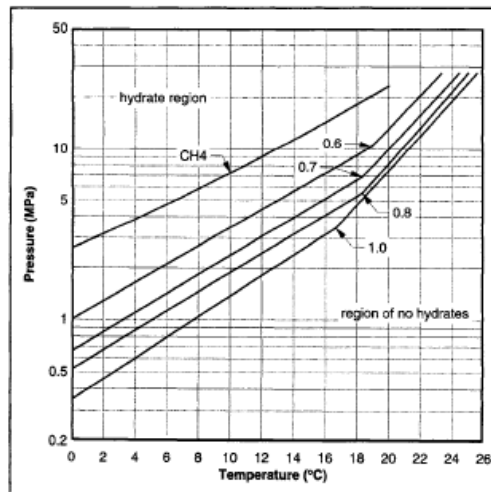


Figure 3-1. Hydrate locus for sweet natural gas using the gas gravity method (SI Units)

### K-Factor Method

The second method that lends itself to hand calculations is the K-factor method. This method originated with Carson and Katz (1942) (also see Wilcox et al., 1941), although additional data and charts have been reported since then. One of the ironies of this method is that the original charts of Carson and Katz (1942) have been reproduced over the years even though they were originally marked as “tentative” by the authors.

The K-factor is defined as the distribution of the component between the hydrate and the gas:

$$K_i = \frac{y_i}{s_i} \quad (3-2)$$

where  $y_i$  and  $s_i$  are the mole fractions of component  $i$  in the vapor and hydrate, respectively. These mole fractions are on a water-free basis, and water is not included in the calculations. It is assumed that sufficient water is present to form a hydrate.

---

#### 54 *Natural Gas Hydrates: A Guide for Engineers*

A chart is available for each of the components commonly encountered in natural gas that is a hydrate former: methane, ethane, propane, isobutane, n-butane, hydrogen sulfide, and carbon dioxide. Versions of these charts, one set in SI Units and another in American Engineering Units, are included in Appendix 3.

All nonformers are simply assigned a value of infinity. This is true by definition because  $s_i = 0$  for nonformers, so there is no nonformer in the hydrate.

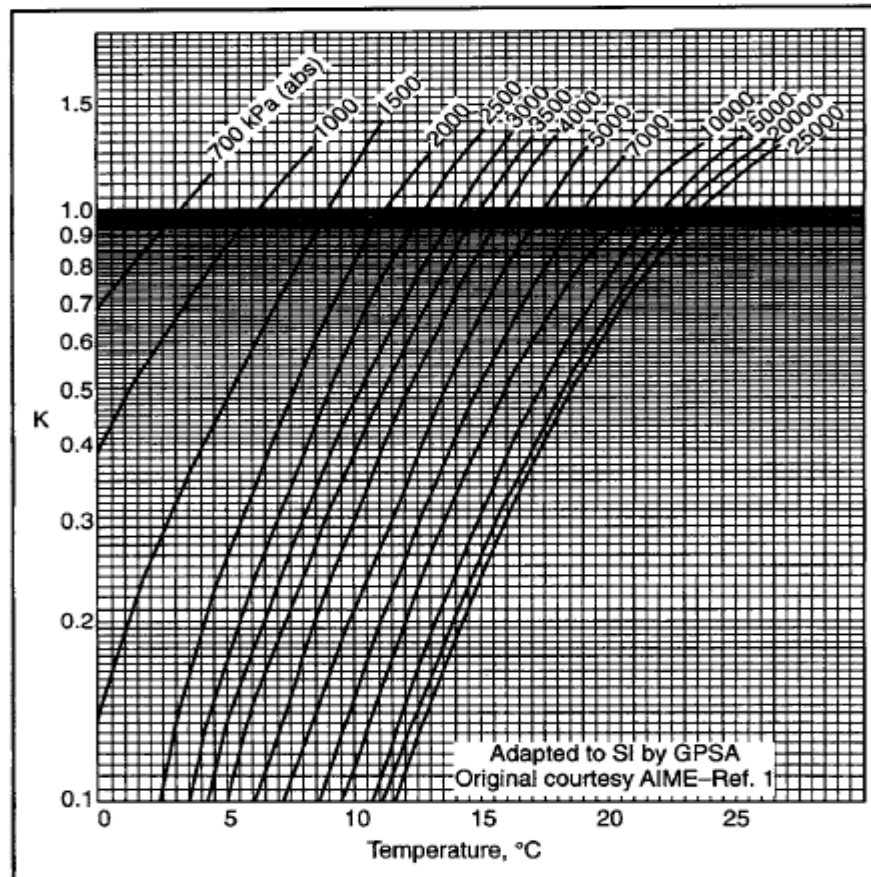


**Figure 3-2a. Vapor-solid equilibrium K-factor for ethane in SI Units.** Reprinted from the *GPSA Engineering Data Book*, 11th ed. Reproduced with permission



1. Input the temperature, T.
2. Input the vapor composition,  $y_i$ .
3. Assume a value for the pressure, P.
4. Set the K-factors for all nonformers to infinity.
5. Given P and T, obtain K-factors from the Katz charts (or from correlations) for the hydrate-forming components in the mixture.
6. Calculate the summation:
 
$$\sum y_i/K_i$$

Note for nonformers the expression  $y_i/K_i$  is zero.
7. Does the summation equal unity?
 

That is, does  $\sum y_i/K_i = 1$ ?

  - 7a. Yes - Go to Step 10.
  - 7b. No - Go to Step 8.
8. Update the pressure estimate.
  - 8a. If the sum is greater than 1, reduce the pressure.
  - 8b. If the sum is less than 1, increase the pressure.
  - 8c. Use caution if the sum is significantly different from 1.
9. Go to Step 4.
10. Convergence! Current P is the hydrate pressure.
11. Stop.

**Figure 3-3. Pseudocode for performing a hydrate pressure estimation using the Katz K-factor method**

### *Incipient Solid Formation*

The other two methods are incipient solid formation points and are basically equivalent to a dew point. This is the standard hydrate calculation. The purpose of this calculation is to answer the question, "Given the temperature and the composition of the gas, at what pressure will a hydrate form?" A similar calculation is to estimate the temperature at which a hydrate will form given the pressure and the composition. The execution of these calculations is similar.

The objective functions to be solved are:

$$f_1(T) = 1 - \sum y_i / K_i \quad (3-6)$$

$$f_2(P) = 1 - \sum y_i / K_i \quad (3-7)$$

Depending on whether you want to calculate the pressure or the temperature, the appropriate function, either Equation 3-6 or 3-7, is selected. Iterations are performed on the unknown variable until the summation is equal to unity. So, to use the first equation (Equation 3-6), the pressure is known and iterations are performed on the temperature.

Figure 3-3 shows a simplified pseudocode description of the algorithm for performing a hydrate formation pressure calculation using the K-factor method.

# Hydrate physical properties

### Molar Mass

The molar mass (molecular weight) of a hydrate can be determined from its crystal structure and the degree of saturation. The molar mass of the hydrate,  $M$ , is given by:

198

*John J. Carroll 199*

$$M = \frac{N_w M_w + \sum_{j=1}^c \sum_{i=1}^n Y_{ij} v_i M_j}{N_w + \sum_{j=1}^c \sum_{i=1}^n Y_{ij} v_i} \quad (8-1)$$

where  $N_w$  is the number of water molecules per unit cell (46 for Type I and 136 for Type II),  $M_w$  is the molar mass of water,  $Y_{ij}$  is the fractional occupancy of cavities of type  $i$  by component  $j$ ,  $v_i$  is the number of type  $i$  cavities,  $n$  is the number of cavity types (2 for both Type I and II, but 3 for Type H), and  $c$  is the number of components in the cell.

Although this equation looks fairly complicated, it is just accounting for all of the molecules present and then using a number average to get the molar mass.

Table 8-1 summarizes the molar masses of a few hydrate formers. It is a little surprising that the molar masses of all six components are approximately equal (~20 g/mol). This is because the hydrate is composed mostly of water (18.015 g/mol).

**Table 8-1**  
**Molar Masses of Some Hydrates at 0°C**

	Hydrate Type	Saturation		Molar Mass (g/mol)
		Small	Large	
Methane	I	0.8723	0.9730	17.74
Ethane	I	0.0000	0.9864	19.39
Propane	II	0.0000	0.9987	19.46
Isobutane	II	0.0000	0.9987	20.24
CO <sub>2</sub>	I	0.7295	0.9813	21.59
H <sub>2</sub> S	I	0.9075	0.9707	20.87

**Note:** Calculated using Equation 8-1.  
The saturation values were calculated using *CSMHYD*.

### Density

The density of a hydrate,  $\rho$ , can be calculated using the following formula:

$$\rho = \frac{N_w M_w + \sum_{j=1}^c \sum_{i=1}^n Y_{ij} v_i M_j}{N_A V_{\text{cell}}} \quad (8-2)$$

where  $N_w$  is the number of water molecules per unit cell (46 for Type I and 136 for Type II),  $N_A$  is Avogadro's number ( $6.023 \times 10^{23}$  molecules/mole),  $M_w$  is the molar mass of water,  $Y_{ij}$  is the fractional occupancy of cavities of type  $i$  by component  $j$ ,  $v_i$  is the number of type  $i$  cavities,  $V_{\text{cell}}$  is the volume of the unit cell (see Table 2-1),  $n$  is the number of cavity types (2 for both Types I and II, but 3 for Type H), and  $c$  is the number of components in the cell.

Equation 8-2 can be reduced for a single component in either a Type I or Type II hydrate to:

$$\rho = \frac{N_w M_w + (Y_1 v_1 + Y_2 v_2) M_j}{N_A V_{\text{cell}}} \quad (8-3)$$

**Table 8-2**  
**Densities of Some Hydrates at 0°C**

	<b>Hydrate Type</b>	<b>Density (g/cm<sup>3</sup>)</b>	<b>Density (lb/ft<sup>3</sup>)</b>
Methane	I	0.913	57.0
Ethane	I	0.967	60.3
Propane	II	0.899	56.1
Isobutane	II	0.934	58.3
CO <sub>2</sub>	I	1.107	69.1
H <sub>2</sub> S	I	1.046	65.3
Ice	—	0.917	57.2
Water	—	1.000	62.4

**Note:** Calculated using Equation 8-3.  
 The saturation values were calculated using *CSMHYD*.  
 Properties of ice and water from Keenan et al. (1978).

**Table 8-3**  
**Enthalpies of Fusion for Some Gas Hydrates**

	<b>Hydrate Type</b>	<b>Enthalpy of Fusion (kJ/g)</b>	<b>Enthalpy of Fusion (kJ/mol)</b>	<b>Enthalpy of Fusion (MBtu/lb)</b>
Methane	I	3.06	54.2	23.3
Ethane	I	3.70	71.8	30.9
Propane	II	6.64	129.2	55.5
Isobutane	II	6.58	133.2	57.3
Ice	—	0.333	6.01	143

**Note:** Original values from Sloan (1998). Molar enthalpies of fusion converted to specific values (i.e., per unit mass) using the molar masses from Table 8-1.  
Properties of ice and water from Keenan et al. (1978).

to a gas). For water, this is 2.83 kJ/g or 51.0 kJ/mol. This process is probably more comparable to the formation of a hydrate than the simple melting of ice.

One method for estimating the effect of temperature on the heat of fusion is the so-called Clapeyron approach. A Clapeyron-type equation is applied to the three-phase locus. The Clapeyron-type equation used in this application is:

$$\frac{d \ln P}{d(1/T)} = \frac{\Delta H}{zR} \quad (8-4)$$



### Heat Capacity

Limited experimental data are available for the heat capacity of hydrates. Table 8-4 lists some values. For comparison, ice is also included in this table. Over the narrow range of temperatures that hydrates can exist, it is probably safe to assume that these values are constants.

### Thermal Conductivity

There have been limited studies into the thermal conductivity of hydrates; however, they show that hydrates are much less conductive than ice. The thermal conductivity of ice is 2.2 W/m·K, whereas the thermal conductivities of hydrates of hydrocarbons are in the range  $0.50 \pm 0.01$  W/m·K.

### Mechanical Properties

In general, the mechanical properties of hydrates are comparable to those of ice. In the absence of additional information, it is safe to assume that the mechanical properties of the hydrate equal those of ice. One should not

**Table 8-4**  
**Heat Capacities for Some Gas Hydrates**

	Hydrate Type	Heat Capacity (J/g·°C)	Heat Capacity (J/mol·°C)	Heat Capacity (Btu/lb·°F)
Methane	I	2.25	40	0.54
Ethane	I	2.2	43	0.53
Propane	II	2.2	43	0.53
Isobutane	II	2.2	45	0.53
Ice	—	2.06	37.1	0.492

**Note:** Original values from Makogon (1997).  
Properties of ice and water from Keenan et al. (1978).

### Volume of Gas in Hydrate

The purpose of this section is to demonstrate the volume of gas encaged in a hydrate. Therefore, we examine only the methane hydrate.

The following are the properties of the methane hydrate at 0°C: the density is 913 kg/m<sup>3</sup>, the molar mass (molecular weight) is 17.74 kg/kmol, and methane concentration is 14.1 mole percent; this means there are 141 molecules of methane per 859 molecules of water in the methane hydrate. The density and the molar mass are from earlier in this chapter and the concentration is from Chapter 2.

This information can be used to determine the volume of gas in the methane hydrate. From the density, 1 m<sup>3</sup> of hydrate has a mass of 913 kg. Converting this to moles  $913/17.74 = 51.45$  kmol of hydrate, of which 7.257 kmol are methane.

The ideal gas law can be used to calculate the volume of gas when expanded to standard conditions (15°C and 1 atm or 101.325 kPa).

$$V = nRT/P = (7.257)(8.314)(15 + 273)/101.325 = 171.5 \text{Sm}^3$$

Therefore 1 m<sup>3</sup> of hydrate contains about 170 Sm<sup>3</sup> of methane gas. Or in American Engineering Units, this converts to 1 ft<sup>3</sup> of hydrate contains 170 SCF of gas—not a difficult conversion. And 1 ft<sup>3</sup> of hydrate weighs about 14.6 lb, so 1 lb of hydrate contains 11.6 SCF of methane.

By comparison, 1 m<sup>3</sup> of liquid methane (at its boiling point 111.7K or -161.5°C) contains 26.33 kmol, which converts to 622 m<sup>3</sup> of gas at standard conditions. Alternately, 1 m<sup>3</sup> compressed methane at 7 MPa and 300 K (27°C) (1,015 psia and 80°F) contains 3.15 kmol or 74.4 Sm<sup>3</sup> of methane gas. The properties of pure methane are from Wagner and de Reuck (1996).

To look at this another way, to store 25,000 Sm<sup>3</sup> (0.88 MMSCF) of methane requires about 150 m<sup>3</sup> (5,300 ft<sup>3</sup>) of hydrates. This compares with 40 m<sup>3</sup> (1,400 ft<sup>3</sup>) of liquefied methane or 335 m<sup>3</sup> (11,900 ft<sup>3</sup>) of compressed methane.

# Hydrate Prevention

### **20.3 Hydrate Prevention**

Gas subsea systems typically contain small quantities of water, which allows them to be continuously treated with methanol or glycol to prevent hydrate formation. These inhibitors prevent the formation of hydrates by shifting the hydrate stability curve to lower temperatures for a given pressure. If the systems produce too much water, it is difficult to economically treat with methanol. As a result, the system designs have to incorporate insulation of almost all components of system and develop complex operating strategies to control hydrate formation during transient activities such as system start-up and shut-in.

Hydrate prevention techniques for subsea system include:

- Thermodynamic inhibitors
- Low-dosage hydrate inhibitors (LDHIs)
- Low-pressure operation
- Water removal
- Insulation, and
- Active heating.

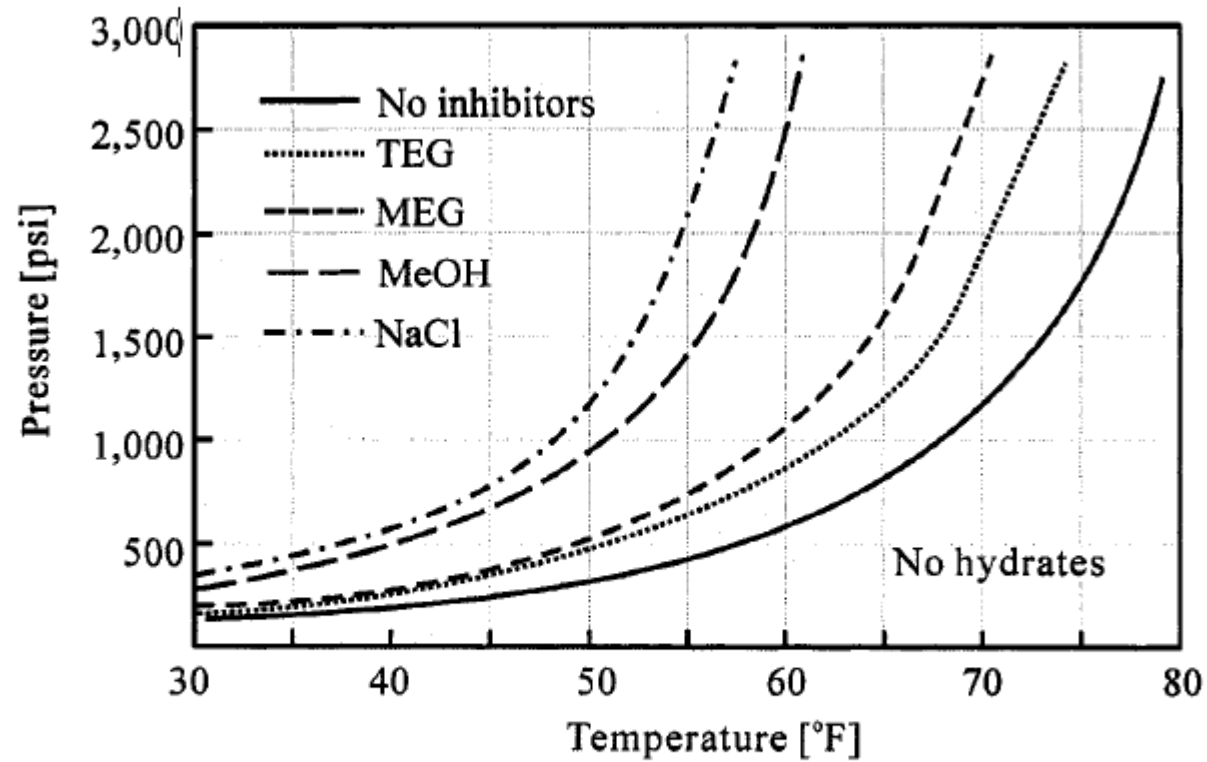


**Figure 20.6 Effect of thermodynamic inhibitors on hydrate formation.**

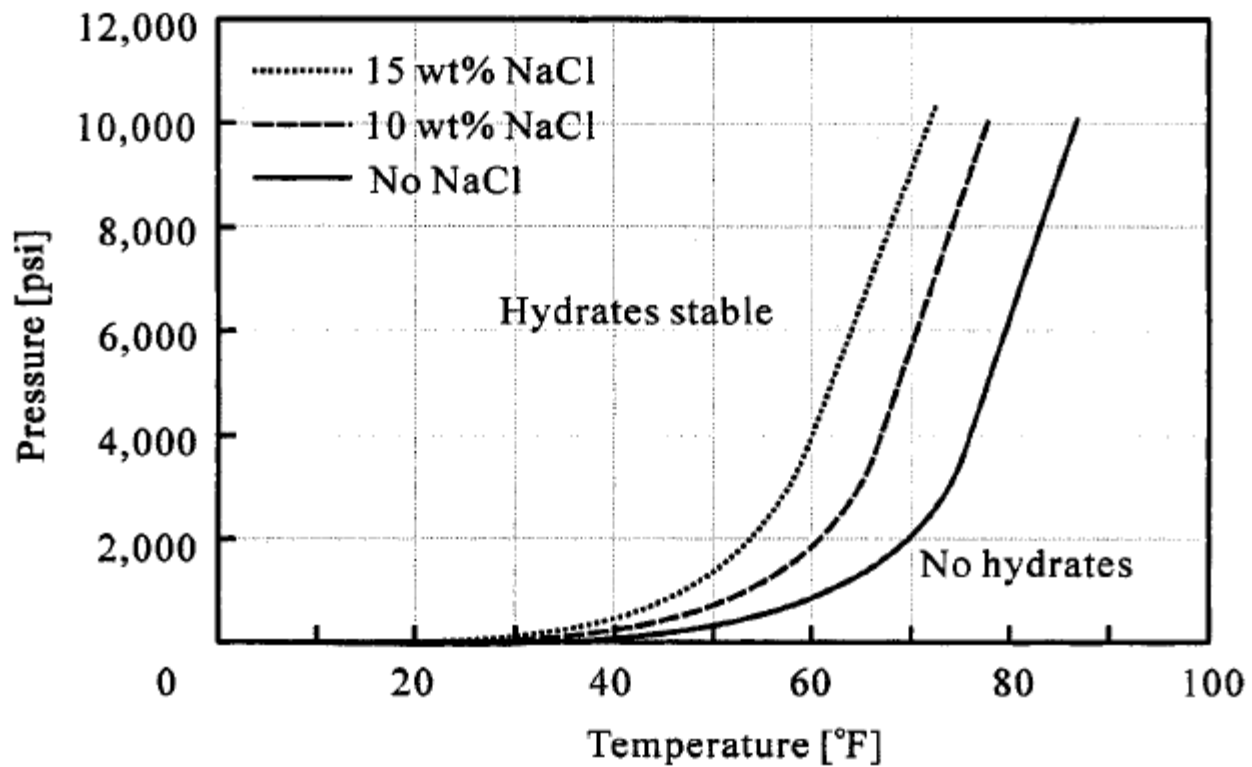


**Figure 20.7** Effect of salts on hydrate formation.

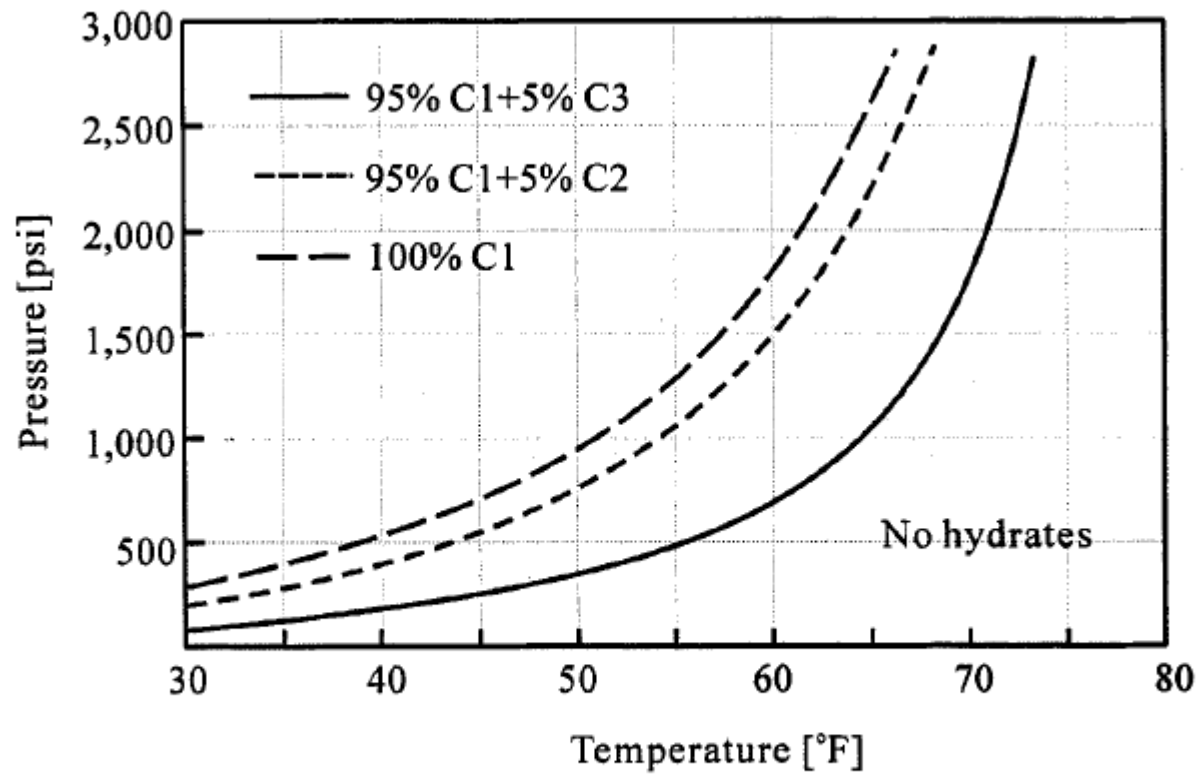


**Figure 20.8 Effect of gas composition on hydrate formation.**

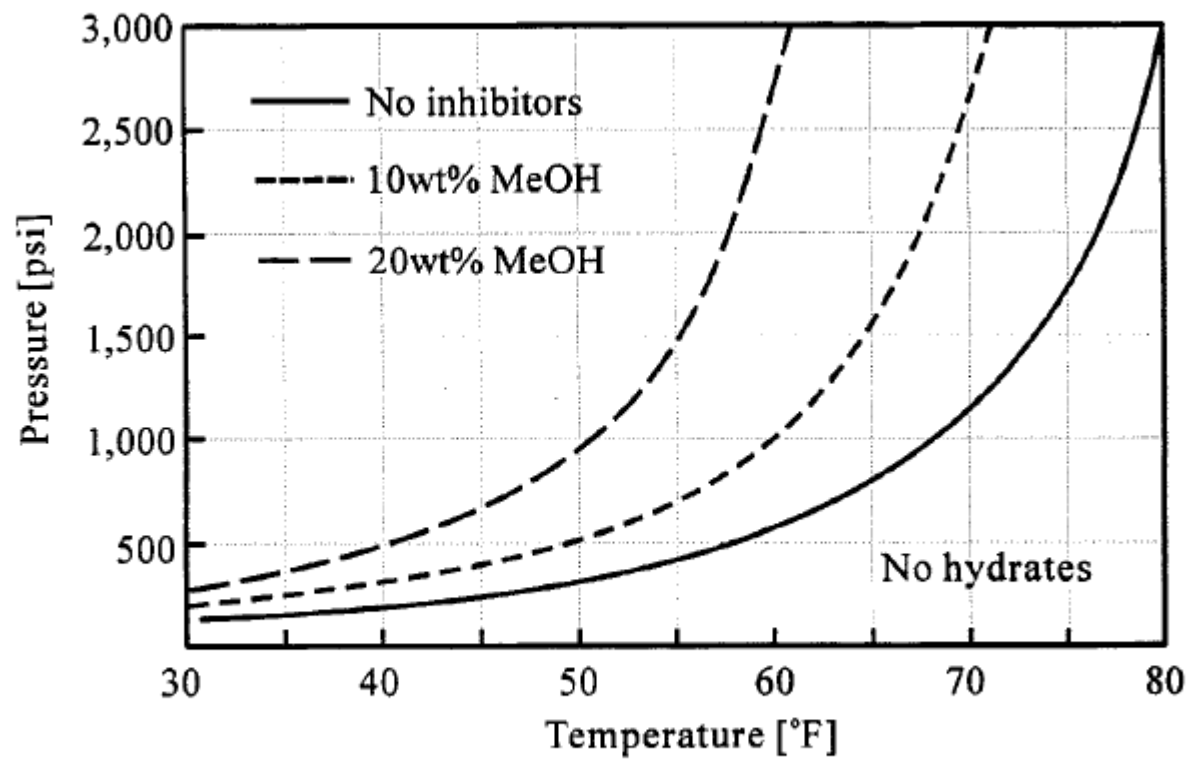


**Figure 20.9** Effect of MeOH on hydrate formation.



### 20.2.3 Effects of Salt, MeOH, Gas Composition

The hydrate dissociation curve may be shifted towards lower temperatures by adding a hydrate inhibitor. Methanol, ethanol, glycols, sodium chloride, and calcium chloride are common thermodynamic inhibitors. Hammerschmidt (1969) suggested a simple formula to roughly estimate the temperature shift of the hydrate formation curve.

$$\Delta T = \frac{KW}{M(100 - W)} \quad (20.1)$$

where,  $\Delta T$  : temperature shift, hydrate depression [ $^{\circ}\text{C}$ ]

$K$  : constant [ - ], which is defined in Table 20.1.

$W$  : concentration of the inhibitor in weight percent in the aqueous phase.

$M$  : molecular weight of the inhibitor divided by the molecular weight of water.

Table 20.1 Constant of Equation (20.1) for various inhibitors.

Inhibitor	K value
Methanol	2335
Ethanol	2335
Ethylene glycol (MEG)	2700
Diethylene glycol (DEG)	4000
Triethylene glycol (TEG)	5400

#### **20.2.4 Mechanism of Hydrate Inhibition**

There are two types of hydrate inhibitors used in subsea engineering: thermodynamic inhibitors (THIs) and low-dosage hydrate inhibitors (LDHIs).

The most common thermodynamic inhibitors are methanol and MEG, even though ethanol, other glycols (DEG, TEG), and salts can be effectively used. They inhibit hydrate formation by reducing the temperature at which hydrates form. This effect is the same as adding anti-freeze to water to lower the freezing point. Methanol and MEG are the most commonly used inhibitors,

LDHIs include anti-agglomerants and kinetic inhibitors. LDHIs have found many applications in subsea systems in recent years. LDHIs prevent hydrate blockages at significantly lower concentrations, e.g., less than 1 weight percent, than thermodynamic inhibitors such as methanol and glycols. Unlike thermodynamic inhibitors, LDHIs do not change the hydrate formation temperature. They either interfere with formation of hydrate crystals or agglomeration of crystals into blockages. Anti-agglomerates can provide protection at higher subcooling than kinetic hydrate inhibitors. However, low dosage hydrate inhibitors are not recoverable and they are expensive. The difference in hydrate inhibition mechanism between LDHIs and THIs is shown in Figure 20.10.